Molecular mechanisms underlying sensory-driven structural and functional plasticity in the awake developing brain

by

Simon Chen

B.Sc., The University of British Columbia, 2007

A THESIS SUBMITTED IN PARTIAL FULFILLMENT OF
THE REQUIREMENTS FOR THE DEGREE OF

DOCTOR OF PHILOSOPHY

in

THE FACULTY OF GRADUATE STUDIES

(Neuroscience)

THE UNIVERSITY OF BRITISH COLUMBIA

(Vancouver)

July 2012

Abstract

During early brain development, formation of functional neural circuits requires correct neuronal morphological growth and formation of appropriate synaptic connections. In addition, sensory experience and neural activity impart lasting effects on morphological and functional complexity by directing synapse formation and synaptic plasticity. Errors in these events may result in the creation of dysfunctional circuits underlying common neurodevelopmental disorders, including Autism Spectrum Disorder (ASDs), schizophrenia, and epilepsy. Therefore, to understand the normal development and the pathophysiology of these disorders, we must decipher the molecular mechanisms regulating developmental neural circuit structural and functional plasticity. This dissertation discusses work on the molecular mechanisms underlying structural and functional plasticity in the developing brain, ranging from cell adhesion molecules involved with initial synapse formation to transcription factors regulating sensory experience-driven functional plasticity. In the first half of the dissertation, using two-photon time-lapse imaging of individual growing neurons within intact and awake embryonic *Xenopus* brains, I found that the cell adhesion molecules, neurexin (NRX) and neuroligin-1 (NLG1), confer stabilization to labile dendritic filopodia, supporting their transition into longer and persistent branches through an activity-dependent multistep process. Disrupting NRX-NLG1 function destabilizes filopodia and culminates in reduced dendritic arbor complexity as neurons mature over days. These findings suggest that abnormalities in brain neuron structural development may contribute to ASDs. In the second half of the dissertation, I used *in vivo* two-photon calcium imaging of visual network activity and rapid time-lapse imaging of individual growing brain neurons to identify morphological correlates of experience-driven functional potentiation and

depression during critical periods of neural circuit formation. Further, I identified the transcription factor MEF2A/2D as a major regulator of neuronal response to plasticity-inducing stimuli directing both structural and functional changes. Unpatterned sensory stimuli that change plasticity thresholds induce rapid degradation of MEF2A/2D through a classical apoptotic pathway requiring NMDA receptors and caspases-9, 3 and 7, demonstrating natural sensory experience fine-tunes the plasticity thresholds of neurons during neural circuit formation. Together, work in this dissertation provides new insights into the molecular and cellular mechanisms of how sensory experience and synapse formation direct structural and functional plasticity in the embryonic developing brain.

Preface

The work in Chapter 2, entitled "Neurexin-neuroligin cell adhesion complexes contribute to synaptotropic dendritogenesis via growth stabilization mechanisms in vivo" has been published in

Chen, S.X., Tari, P.K., She, K., and Haas, K. (2010). Neurexin-neuroligin cell adhesion complexes contribute to synaptotropic dendritogenesis via growth stabilization mechanisms in vivo. **Neuron** *67*, 967-983.

All the experiments were conceived and designed by myself, and I conducted most of the data collection, analysis, and manuscript preparation. Parisa Tari assisted with the immunohistochemistry and western blotting, and Kevin She conducted the Neurexin-Neuroligin binding assay. Dr. Kurt Haas provided advice on experimental design and helped with editing the manuscript.

The work in Chapter 3, entitled "The transcription factor MEF2 directs developmental visually-driven functional and structural metaplasticity" has been published in

Chen, S.X., Cherry, A., Tari, P.K., Podorgski, K., Kwong, KH, Haas, K. (2012). The transcription factor MEF2 directs developmental visually-driven functional and structural metaplasticity. **Cell** ***in press***

All the experiments were conceived and designed by myself, and I conducted most of the experimental work and data analysis, prepared the figures and wrote the manuscript. Angus Cherry assisted with *in vivo* calcium imaging, Parisa Tari assisted with the western blotting, Kali Kwong assisted with single-cell electroporation, and Kasper Podgorski wrote the program to analyze calcium imaging results. Dr. Kurt Haas provided advice on experimental design and helped with editing the manuscript.

Certificate of approval:

The animal studies presented in this thesis were performed with ethics approval from the University of British Columbia Animal Care Committee (certificate # - A09-0021)

Table of Contents

Abstract ii
Preface iv
Table of Contents v
List of Tables viii
List of Figures ix
List of Acronyms xi
Acknowledgement xiii

1. GENERAL INTRODUCTION 1
1.1. The Albino *Xenopus laevis* Tadpole as a Model of Early Brain Development 1
1.2. Dendritogenesis 6
1.2.1. An overview of dendritic arborization in early development 6
1.2.2. Intrinsic factors regulating dendrite growth 7
1.2.3. Extrinsic factors regulating dendrite growth 9
1.2.4. Neural activity regulating dendrite growth 11
1.2.5. Synaptotropic model of dendrite growth 13
1.3. Synaptogenesis 17
1.3.1. Synapse assembly 17
1.3.2. Synapse maturation 24
1.3.3. Synapse elimination 26
1.4. Long-Term Potentiation and Depression 28
1.4.1. Molecular mechanisms underlying LTP 29
1.4.2. Molecular mechanisms underlying LTD 32
1.4.3. LTP/LTD and structural plasticity 33
1.5. Metaplasticity 36
1.5.1. The Bienenstock, Cooper and Munro (BCM) computational model of synaptic plasticity 38
1.5.2. Molecular mechanisms underlying metaplasticity 41
1.6. Experience-Driven Plasticity and Metaplasticity in The Developing Brain 42
1.6.1. Visual-driven synaptic plasticity 42
1.6.2. Visual-driven functional plasticity and metaplasticity 43
1.7. Research Aims and Hypothesis 45
1.7.1. Examining the role of the cell adhesion molecules, NRXs and NLGs in brain neuronal growth and function in vivo 45
1.7.2. Determining the morphological correlates of physiological plasticity and metaplasticity in vivo. 45
1.7.3. Deciphering the molecular mechanisms mediating functional and structural metaplasticity 46

2. NRX-NLG CELL ADHESION COMPLEXES CONTRIBUTE TO SYNAPTOTROPIC DENDRITOGENESIS VIA GROWTH STABILIZATION MECHANISMS IN VIVO 47
2.1. Specific Background 48
2.1.1. Neurexin and neuroligin 48
2.2. Introduction 53

2.3. Material and Methods 56
2.3.1. Animals 56
2.3.2. Plasmids and morpholinos 56
2.3.3. Immunoblotting 57
2.3.4. Immunohistochemistry 57
2.3.5. Neurexin-neuroligin binding assay 58
2.3.6. In vivo single cell transfection and loading with dyes and morphlinos 59
2.3.7. In vivo time-lapse imaging of dendrite growth dynamics 60
2.3.8. Morphometric analysis 61
2.3.9. Statistical tests 62
2.4. Results 62
2.4.1. Endogenous NLG1 expression in developing Xenopus brain 62
2.4.2. Cell-autonomous NRX-NLG1 disruption prevents dendritic filopodia stabilization 72
2.4.3. Increased NLG1 function hyper-stabilizes dendritic filopodia 76
2.4.4. Knock-down of NLG1 blocks dendritic filopodia stabilization 79
2.4.5. NRX-NLG1 adhesion creates transient stabilization 81
2.4.6. NLG1 over-expression mediated filopodial stabilization requires NMDA receptor transmission 85
2.4.7. NRX-NLG1 interactions influence long-term dendritic arbor patterning 87
2.5. Discussion 89

3. THE TRANSCRIPTIONA FACTOR MEF2 IS A MASTER REGULATOR OF VISUAL EXPERIENCE-DRIVEN FUNCTIONAL AND STRUCTURAL METAPLASTICITY IN THE DEVELOPING BRAIN 97
3.1. Specific Background 98
3.1.1. Transcription Factor MEF2 98
3.2. Introduction 100
3.3. Material and Methods 103
3.3.1. Animals 103
3.3.2. Western blotting 103
3.3.3. In vivo two-photon calcium imaging 104
3.3.4. Visual stimulation and training 105
3.3.5. Fluorescence data processing 105
3.3.6. In vivo single neuron labeling 106
3.3.7. In vivo time-lapse imaging of dendrite growth dynamics 106
3.3.8. Dynamics morphometric analysis 107
3.4. Results 107
3.4.1. Sensory experience drives simultaneous morphological and functional plasticity 107
3.4.2. White noise priming induces functional and structural metaplasticity 114
3.4.3. NMDARs are required for both functional and structural metaplasticity 117
3.4.4. WN induces a rapid decrease in expression of the transcription factor MEF2 119

3.4.5. The time course of metaplastic shift in plasticity outcomes matches MEF2 levels 121
3.4.6. WN-induced reduction in MEF2 is mediated by digestion through caspase-9, -3/7 123
3.4.7. MEF2A/2D knockdown is sufficient to induce a metaplastic shift in functional plasticity 126
3.4.8. MEF2 knockdown induces structural metaplasticity 127
3.5. Discussion 129
3.5.1. Coordination of developmental structural and functional plasticity and metaplasticity 129
3.5.2. MEF2 is necessary and sufficient to shift developmental plasticity thresholds 130

4. CONCLUSION 135
4.1. Summary of Findings 135
4.2. Future Directions 138
4.2.1. Role of other NLG isoforms on dendrite growth 138
4.2.2. Do autism-associated NLG mutants alter dendrite growth? 139
4.2.3. Role of NRX-NLG1 interactions on the functional properties and connectivities of neural circuit 142
4.2.4. Identifying molecular cascades downstream of MEF2 142
4.3. Significance 143

REFERENCES 145

List of Tables

Table 2.1. Summary of the Effects of Different NLG1 Constructs on Filopodial Dynamics, Arbor growth, and Synapses. 96

Table 3.1. Summary of the Effects of Different Visual Stimuli and Pharmacological Treatments on Visual-Evoked Responses and Dendrite Growth 134

List of Figures

Figure 1.1 Retinal System of Xenopus laevis Tadpoles. 3
Figure 1.2 Neuronal Cell Types in the Optic Tectum of Xenopus laevis 5
Figure 1.3 Dendritic Diversity in Mammals. 7
Figure 1.4 Synaptotropic Dendrite Growth 16
Figure 1.5 Synaptic Adhesion Molecules Function Throughout the Life of a Synapse 19
Figure 1.6 Model for CNS Synaptogenesis 21
Figure 1.7 Cell Adhesion Molecules 23
Figure 1.8 Dynamic Regulation of AMPA-receptor Signaling in Synaptic Plasticity 30
Figure 1.9 Metaplasticity and Plasticity Modulation 37
Figure 1.10 The Bienenstock, Cooper and Munro (BCM) Model 40
Figure 1.11 In vivo Calcium Imaging Setup in Xenopus tadpole 45
Figure 2.1 Structure of Neuroligin and Neurexin 52
Figure 2.2. Characterization of Xenopus laevis NLG1 65
Figure 2.3 Dual Imaging of PSD-95 Puncta and Dendritic Filopodia. 68
Figure 2.4 Blocking NRX-NLG1 Interactions Prevents Dendritic Filopodial Stabilization, Dendritic Arbor Growth, and Reduces Synapse Number. 72
Figure 2.5 Expression of NLG1-swap Increases Filopodia Turnover and Decreases Postsynaptic Specializations. 76
Figure 2.6 Over-Expression of NLG1 Hyper-Stabilizes Dendritic Filopodia and Increases Postsynaptic Specializations. 79
Figure 2.7 Morpholino-Mediated Knockdown of NLG1 Inhibits Dendrite Growth and Impairs Synaptic Transmission 81
Figure 2.8 Expressing of NLG1-ΔC Increases Filopodia Lifetime Without Persistent Stabilization and Decreases Postsynaptic Specializations 85
Figure 2.9 NRX-NLG1 Interactions Influence Long-Term Dendritic Arbor Patterning. 88
Figure 2.10 Model of NRX-NLG1 Regulation of Dendritogenesis 95
Figure 3.1 Visual-Experience Driven Potentiation is Associated with Morphological Stabilization and Sprouting 111
Figure 3.2 Visual-Experience Driven Depression Destabilizes Dendritic Growth 113
Figure 3.3 Brief Unpatterned Visual Stimulation Alters Subsequent Morphological Response to Plasticity Stimuli 116

Figure 3.4 NMDAR Blockade Inhibits the WN-Mediated Metaplasticity Shift in Morphological Plasticity..... 118
Figure 3.5 Time Course of MEF2 Reduction Following WN Corresponds to the Duration Altered Plasticity Response. 122
Figure 3.6 Transient Activation of Caspase-3 Leads to MEF2 Degradation and is Required for WN-mediated Shift in Plasticity Response. 125
Figure 3.7 Knockdown of MEF2 Shifts Plasticity Responses. 128
Figure 4.1 Expression of ASD-associated NLG Mutants Results in Simple and Less Complex Dendritic Arbors..... 141

List of Acronyms

AChE	Acetylcholinesterase
AMPA	α-Amino-3-Hydroxy-5-Methyl-4-Isoxazole Propionic Acid
AMPAR	AMPA Receptor
AKAP	A-Kinase-Anchoring Protein
AP5	(2*R*)-Amino-5-Phosphonovaleric Acid
ASD	Autism Spectrum Disorder
BDNF	Brain-Derived Neurotrophic Factor
CAM	Cell Adhesion Molecule
CaMKII	Calcium/Calmodulin-Dependent Protein Kinase II
Cdc42	Cell Divison Cycle 42
CNS	Central Nervous System
CNQX	6-Cyano-7-Nitroquinoxaline-2,3-Dione
ER	Endoplastic Reticulum
fEGFP	(farnesylated) Enhanced Green Fluorescent Protein
GABA	γ-Aminobutyric Acid
GluR	Glutamate Receptor
GRIP	Glutamate Receptor Interacting Protein
HA	Heamagglutinin
HRP	Horseradish Peroxidase
KO	Knockout
LGN	Lateral Geniculate Nucleus
LTP	Long-Term Potentiation
LTD	Long-Term Depression
MAGUK	Membrane-Associated Guanylate Kinase
MAPK	Mitogen-Activated Protein Kinase
MEF2	Myocyte Enhancer Factor 2
mGluR	Metabotropic Glutamate Receptor
mEPSC	Miniature Excitatory Postsynaptic Current
MS222	3-Aminobenzoic Acid Ethyl Ester
RGC	Retinal Ganglion Cell
NGL	Neuregulin

NLG	Neuroligin
NMDA	*N*-methyl-D-aspartate Receptor
NR	NMDA Receptor
NRX	Neurexin
OGB1-AM	Oregon Green 488 BAPTA-1, AM
PCR	Polymerase Chain Reaction
PDZ	PSD-95, Dlg and ZO-1
PICK	Protein Interacting with C Kinase
PKA	cAMP-Dependent Protein Kinase
PKC	Protein Kinase C
PKM	Protein Kinase M
PSD	Postsynaptic Density
SNAP25	Synaptosomal-Associated Protein 25
TTX	Tetrodotoxin

Acknowledgement

I would like to thank, first and foremost, my supervisor Dr. Kurt Haas for his guidance and support throughout my Ph.D. study. Kurt gave me a lot of space and freedom to mature and develop my own research interest. Without Kurt I would not get to understand how much fun research and science is about. I also want to thank Dr. Catherine Rankin for her endless support and encouragement during my Ph.D., and my research advisory committee, Dr. Ann Marie Craig, Dr. Shernaz Bamji, and Dr. Vanessa Auld, for their invaluable advice on my projects.

I want to extend my genuine appreciation to all the members in Haas Lab, in particular, to Sesath Hewapathirane, Xuefeng Liu, and Derek Dunfield. I had the pleasure to work each of them when I first joined the lab, and I really learned a lot from them. The experience is invaluable to me and will stay with me forever. I also want to thank all the students who helped me with my experiments - Parisa Tari, Angus Cherry, and Kali Kwong.

I am truly grateful for the funding support I received - the Frederick Banting and Charles Best Canadian Graduate Scholar from the Canadian Institute of Health Research .

Lastly, I would like to thank my parents and my brother. This journey would not have been possible without their supports. To Patrick, thank you for being the wonderful brother you are, I have been following your path for most of my life and you are truly a role model to me.

1. GENERAL INTRODUCTION

1.1. The Albino *Xenopus laevis* Tadpole as a Model of Early Brain Development

Over the past decades, the African claws frog, *Xenopus laevis*, has been an important model system for studying early stages of central nervous system development (Aizenman and Cline, 2007; Baudet et al., 2011; Borodinsky et al., 2004; Engert et al., 2002; Hu et al., 2005; McFarlane and Lom, 2011; Meyer, 1998; Ruthazer et al., 2003; Sin et al., 2002; Sperry, 1963; Zhang et al., 2000). The physiological events of neuronal growth and circuit refinement appear to be highly conserved between *Xenopus* and higher mammals, including glutamatergic synaptic maturation and plasticity (Wu et al., 1996; Wu and Cline, 2003). However, the retinotectal pathway of the albino *Xenopus* tadpole provides an accessible central neural circuit for study during critical periods of neurogenesis, neuronal morphogenesis, and wiring, which are difficult to directly examine in the developing mammalian brain. The tadpole retinotectal circuit develops over a period of weeks as axons from retinal ganglion cells (RGC) of the eye follow guidance cues to locate imprecise termination zones within the optic tectum to create a rough retino-topographic map (**Figure 1.1**) (Cline, 1991; McFarlane and Lom, 2011; Ruthazer et al., 2003; Sperry, 1963). At the same time, tectal neurons extend nascent dendrites into the tectal neuropil and form synapses with RGC axons. During a

maturation period spanning days to weeks, tectal dendrites, RGC axons, and synapses that are formed undergo activity-dependent remodeling to produce circuits optimized to process visual stimuli (Aizenman and Cline, 2007; Cline, 1991). Studies in the 70s, using Golgi stain have characterized different cell types that are present at different stages of *Xenopus laevis*. For example, at stage 49, the optic tectum contains projection neurons such as pyramidal-like cells, pear-like shape cells, ganglionic cells, and many other cell types like stellate, amacrine, horizontal, bipolar cells, etc (**Figure 1.2**) (Lazar, G.Y. 1973), suggesting the optic tectum of *Xenopus laevis* contains neuronal cell types that are similar as higher vertebrates. Moreover, the relevance of similar activity-dependent circuit formation in early mammalian development is supported by findings that dark-rearing prior to eyelid opening in ferrets and cats prevents normal circuit formation in the lateral geniculate nucleus, colliculus and primary visual cortex (Dong et al., 2009; Feller and Scanziani, 2005).

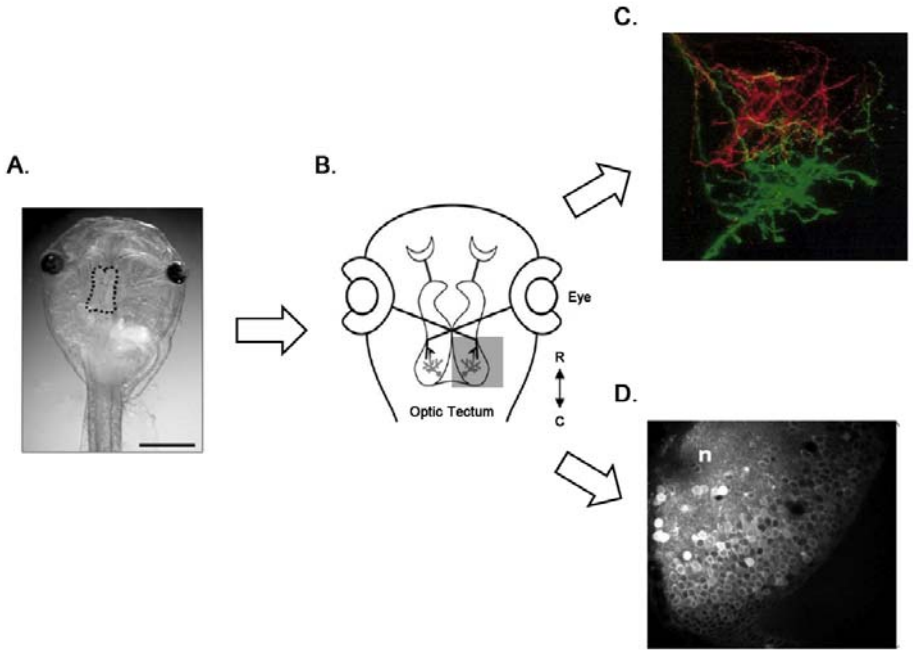

Figure 1.1 Retinal System of Xenopus laevis Tadpoles.

(A) Stage 47 albino *Xenopus laevis* tadpole. **(B)** Cartoon Diagram of the retinotectal system in the *Xenopus* tadpole. Axons from RGCs from the eye project and innervate optic tectal neurons. *Reprinted with permission from (Chiu et al., 2008)* **(C)** RGC axonal terminal in the optic tectum. Temporal and nasal retina were labeled with dil (red) and FITC-dextrane (green), respectively Scale bar = 20μm. *Reproduced with permission from (Ruthazer and Cline, 2004)* **(D)** Optic tectum loaded with calcium dye to demonstrate the location of tectal neuronal soma and neuropil (n).

Two recent major technological innovations have established the *Xenopus laevis* tadpole as a leading model for studying early brain circuit development – two-photon fluorescence microscopy and single-cell electroporation. The transparency of the albino *Xenopus laevis* tadpoles provides a clear window allowing direct in vivo imaging of the intact developing brain (**Figure 1.1**), and two-photon microscopy allows imaging of living neurons deep within the brain with reduced phototoxicity (Denk et al., 1990). The transparent tadpole preparation provides a relatively easy means to image early brain circuit formation compared to similar stages of mammalian development, which largely

occurs *in utero* and at early postnatal periods. Single-cell electroporation (SCE) is an *in vivo* transfection method that allows delivery of dye, DNA, peptides or other macromolecules to individual cells within intact tissues (Haas et al., 2002; Haas et al., 2001). SCE can be used to label neurons with plasmid DNA encoding protein fluorophores along with additional genetic constructs for exogenous protein expression. By restricting gene expression to individual neurons within intact circuits, one can discern cellular morphology, which is occluded when multiple cells are labeled, and allows identification of cell-autonomous effects of genetic manipulations. Following SCE, labeled neurons can be imaged using *in vivo* time-lapse two-photon microscopy to achieve high-resolution 3D images for accurate morphometric measurements of neuronal growth dynamics.

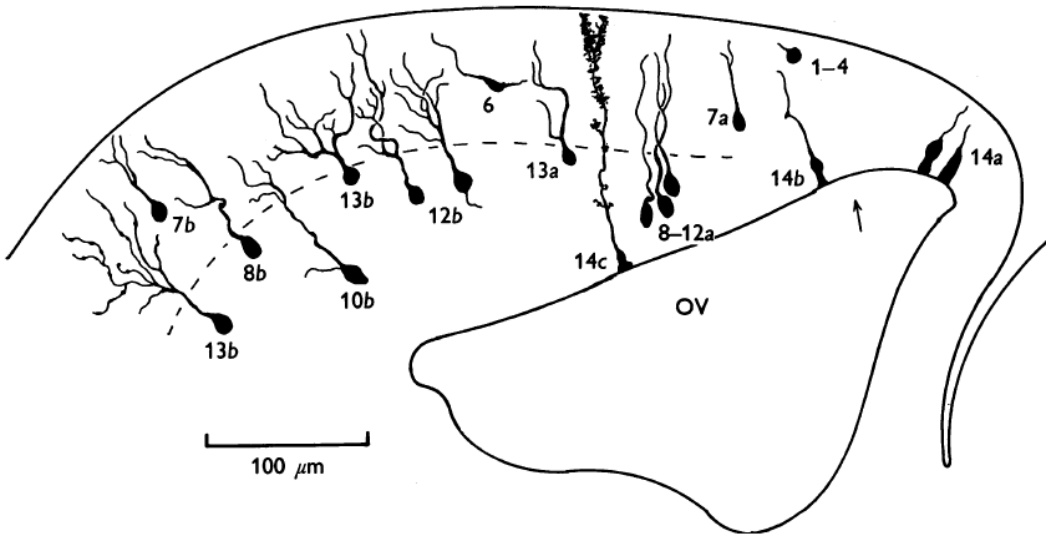

Figure 1.2 Neuronal Cell Types in the Optic Tectum of Xenopus laevis

Structure of the optic tectum at stage 49. The interrupted line represents the outer surface of layer 6. The arrow indicates the region of intensive cell division. OV, optic ventricle. Rostral is to the left. 7 – small pear-shaped cell with recurrent axon; 8 – pear-shaped cell with ascending axon and narrow dendritic tree; 9 – axonless pear-shaped cell; 10,11 – pear-shaped cells in the deep periventricular layers; 12 – pear-shaped cell with intratectal axon; 13 – pyramidal cells; 14 – ependymal cells (Lazar G.Y. 1973).

1.2. Dendritogenesis

1.2.1. An overview of dendritic arborization in early development

The human brain is an architectural marvel. The structure of each brain neuron and the interconnected networks they create are critical to all brain functions, and structural abnormalities are directly associated with neurological disorders. The human brain is estimated to be composed of hundreds of billions of neurons interconnected by trillions of synapses. Each brain neuron has an elaborate and unique morphology critical to its functions of collecting, processing and disseminating information. Brain neurons are typically polar cells, composed of a tree-like dendritic arbor that receives and integrates synaptic input from upstream sources, a cell body and an output axonal process and arbor that terminate locally or distantly to transmit signals to downstream targets (**Figure 1.3**). The morphologies of dendritic arbors follow neuronal-type basic patterns and each neuron is unique in the number and position of dendritic branches. The size and shape of dendritic arbor are important to provide appropriate dimensions for sampling the correct field of axonal innervations. Moreover, the physical dimensions of dendrites, including diameter, branching and length directly influence the function of integrating synaptic electrical signals that contribute to action potential generation at the cell body (Spruston, 2008). Hence, deciphering how such complex neuronal morphologies are formed is a leading question in developmental neuroscience, central to understanding the origins of numerous common neurodevelopmental disorders, such as Autism Spectrum Disorders (ASDs), schizophrenia and epilepsy.

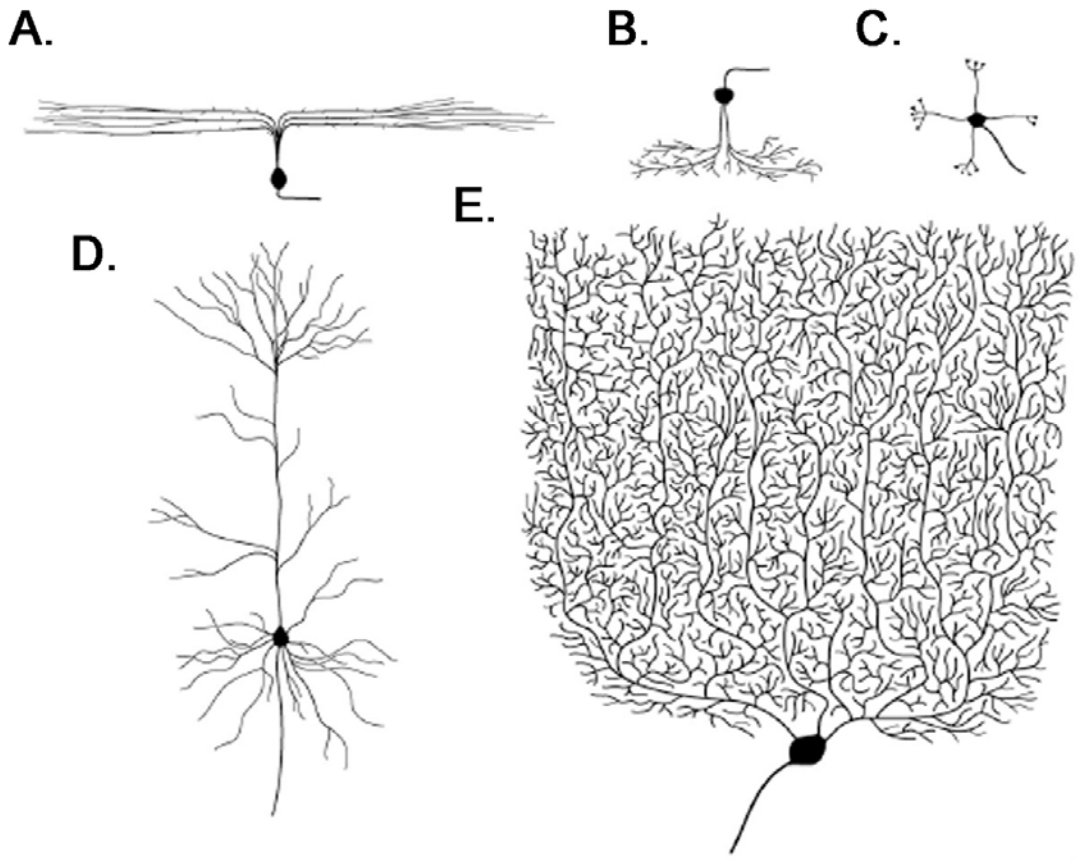

Figure 1.3 Dendritic Diversity in Mammals.

(A) side view of a retinal ganglion cell. **(B)** side view of an amacrine cell. **(C)** a cerebellum granule neuron. **(D)** a cortical pyramidal neuron. **(E)** a purkinje cell. *Adapted with permission from (Gao, 2007)*

1.2.2. Intrinsic factors regulating dendrite growth

Since the time of Golgi and Cajal, studying the complexity and diversity of dendritic arbors has been important to our understanding of nervous system structure and function. Yet, the molecular and cellular mechanisms underlying dendritic morphogenesis remain largely undefined. Dendritic arbor development is believed to be controlled intrinsically by genetically encoded patterns due to the conserved arbor

patterns between distinct subtypes of neurons (**Figure 1.2**). The application of genetic approaches in invertebrates and vertebrates has uncovered a complex network of transcription factors and ligand/receptors that control dendritic outgrowth and branching. One seminal finding came from study of the dendritic arborization (DA) neurons of the *Drosophila melanogaster* larval peripheral nervous system. *D. melanogaster* have four classes of DA neurons, categorized by their dendritic arbor complexity. Class I DA neurons have simple dendritic arbors and class IV neurons have a much more complex branch patterns. Using a systematic RNA interference screen, work from the Jan lab has identified multiple transcription factors that are critical for regulating DA neuronal complexity (Parrish et al., 2006). For example, one of the transcription factors, the BTB-zinc finger protein *Abrupt*, is expressed only in the class I DA neurons. Ectopically expressing Abrupt in class II, III, IV DA neurons results in the production of a simple dendritic arbor, similar to class I DA neurons (Li et al., 2004; Sugimura et al., 2004). Each of the four classes of DA neurons also expresses different levels of the homeodomain-containing transcription factor, *CUT*. Loss-of-function and neuron-specific over-expression studies showed that the levels of CUT expression dictate the distinct features of different classes of DA neurons (Grueber et al., 2003). Lastly, class IV DA neurons uniquely express the transcription factor *Collier*, which functions to suppress the actions of CUT. Loss-of-function of Collier in class IV DA neurons resulted in a morphological phenotype similar to class III DA neurons, suggesting that balanced co-expression of CUT and Collier is necessary to produce the appropriate morphology of class IV DA neurons (Jinushi-Nakao et al., 2007). These studies reveal the significance of transcription factors in regulating dendritic arbor patterning, in which a distinct morphology can be achieved through varying the levels of a single transcription factor or a combinatorial mechanism with multiple transcription factors (Jan and Jan, 2010).

Transcription factors have also been shown to regulate dendrite morphology in mammalian neurons. In the rodent cortex, the bHLH (basic helix-loop-helix) transcription factor Neurogenin2 promotes outgrowth of a polarized leading process in pyramidal neurons (Hand et al., 2005). Dendritic development is also under control by multiple activity-dependent transcription factors such as neurogenic differentiation factor 1 (NEUROD1), cAMP response element-binding protein (CREB), and Ca2+-responsive transactivator (CREST) (Aizawa et al., 2004; Gaudilliere et al., 2004; Redmond et al., 2002).

1.2.3. Extrinsic factors regulating dendrite growth

In addition to genetic regulation, many extrinsic molecules have been identified to regulate dendritic arbor patterning by influencing branch stabilization, retraction, and directional guidance. Many axonal guidance molecules such as Slit and Semaphorins have also been shown to direct dendrite growth. In *D. melanogaster,* Robo receptor activation by binding to its secreted ligand Slit promotes dendritic branching and elongation of class IV DA neurons, but does not affect other classes of DA neurons (Dimitrova et al., 2008). In the retinotectal system of zebrafish, Robo2 and Slit are responsible for directing RGCs into specific layers of the midbrain optic tectum. The Baier lab has recently shown that Slit/Robo2 signaling is also important for tectal dendrite stratification (Xiao et al., 2011), suggesting the shared responsiveness of axons and dendrites to Slit is essential for bringing matching synaptic partners into the correct layer of the tectum. Furthermore, in the developing olfactory system of *D. melanogaster*, Semaphorin 1A (Sema 1A) is expressed in a gradient fashion along the dorsolateral to ventromedial axis to direct axonal pathfinding in the antennal lobe. Komiyama *et al*.

found that the graded expression of Sema-1A is also important for the dendrite targeting of projection neurons by acting as receptors to guide dendrites to the appropriate glomeruli (Komiyama et al., 2007). In their later study, they identified two other secreted semaphorins, Sema-2a and Sema-2b that act as ligands to Sema-1A to provide unique spatial distribution for projection neuron dendrite targeting (Sweeney et al., 2011). In mammalian cortical neurons, semaphorins have also been shown to regulate neuron polarity and dendrite orientation. Sema-3A, localized near the marginal zone, attracts the apical dendrite of pyramidal neurons to extend the processes toward the pial layer. In contrast, Sema-3A acts as a chemorepellant in axons of pyramidal neurons (Polleux et al., 2000), demonstrating that the differential response of axons and dendrites to the same guidance molecule can help establish neuronal polarity.

The neurotrophins is another class of molecules that plays a critical role in dendrite growth. Neurotrophins are composed of four families of proteins: nerve growth factor (NGF), brain-derived neurotrophic factor (BDNF), neurotrophin-3 (NT-3), and neurotrophin-4 (NT4). These factors trigger signaling cascades through binding to the Trk family of tyronsine kinase receptors, in which NGF preferentially binds to TrkA, BDNF and NT4 bind to Trk B, and NT-3 binds to TrkC. All neurotrophins also bind to the p75 neurotrophin receptor (p75NTR) with low-affinity (for review, please see (Reichardt, 2006)). Experimental studies using slice cultures showed acute application of NT3 has a profound effect on dendrite growth by increasing total dendritic length, number of branch points, and number of primary dendrites. Application of NT3 to organotypic cortical slices for 36 h also induced dendrite growth and increased the morphological complexity of neurons (Baker et al., 1998; McAllister et al., 1995). In contrast, over-expression of BDNF in cortical pyramidal neurons caused structural instability evident from an increase

in both sprouting and retraction of dendritic filopodia (Horch et al., 1999). Hence, it is proposed that the two neurotrophins, BDNF and NT-3, may interact in a “push-pull” fashion to regulate dendritic arborization (McAllister, 2000). Strikingly, In the retinotectal system of *Xenopus* tadpoles, treatments with recombinant BDNF or blocking antibodies to BDNF that alter endogenous free BDNF levels in the tadpole optic tectum only affects the morphology of RGC axons but not tectal dendrites (Hu et al., 2005; Sanchez et al., 2006).

1.2.4. Neural activity regulating dendrite growth

During early brain development, neural activity plays a critical role in establishing, strengthening or weakening, and breaking synaptic connections. Since dendrite growth occurs concurrently with synapse formation, such observation raises the question of whether neural activity also plays a role in shaping dendritic arbors. Animals raised in enriched environment with complex sensory stimuli exhibit more complex cortical neuronal dendritic arbor morphologies than animals raised with sparse environmental stimulation (Volkmar and Greenough, 1972b). Similarly, monocular deprivation alters dendrite development in LGN and visual cortex of the visual system. These findings demonstrate that sensory experience exerts long-lasting effects on dendritic arbor morphology (Coleman and Riesen, 1968; Wiesel and Hubel, 1963).

The term ‘neural activity’ encompasses a number of different events including receptor cell activation by sensory experience, action potential firing, and synaptic transmission. A large amount of research has accumulated implicating an important role of activity in contributing to dendritic arbor growth. However, blocking action potential activity by exposing developing neurons to the sodium channel blocker tetrodotoxin

(TTX) has generated varying effects on dendrite growth. In acute cortical slices, TTX exposure increases density and length of interstitial shaft filopodia, without affecting their motility and turnover. However, the overall dendritic arbor size and growth rate was not measured in this study (Portera-Cailliau et al., 2003). In contrast, TTX injected into the eyes has no detectable effect on dendrites of neurons in the LGN, and its direct application fails to alter dendrite growth *in vivo* in the optic tectum of *Xenopus* tadpoles (Dalva et al., 1994; Goodman and Model, 1990; Riccio and Matthews, 1987; Wong et al., 2000). One possible explanation is that TTX only eliminates action potential-mediated synaptic transmission, but does not affect spontaneous vesicular neurotransmitter release. Therefore, activity-dependent mechanisms may still be driven by weak spontaneous input.

Since glutamatergic synaptic transmission is the primary excitatory synaptic transmission in the brain, the effects of glutamatergic transmission on dendrite growth have also been examined. In acute cortical brain slices, pharmacological blockade of both NMDA and AMPA subtypes of glutamate receptors results in an overall reduction in dendritic shaft filopodia turnover and density, whereas focal glutamate application increases the length of shaft filopodia (Portera-Cailliau et al., 2003). Chronic blockade of NMDA and AMPA receptors elicits a decrease in dendrite growth in pyramidal neurons of neonatal rat cortex organotypic cultures (Baker et al., 1997) and *in vivo* in tectal neurons of *Xenopus* tadpoles (Rajan and Cline, 1998). *In vivo* time-lapse imaging of individual neurons showed that NMDA receptor antagonist APV blocks the development of immature tectal neurons while AMPA receptor antagonist CNQX, and sodium channel blocker, TTX do not (Rajan and Cline, 1998; Rajan et al., 1999). However, both APV and CNQX affect the maintenance of dendritic structure in mature tectal neurons. These

findings suggest a developmental shift in glutamatergic receptor function in dendritogenesis in the *Xenopus* tectum during early development (Rajan and Cline, 1998; Rajan et al., 1999) (See. Section 1.3.2).

Activity driven by patterned sensory visual stimulation has also been shown to regulate the growth of brain neurons in the developing *Xenopus* tectum. Using a visual stimulation assay consisted of 4 hr of dark followed by 4 hr of moving bar visual stimulation of freely swimming *Xenopus* tadpoles, Sin and colleagues showed that patterned visual stimulation increases dendritic arbor growth in an NMDAR-dependent manner (Chiu et al., 2008; Haas et al., 2006; Sin et al., 2002). In addition, they found that when a brief period of visual stimulation precedes exposure to darkness, the growth-promoting effect from the patterned stimulation persists even after the stimulus is removed (Sin et al., 2002). Together, these results demonstrate that neural activity such as that driven by sensory experience mediated by glutamatergic synaptic transmission plays a significant role in regulating dendrite growth.

1.2.5. Synaptotropic model of dendrite growth

Recent advances in two-photon microscopy have provided observation of growing neurons within an intact environments complete with the full complement of growth factors and proper neuronal activity. *In vivo* two-photon rapid time-lapse imaging of growing neurons adds a new layer of understanding of the processes underlying dendritogenesis. Such imaging of actively growing brain neurons reveals a surprising amount of motility and turnover of dendritic processes over periods of minutes, which could not be predicted from long interval imaging (Liu et al., 2009; Niell et al., 2004). Short dendritic filopodia and longer branches are added and extend, retract and are

eliminated. Remarkably, almost all dendritic filopodia retract within minutes of initial extension. A leading theory to explain this pattern of dynamic growth is the synaptotropic model of dendritogenesis, in which motile processes seek appropriate presynaptic partners, and synapse formation confers morphological stabilization (Vaughn, 1989). The high intrinsic rate of filopodial elimination reflects the high threshold for strong synapse formation. Support for this model comes from *in vivo* time-lapse imaging of dendritic growth in zebrafish tectal neurons expressing fluorescently tagged postsynaptic protein PSD-95, which demonstrates strong correlation between formation of PSD-95 puncta and stabilization of dendritic filopodia (**Figure 1.4**) (Niell et al., 2004).

An important implication of the synaptotropic model is that this mechanism allows function to drive form, since the appropriateness of new synapses to circuit function is constantly tested leading either to further synapse maturation and strengthening, or synapse elimination (Cline and Haas, 2008; Liu et al., 2009; McAllister, 2000; Tan et al., 2010; Wu and Cline, 1998; Yu and Malenka, 2003). Therefore, even though the vast majority of dendritic filopodia are rapidly retracted, they function to sufficiently search the local volume of neuropil for appropriate axonal contacts. The number of filopodia added, their orientation and distance extended, determines the extracellular volume sampled, and thus, the potential for identifying and connecting to the best presynaptic axons. Once synapses are formed and tested, filopodia are stabilized to prevent retraction and can then extend further to create persistent branches. Indeed, rapid time-lapse imaging over periods of hours finds that dendritic filopodia can stabilize, elongate and transition into branches that support further filopodial extension (**Figure 1.4**). Since the mature arbor is relatively stable, and each dendritic branch in the mature arbor makes a significant contribution to neuronal and network function, high filopodial turnover and appropriate extracellular searching ensures that each mature branch formed is optimal.

In this manner, brain neuronal dendritic arbors grow through use-tested self-organization to create functional structures and circuits.

However, there are also studies showing that axonal and dendritic patterning is independent from synapse formation (Kerschensteiner et al., 2009; Nevin et al., 2008). The Baier lab demonstrated that in the visual system of zebrafish, blockage of visual experience, correlated activity, or synaptic transmission does not affect the patterning and stratification of bipolar cells and ganglion cells, suggesting that neuronal connections in the the retina and tectum of larval zebrafish may be genetically hardwired and are independent from synapse formation and activity-dependent competition (Nevin et al., 2008). Another seminal study came from work done by the Wong lab, in which they generated transgenic mice with expression of tetanus toxin (TeNT) in the ON bipolar, but not the OFF bipolar cells, so only one type of cell's input is inhibited. Strikingly, they found that ON RGCs can correctly innervate with the silenced ON bipolar cell over the transmitted OFF bipolar cell. Moreover, the morphology of these innervations appears to be normal compared to OFF RGCs but with less synaptic connections. Time-lapse imaging studies showed that the decrease in synapse number is due to a reduced rate of synapse formation instead of an increase in synapse elimination. They demonstrated a selective role of activity in regulating synapse formation but not elimination, while affecting synapse number but not dendritic and axonal arbor morphology (Kerschensteiner et al., 2009). Hence, it is possible that in some systems in the brain, activity-dependent competition of circuit refinment is not ideal for processing distinct information, and other mechanisms are involved to shape the neuronal connectivity.

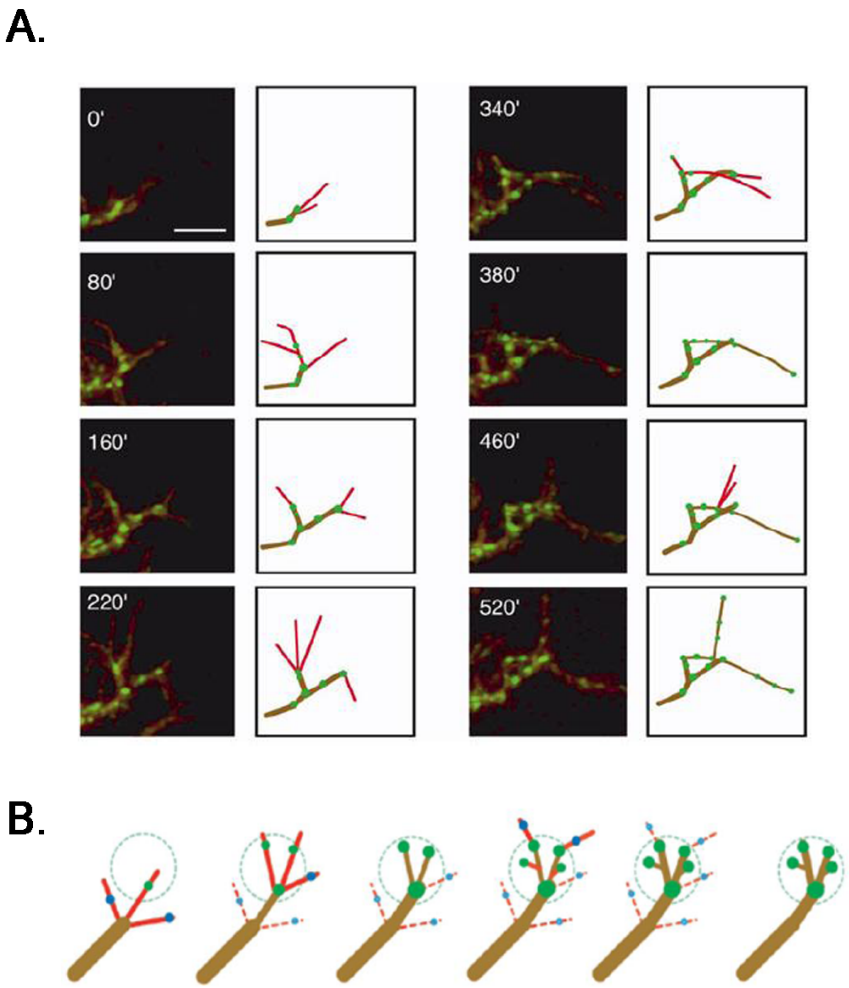

Figure 1.4 Synaptotropic Dendrite Growth

(A) Dendrite growth occurs by an iterative sequence of selective filopodial stabilization and punctum formation. Still images from a time-lapse series, accompanied by a schematic rendering for clarity. Green represents PSD-95:GFP puncta (a post-synaptic marker), red lines are newly formed (often transient) branches, and brown are persistent branches. Scale bar = 5μm. **(B)** Model of synaptotropic guidance of dendrite growth. A number of filopodia (solid red) extend from a dendritic branch. Those that encounter correct partners and form synaptic contacts (green dots) are stabilized as new branches (brown), whereas those that establish inappropriate contacts (blue dots) are retracted (dashed red). Successive rounds of selective stabilization result in arborization within a field of appropriate synaptic connections (dashed green region). *Reprinted with permission from (Niell et al., 2004).*

1.3. Synaptogenesis

1.3.1. Synapse assembly

The molecular mechanisms mediating dendritogenesis are emerging and have provided further support for the synaptotropic model, since discrete components of synapse formation and maturation have now been linked to specific aspects of dynamic growth behavior (Chen et al., 2010; Haas et al., 2006; Liu et al., 2009; Wu and Cline, 1998). Synapses are junctions between neurons in the brain that allow transmission of electrochemical signals from neuron to another, and communications between neurons are mediated primarily through neurotransmitter release and activation of postsynaptic receptors and ion channels. Synapses are held together by membrane-bound cell adhesion molecules (CAMs) that bind in a homo- or heterophilic fashion across the synaptic cleft (**Figure 1.5**) (Craig et al., 2006; Lise and El-Husseini, 2006). Mounting evidence suggests that the actions of cell adhesion molecules is not only limited to providing adhesive support and inter-neuronal recognition during initial axo-dendritic contact but are also essential for subsequent multiple stages of synapse formation and maturation (Dalva et al., 2007; Washbourne et al., 2004). Synapse development is a multi-step event that involves contact initiation, recruitment of pre- and postsynaptic proteins, and either synapse maturation or weakening and elimination (Lise and El-Husseini, 2006; McAllister, 2007). The initial contact between axons and dendrites is important to provide specific target recognition conferred by a large assortment of distinct families and splice variant isoforms of cell adhesion molecules (Siddiqui and Craig, 2011). Following the trans-synaptic interactions that confers initial recognition of appropriate partners, cell adhesion molecules binding initiates the next step of

development by acting as nucleators to attract additional synaptic proteins to both pre- and postsynaptic sites (**Figure 1.6**) (Lise and El-Husseini, 2006; McAllister, 2007).

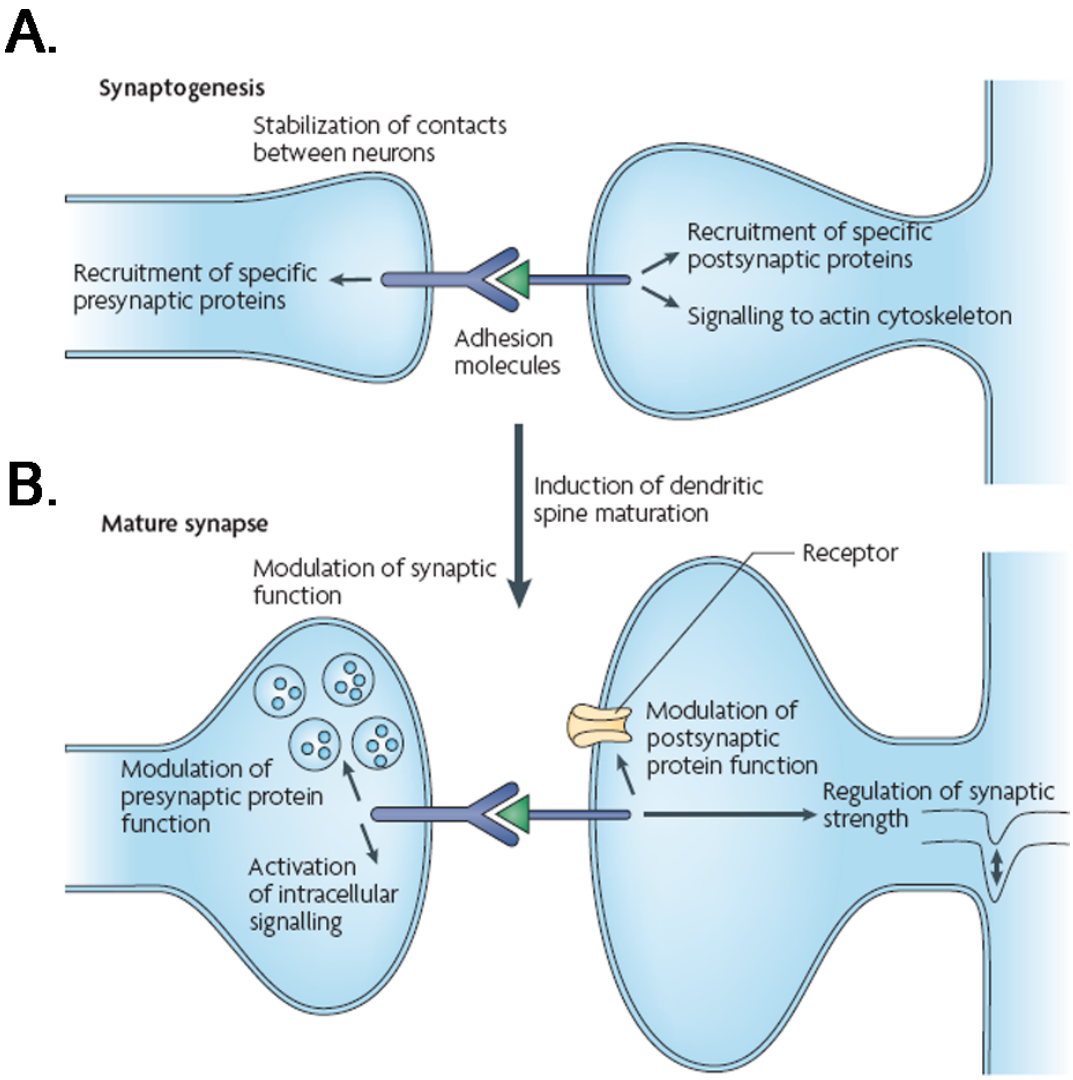

Figure 1.5 Synaptic Adhesion Molecules Function Throughout the Life of a Synapse

(A) At the nascent synaptic site, synaptic adhesion molecules stabilize the initial contact between axons and dendrites. Clustering and binding of adhesion proteins can lead to the recruitment of synaptic proteins via specific cytoplasmic or extracellular domains on these molecules, including PDZ-binding domains. Interactions between adhesion molecules can also lead to the activation of intracellular signaling events that can drive synapse maturation. In particular, signaling to the actin cytoskeleton can lead to the induction of dendritic spine formation. **(B)** In the mature or maturing synapse, synaptic adhesion molecules can interact with channels and other synaptic proteins to modulate their function, either by direct interaction with these proteins or through the activation of intracellular signaling events. In addition, synaptic adhesion proteins can regulate synaptic plasticity. *Reprinted with permission from (Dalva et al., 2007)*

Presynaptic proteins are transported in two major multi-molecular complexes: piccolo transport vesicles (PTVs) and synaptic vesicle (SV) protein transport vesicles (STVs) (McAllister, 2007; Sabo et al., 2006). PTVs transport molecules that are associated with the active zone such as piccolo, bassoon, Mun13, Mun18, syntaxin, and snap25 (Zhai et al., 2001). In contrast, STVs carry synaptic vesicle-associated proteins and other proteins critical for exo- and endocytosis (**Figure 1.6**) (Ahmari et al., 2000; Zhai et al., 2001). Proteins carried by the PTVs are responsible for maintaining the structure of presynaptic sites and connecting with the postsynaptic reception apparatus. Piccolo (Cases-Langhoff et al., 1996; Fenster et al., 2000) and Basson (tom Dieck et al., 1998) have been well characterized over the past decade. Both proteins contain multiple different binding motifs that can interact with other scaffolding proteins to form a large mesh of active zone protein networks, and Piccolo has also been shown to regulate endo- and exocytosis of synaptic vesicles (Gerber et al., 2001). Time-lapse imaging in cultured hippocampal neurons has demonstrated that the active zone assembly can occur within 1-2 hr after initial axo-dendritic contact (Ahmari et al., 2000; Antonova et al., 2001; Friedman et al., 2000; Okabe et al., 2001; Sabo et al., 2006; Zhai et al., 2001).

At the postsynaptic side, assembly of synaptic proteins at the contacted site form a specialized membrane micro-domain called the postsynaptic density (PSD) (Sheng and Hoogenraad, 2007). The PSD consists of a large mesh of protein networks containing neurotransmitter receptors, scaffolding proteins, and molecules important for cytoskeletal organization and signal transduction. In particular, scaffolding proteins provide an infrastructure of protein interactions connecting cell membrane, receptors, signaling molecules, and regulators of the cytoskeleton (Kim and Sheng, 2004). The protein PSD-95 is a member of the membrane-associated guanylate kinase (MAGUK) family of proteins, and is one of the central scaffolding proteins at the postsynaptic terminal. PSD-95 contains multiple PDZ (PSD95, discs large, and zona occluden) domains that can bind to and form dimmers with other proteins with PDZ domains, allowing protein-multimerization to form large assemblies of protein networks (Garner et al., 2002; Sheng and Hoogenraad, 2007; Ziv, 2001). Scaffolding proteins may also confer stabilization of dendritic processes by acting as a nucleation site linking the trans-synaptic adhesive interactions with the intracellular the cytoskeleton network.

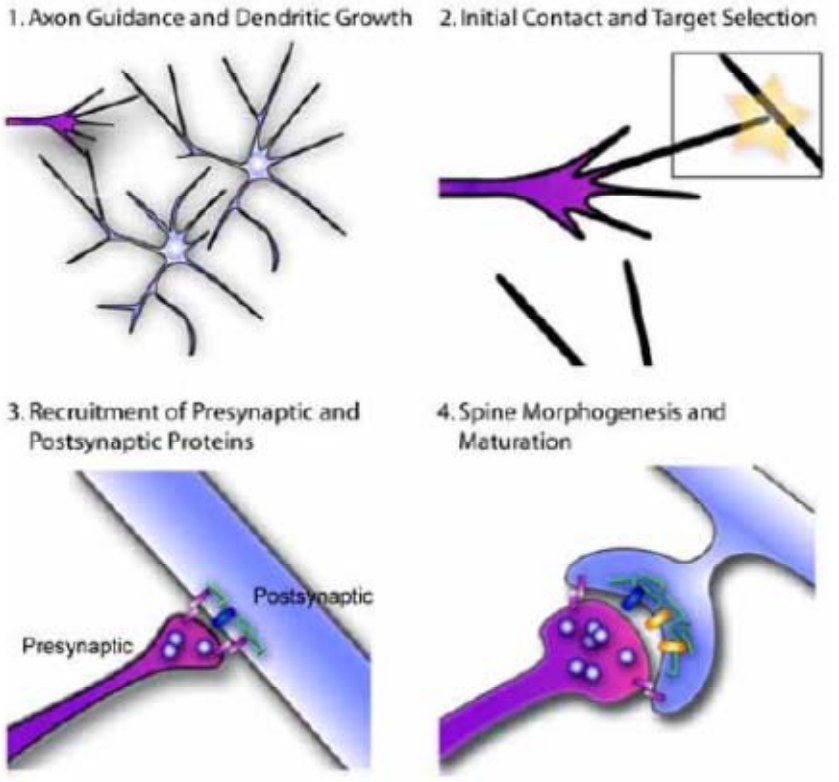

Figure 1.6 Model for CNS Synaptogenesis

Synapse formation is divided into characteristic stages typically including axon and dendrite growth and guidance (1) followed by the formation of initial contact between axon and dendrite (2) Following contact initiation, recruitment of appropriate synaptic proteins to nascent sites of contact (3) and maturation and stabilization of these synaptic contacts (4) result in functional synapses. Additionally, the stage of synapse elimination is often included in the process of synapse formation, due to its important role in the assembly of functional synaptic networks. *Reprinted with permission from(Gerrow and El-Husseini, 2006)*

A number of CAMs has been identified to mediate the assembly of the highly ordered pre- and postsynaptic protein complexes. Neurexins (NRX) and neuroligins (NLGs) were the first CAMs shown to be potent inducers for pre- and postsynaptic specialization (Graf et al., 2004; Ichtchenko et al., 1995; Scheiffele et al., 2000). Expressing NRXs or NLGs in non-neuronal cells and co-cultured with neurons induces

post or pre-synaptic differentiation, respectively (Graf et al., 2004; Scheiffele et al., 2000). Neurexins contain intracellular PDZ binding domains that interact with scaffolding molecules such as calcium/calmodulin-dependent serine protein kinase (CASK) and MINT (Munc 18 interacting protein) to form a linkage with the presynaptic actin cytoskeleton (Dean and Dresbach, 2006; Sudhof, 2008). Deletion of CASK in mice causes synaptic abnormalities and results in a lethal phenotype (Atasoy et al., 2007). Postsynaptically, NLG1 promotes postsynaptic differentiation and maturation by recruiting PSD-95 (Irie et al., 1997) and NMDA receptors (Barrow et al., 2009; Chih et al., 2005; Nam and Chen, 2005) through interactions with an intracellular C-terminal PDZ binding domain. Many other synaptogenic cell adhesion molecules such as leucine-rich repeat transmembrane neuronal proteins (LRRTMs) (Linhoff et al., 2009), synaptic cell adhesion molecule (synCAM) (Biederer et al., 2002), and netrin G2 ligand (NGL2) (Kim et al., 2006) have also been identified to promote pre- and postsynaptic differentiation (**Figure 1.7**) (for review, see (Siddiqui et al., 2011)).

Other CAMs that do not induce pre- and postsynaptic differentiation are also important for synaptic protien recruitment, and dysfunction in these CAMs can interfere with proper synapse formation. For example, neuronal cadherin (N-cadherin) is found in both pre- and postsynaptic compartments, and the intracellular domain of N-cadherin dynamically interacts with α-, β-, δ- and p120 catenin (Brigidi and Bamji, 2011) to stabilize the synapse and modulate synaptic function. The localization of synaptic vesicles is found to be partly dependent on cadherin's association with β-catenin and the recruitment of the PDZ protein (Scribble) and the Rac/Cdc42 guanine nucleotide exchange factor (β-pix) at the nascent axon-dendrite contact (Bamji et al., 2003; Sun et al., 2009). The Bamji Lab revealed that β-pix increases actin polymerization at the

discrete sites, thus trapping synaptic vesicles as they translocate along the axon (Sun and Bamji, 2011). Functional-blockade and catenin-knockout studies show a clear dispersal and reduction in reserve pool of synaptic vesicles when cadherin-catenin interactions are perturbed (Bamji et al., 2003; Sun et al., 2009; Sun and Bamji, 2011).

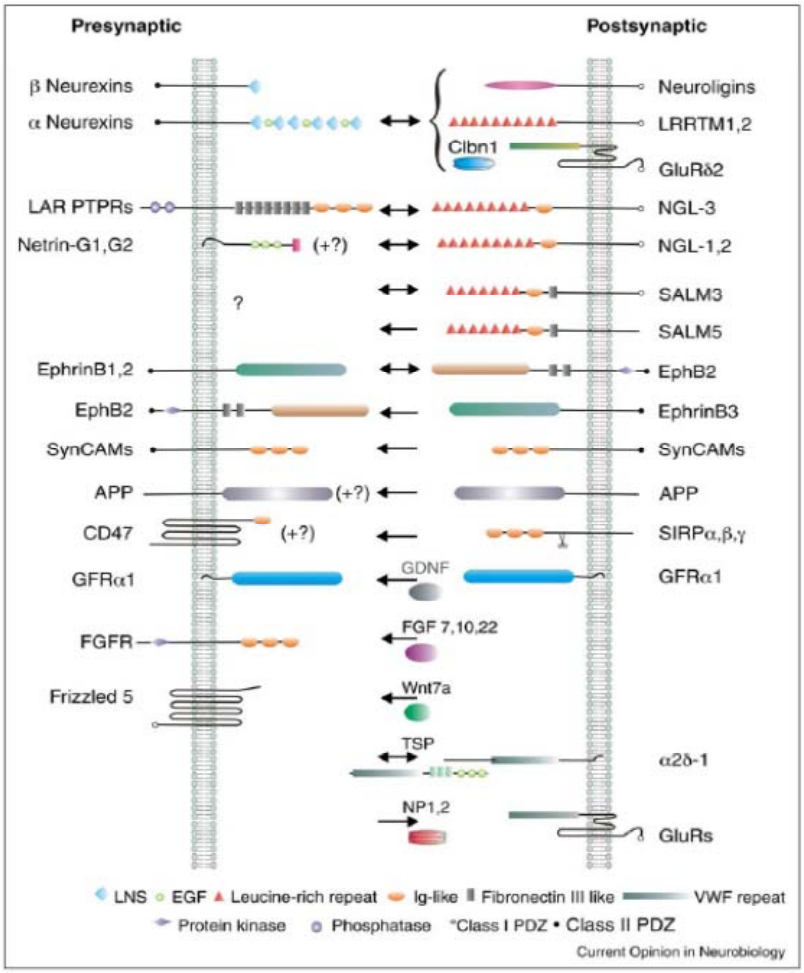

Figure 1.7 Cell Adhesion Molecules

An inventory of synaptogenic molecules, defined here as proteins that induce presynaptic (←) or postsynaptic (→) differentiation when present at axons or dendrites, respectively. Many of the adhesion complexes have bidirectional synaptogenic activity. The main receptors are also shown for the secreted synaptogenic factors. PDZ domain binding sites and common protein domains are indicated. *Reproduced with permission from (Siddiqui and Craig, 2011)*

1.3.2. Synapse maturation

Initial nascent synapse formation is followed by a process of maturation. During this maturation phase, a stepwise accumulation or shift in expression of neurotransmitter receptors occurs in order to make immature synapses functional and stronger. NMDARs are the first glutamatergic receptors recruited to nascent synaptic sites, and at this stage, these synapses are generally referred to as “silent synapses”, characterized electrophysiologically by the presence of NMDA, but not AMPA receptor currents. Over the maturation process, AMPA receptors are trafficked into synapses in an activity-dependent manner (Bredt and Nicoll, 2003; Bresler et al., 2004; Nam and Chen, 2005; Washbourne et al., 2002). Activation of AMPARs causes local depolarization that removes Mg^{2+} ions from blocking the pore of NMDARs. Activation of NMDARs allows calcium entry that triggers downstream signaling cascades, promoting more AMPAR insertion into synapses to produce mature, “AMPAfied’ synapses (Isaac et al., 1997; Liao et al., 1995; Wu et al., 1996). Delivery of AMPARs to synapses is regulated by a number of scaffolding proteins, including protein kinase C-interacting protein (PICK) (Daw et al., 2000; Perez et al., 2001), glutamate receptor binding protein (GRIP) (Dong et al., 1997; Osten et al., 2000; Srivastava et al., 1998), and the adaptor protein, Stargazin (Bredt and Nicoll, 2003; Chen et al., 2000; Dakoji et al., 2003; Tomita et al., 2004). In addition to the enhancement of AMPAR neurotransmission, synapse maturation is also associated with a change in subunit composition of NMDARs. NMDARs are tetramers of a combination of subunits. All NMDARs contain NR1 subunits along with NR2 or NR3 subunits. During development, immature synapses contain mainly NR2B subunits, which have slower decay kinetics and therefore larger calcium conductance. As neurons mature, NR2B subunits are gradually replaced with NR2A

subunits that have more rapid decay kinetics, which produce shorter duration of calcium currents (Williams et al., 1993). In summary, during synapse maturation, addition of AMPARs to immature synapses enhances synaptic transmission efficacy while changes in NMDAR subunit composition confer more restricted calcium influx.

A developmental shift in glutamate receptor function in dendrite growth has also been reported in the developing brain of *Xenopus* tadpoles. In the optic tectum, immature tectal neurons with small dendritic arbors express predominantly NMDAR without AMPAR and a majority of the retinotectal synapses at this stage are “silent” synapses (Wu et al., 1996). As tectal neurons grow, AMPAR are incorporated into maturing glutamatergic synapses (Wu et al., 1996). Interfering with the maturation process has profound effects on dendrite growth. Genetic manipulation of individual neurons by expressing peptides corresponding to the cytoplasmic tail of AMPARs alters growth to produce long, sparsely branched dendritic arbors (Haas et al., 2006). Expressing the cytoplasmic tail of AMPARs decreases the amplitude without affecting the frequency of spontaneous excitatory synaptic input, suggesting the peptides block synapse maturation by prohibiting AMPAR to be incorporated into nascent synapses (Haas et al., 2006; Shi et al., 2001). The contributions of the NMDAR subunits NR2A and NR2B on the morphological development of tectal neurons have also been examined. Edwald and colleagues manipulated synaptic NMDAR composition in immature tectal neurons by exogenous expression or endogenous knockdown of different NMDAR subunits. They found that NR2A and NR2B subunits have overlapping functions on dendrite growth, in which knockdown of either subunit decreases branch clustering and stabilization (Ewald et al., 2008). Knocking down either NR2A or NR2B units also blocked visual stimulation-induced increases in dendritic arbor growth. The

role of NR2B in dendrite morphology has also been examined in rodents. In 2009, the Luo lab used the mosaic analysis with double markers (MADM) technique to generate transgenic mice with single neuron knockout of the NR2B subunit. They analyzed two types of neuron in the barrel cortex, dentate gyrus granule cells (dGCs) and barrel cortex layer 4 spiny stellate cells (bSCs), and found that while these neurons have similar dendritic growth rates and arbor size as control neurons, mutant neurons have abnormal dendritic patterning (Espinosa et al., 2009). Normal bSCs locate in the barrel wall and project dendrites to one single barrel and receive sensory information primarily from a single whisker (Inan and Crair, 2007). However, the NR2B knockout cells fail to restrict the growth to only the primary barrel and extend branches to multiple barrels (Espinosa et al., 2009). These results suggest that the developmental shift in glutamate receptor function is important for activity-dependent dendritic remodelling.

1.3.3. Synapse elimination

Synapse elimination is the final stage of synaptogenesis where inappropriate synapses are pruned via activity-dependent competition. Mounting evidence suggests that postsynaptic neurons initially receive imprecise inputs from a wide range of axons and these connections are refined and sharpened as the neural circuits mature (Sakaguchi and Murphey, 1985). In the optic tectum, RGC axons initially branch extensively across a relatively broad region, resulting in tectal dendrites receiving inputs from RGCs spanning the retina. Over maturation, RGC axonal terminal arbors are pared back, and divergent inputs to individual tectal neurons are reduced (Ruthazer et al., 2003; Ruthazer et al., 2006). Recent work from the Cline Lab using *in vivo* two-photon imaging combined with serial section EM-based 3D reconstruction of tectal neurons has

also demonstrated a prominent role of synapse elimination in experiment-dependent circuit refinement in the *Xenopus* optic tectum (Li et al., 2011). They reported that newly extended dendrites from growing neurons form connections with multiple presynaptic axonal boutons, resulting in a high density of immature synapses during early development. As neurons mature, dendritic branch stabilization is correlated with the transition to sparser but more mature synaptic contacts. Taken together with maturational restriction of axonal terminal arborization, these results suggest that tectal neurons progress from exuberant innervations forming immature synapse from widely divergent RGC axons to fewer, but more mature synapses from a restricted subset of appropriate RGCs (Li et al., 2011).

Efforts have been made to dissect the molecular mechanisms involved in activity-dependent synapse elimination. A potential protein that regulates the ability of CNS neurons to eliminate synapses is the transcriptional factors of the myocyte enhancer factors 2 (MEF2) family. In young hippocampal neurons, knockdown of MEF2A and MEF2D dramatically enhances synapse number, whereas over-expressing MEF2A and MEF2D decreases synapse number (Flavell et al., 2006), suggesting MEF2 negatively regulates synapse number. It is possible that MEF2 directly regulates the process of synapse elimination, thus increasing MEF2 functions results in more synapses eliminated and vice versa. However, time-lapse imaging will be essential to confirm whether MEF2 causes elimination of existing synapses or inhibits new synapse formation. Another emerging family of molecules that is thought to regulate activity-dependent synapse elimination is the immune-related proteins, such as C1q of the classical complement cascade (Stevens et al., 2007) and MHCI molecules (Glynn et al., 2011; Goddard et al., 2007; Huh et al., 2000). C1q is the initiating protein of the classical

complement cascade and plays a role in the immune system to eliminate dead cells, debris or pathogens. Interestingly, C1q is highly expressed in developing RGC neurons at developmental stages spanning synaptic pruning. Mice deficient in C1q and C3 have deficits in eye-specific segregation and elimination of excess synapses on dLGN neurons (Stevens et al., 2007). MHC1 has also been reported to be important in retinogeniculate refinement. Retinal projections to the LGN fail to refine completely in mice lacking MHC1 subunits H2-Kb and H2-Db. These mice also have enhanced ocular dominance plasticity but with large mismatch of the ipsilateral projections, reflecting the presence of a large pool of inappropriate connections (Datwani et al., 2009). The McAllister group has also recently demonstrated that MHCI negatively regulates the density and function of cortical synapses during the early stage of development. Manipulations that alter surface levels of MHCI in neurons resulted in increased excitatory synapse density (Glynn et al., 2011).

1.4. Long-Term Potentiation and Depression

Long-term potentiation (LTP) and depression (LTD) are forms of synaptic plasticity characterized by a persistent increase or decrease of excitatory synaptic transmission, respectively (Malenka and Bear, 2004). Since this phenomenon is believed to be a physiological substrate of learning and memory in the mature brain, molecular mechanisms underlying these processes have been extensively investigated over the past two decades.

1.4.1. Molecular mechanisms underlying LTP

Long-lasting LTP is typically divided into two phases i) early-phase LTP (E-LTP), from 30 min to 2-3 hr following induction mediated by the persistent activation of protein kinases , and ii) late-phase LTP (L-LTP), which can persist for hours to days and is dependent on gene expression (Malenka and Bear, 2004). One of the most extensively studied forms of synaptic plasticity is the NMDAR-dependent LTP of glutamatergic synapses at CA3-CA1 region of the hippocampus (Bliss and Collingridge, 1993). LTP is induced by electrical stimulation of the Schaffer collaterals, axons from CA3 pyramidal cells, and recorded by electrodes in the dendritic or somatic layers of CA1 pyramidal neurons (Bliss and Collingridge, 1993; Rose and Dunwiddie, 1986). Delivery of high-frequency stimulation (HFS) or theta burst patterned stimulation (TBS) evokes successive excitatory postsynaptic potentials (EPSPs) and results in accumulation of depolarization that removes Mg^{2+} ions from blocking the pore of NMDARs at postsynaptic CA1 synapses (Nowak et al., 1984). NMDAR activation allows Ca^{2+} influx that initiates signaling cascades necessary for triggering LTP induction. Ca^{2+} ions bind to calmodulin to activate Ca2+/calmodulin-dependent kinase II (CaMKII) and adenylate cyclase (AC) for production of cAMP (Malenka et al., 1989; Malinow et al., 1989). CaMKII is a protein kinase that is highly enriched in the PSD, and its activation is critical for the expression of E-LTP. Loss-of-function of CaMKII results in blockade of LTP induction, and over-expressing constitutively active CaMKII enhances basal synaptic transmission and occludes LTP induction (Lledo et al., 1995; Pettit et al., 1994). Activated CaMKII directly phosphorylates AMPAR subunits to increase channel conductance, and promotes the delivery of AMPARs from intracellular stores to synapses resulting in increased AMPAR number at the synapse (**Figure 1.8**) (Derkach

et al., 1999; Shi et al., 2001). Together, these changes result in enhanced postsynaptic responses to presynaptic innervations.

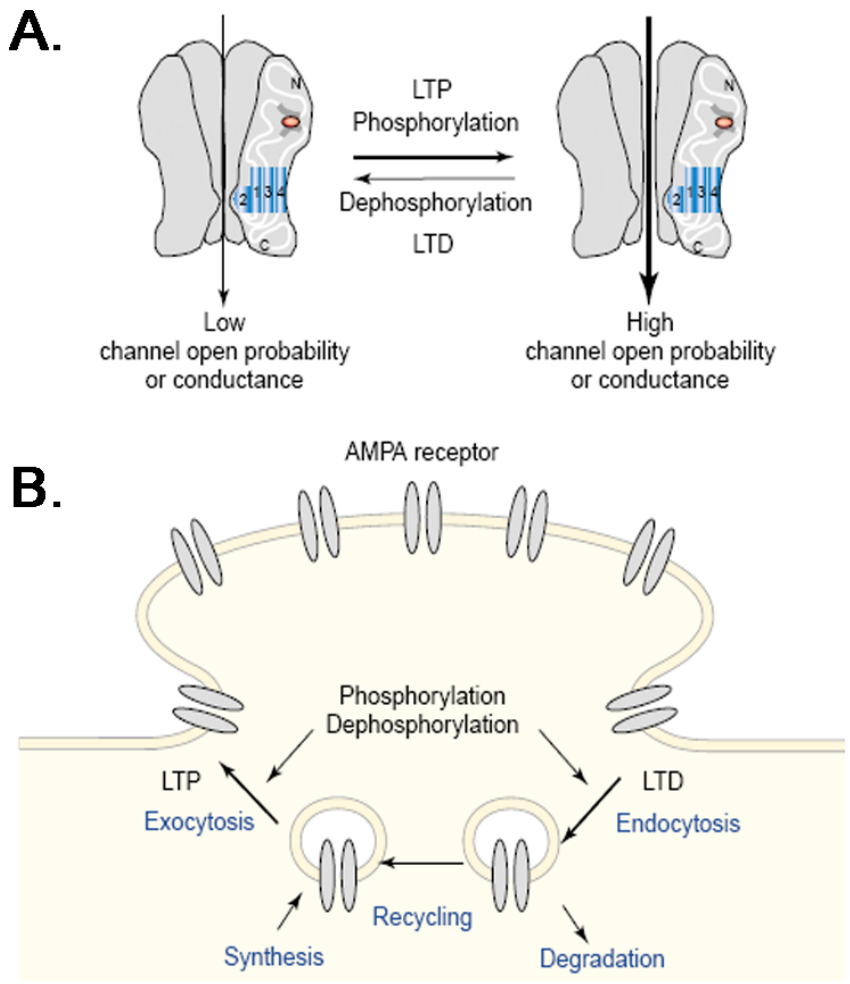

Figure 1.8 Dynamic Regulation of AMPA-receptor Signaling in Synaptic Plasticity

(A) AMPA receptor function can be regulated by the direct phosphorylation of receptor subunits, which, in turn, regulates the ion channel properties of the receptor. Phosphorylation of Ser831 and Ser845 during LTP potentiates ion-channel function, and dephosphorylation during LTD reduces channel function. **(B)** AMPA receptor signaling can also be modulated by dynamic regulation of the levels of receptors at the synaptic surface. Synaptic trafficking of the receptors is regulated by many AMPA-receptor-associated proteins. The association of the receptor with these proteins can be dynamically regulated by phosphorylation. Induction of LTP increases the levels of synaptic AMPA receptors, whereas LTD decreases synaptic AMPA receptor levels.

Regulation of the density of AMPA receptors in the synaptic plasma membrane might occur at several steps along the membrane trafficking pathway, including the insertion and endocytosis of the receptors, sorting of the receptors into recycling versus degradation pathways, and stabilization of the receptors in the synaptic plasma membrane and intracellular pools. Recent studies have shown that several of these processes can be regulated by protein phosphorylation of the receptor subunits and the interaction of AMPA receptor subunits with trafficking proteins.
Reprinted with permission from (Song and Huganir, 2002)

While CaMKII and AMPARs are critical for the expression of E-LTP, what mechanisms are responsible in maintaining this increased synaptic strength for hours or days? Pharmacological studies using protein-synthesis inhibitors, with varying modes of actions, showed that blocking protein synthesis inhibits LTP persistence without affecting induction, suggesting L-LTP requires gene transcription and protein synthesis (Abraham and Williams, 2003; Pittenger and Kandel, 2003). Proteins such as CaMKIV, protein kinase A (PKA), mitogen-activated protein kinase (MAPK), and their convergent downstream transcription factor CREB (cAMP-response element binding protein) have been identified as important contributors for maintaining the persistent increased response of synaptic transmission (Abel et al., 1997; Abraham and Williams, 2003; Pittenger and Kandel, 2003). CREB is rapidly phosphorylated following LTP induction and it binds to cAMP-dependent response element (CRE) to stimulate the expression of transcriptionally linked genes. Knocking down CREB impairs L-LTP similar to inhibitors that block protein synthesis, suggesting that CREB and the proteins it regulates contribute to the stabilization of LTP (Silva et al., 1998). Another recently identified protein implicated in LTP maintenance is the brain-specific, atypical PKC isoform, protein kinase Mzeta (PKMζ). PKMζ is a second messenger-independent kinase, consisting of the independent catalytic domain of PKC lacking the traditional autoinhibitory domain. Therefore, once expressed, it is persistently active during the late phase of LTP (Osten et al., 1996a; Osten et al., 1996b). LTP induction increases new

PKMζ synthesis, and PKMζ activity has been implicated in promoting trafficking of AMPARs containing GluR2 subunits to synapses. This increases the number of postsynaptic AMPARs to increase synaptic strength (Ling et al., 2006). Application of specific cell permeable PKMζ peptide inhibitors reverses established LTP both in hippocampal slices and *in vivo* (Ling et al., 2002).

The influence of LTP induction on sensory information processing and learning and memory has also been demonstrated *in vivo*. In the 1980s, Morris and colleagues found that infusion of AP5, which blocks LTP induction, into hippocampus impairs spatial learning in rats (Morris, 1986). In the adult rat visual cortex, induction of NMDAR-dependent LTP in the dorsal lateral geniculate nucleus using theta burst stimulation significantly enhances visual-evoked responses (Heynen and Bear, 2001). However, saturating the induction of LTP occludes learning in the hippocampus. Rats were implanted with a multielectrode stimulating array and were repeatedly stimulated with tetanus pulse to induce potentiation. Spatial learning was later found to be disturbed in these animals compared to normal animals that were capable ofcdc further potentiation (Moser et al., 1998).

1.4.2. Molecular mechanisms underlying LTD

Similar to LTP, LTD is a phenomenon that causes a long-term decrease in synaptic strength, and most forms of LTD are also NMDAR-dependent. LTD can be induced by low-frequency stimulation (Christie and Abraham, 1992; Dudek and Bear, 1992; Mulkey and Malenka, 1992). LTD can be also divided into two stages – an early phase (E-LTD) and a late phase (L-LTD). Studies have reported that L-LTD only requires mRNA translation but not gene transcription to maintain the response; however,

little is known about the proteins that are required to uphold the stable expression of LTD. On the other hand, induction of E-LTD by low frequency stimulation activates NMDARs to allow low-level of Ca^{2+} entry into postsynaptic neurons (Collingridge et al., 2010; Mulkey and Malenka, 1992). Following NMDAR activation, calmodulin binds to Ca^{2+} ions and activates protein phosphatase 2B (PP2B; also known as calcineurin), which leads to the activation of protein phosphatase 1 (PP1) (Collingridge et al., 2010; Mulkey et al., 1994; Mulkey et al., 1993). Activation of calcineurin-mediated signaling cascades results in dephoshorylaton of AMPAR GluR1 subunits, thereby decreasing AMPAR open channel probability and inducing the rapid internalization of AMPARs from the synapse (Ehlers, 2000; Malenka and Bear, 2004). Moreover, LTD is thought to be correlated with dephosphorylation of postsynaptic substrates such as PKC or PKA (Hrabetova and Sacktor, 2001; Kameyama et al., 1998; Malenka and Bear, 2004; van Dam et al., 2002). Dephosphorylation of PKA inhibits its activity and causes it to dissociate from the intracellular anchoring proteins (AKAP), resulting in a decrease in synaptic transmission (Kameyama et al., 1998). Recent studies from the Sheng Lab have also reported a non-apoptotic role of the mitochondrial pathway (caspases-9 and 3) in LTD, in which NMDAR stimulation transiently activates caspase-3 and induces cleavage of Akt1 kinase, which results in GluR2 internalization and synaptic weakening (Li et al., 2010).

1.4.3. LTP/LTD and structural plasticity

Activity-dependent remodelling of neuronal connections is important for early nervous system development and may also underlie learning and memory functions in the mature brain. In the established neural circuits, most excitatory synapses reside on

dendritic spines. A mature spine has a mushroom-shaped structure, consisting of a spherical head with a thin neck (Engert and Bonhoeffer, 1999; Ziv and Smith, 1996). The unique structural features of dendritic spines serve to compartmentalize calcium and signalling molecules and to electrically modulate synaptic response properties (Bloodgood and Sabatini, 2007; Majewska et al., 2000; Sabatini et al., 2001; Yuste and Denk, 1995). The morphology of dendritic spines is associated with synaptic plasticity. At the Schaffer collateral synapses in the hippocampus, induction of LTP by repetitive uncaging of caged glutamate (Lee et al., 2010; Matsuzaki et al., 2004), high frequency stimulation (Matsuzaki et al., 2004), and theta burst stimulation (Yang et al., 2008) have been shown to dramatically increase the spine head size by two to five-fold. The enlargement of spine size following LTP is attributed by many factors, including reorganization of the actin cytoskeleton (Carlisle and Kennedy, 2005; Cingolani and Goda, 2008) and insertion of AMPARs into synapses (Derkach et al., 2007; Kessels and Malinow, 2009). In contrast, the mechanisms that underlie spine shrinkage and LTD are less known (Hsieh et al., 2006; Okamoto et al., 2004; Zhou et al., 2004). It has been reported that internalization of AMAPRs following LTD is sufficient to induce spine shrinkage (Hsieh et al., 2006); however, a later study suggested the two processes are independent from each other (Wang et al., 2007). Recent advances in imaging techniques have helped us to further understand the dynamic process underlie synaptic plasticity and spine morphology. The Yasuda lab has developed two-photon fluorescence lifetime imaging microscopy (2pFLIM) and new FRET sensors to facilitate the visualization of signalling activities triggered by Ca^{2+} in single dendritic spines following LTP induction (Murakoshi et al., 2008). The Rho family of GTPases such as Rho, Cdc42, and Rac are known to regulate actin cytoskeleton in neurons for neuronal migration (Ridley, 2001), polarity (Iden and Collard, 2008), and neuronal and spine

morphology (Carlisle and Kennedy, 2005; Luo, 2000). The general belief is that Rho activation causes spine shrinkage and retraction whereas Cdc42 and Rac activation promotes actin polymerization to increases spine size (Carlisle and Kennedy, 2005). Combining FRET-FLIM sensors for RhoA and Cdc42 with two-photon glutamate uncaging on single spine to induce LTP, Murakoshi *et al*. have found unexpectedly that the activity of both RhoA and Cdc42 increased rapidly within a minute following LTP induction, and the activation is sustained more than 30 min (Murakoshi et al., 2011). However, the spatial patterns of RhoA and Cdc42 are different, in which RhoA rapidly diffused out from the stimulated spines into the shaft, and Cdc42 activity was restricted in the stimulated spines. Moreover, inhibition of RhoA activity preferentially inhibited the initial phase of spine enlargement, whereas inhibition of Cdc42 affected the maintenance of spine enlargement. Therefore, these results suggest that the simultaneous but sustained activation of RhoA and Cdc42 are important to continuously regulate actin polymerization during LTP; however, the spatial pattern following the activation of different Rho GTPases are critical for regulating spine morphology at different phases of LTP (Murakoshi et al., 2011).

Developmental activity-dependent dendritogenesis appears to share molecular mechanisms with synapse plasticity underlying learning and memory in mature brain. Blocking endogenous CaMKII activity either pharmacologically or by inhibitory peptides induces excessive dendritic arbor growth (Wu and Cline, 1998). In addition, the constitutively active version of PKC, protein kinase Mζ (PKMζ), implicated in L-LTP (Ling et al., 2002), also regulates developmental dendritogenesis (Liu et al., 2009). Inhibiting PKMζ activity by delivering a PKMζ inhibitor peptide promotes dendrite outgrowth. Strikingly, over-expression of CaMKII or PKMζ reduces thresholds for synapse

maturation, producing precocious synapse maturation and decreased growth plasticity by inducing morphological hyper-stabilizing (Liu et al., 2009; Wu and Cline, 1998). In the *Xenopus* tectum, Rho GTPase activity is also activity-dependent regulated. Electrical stimulation at the optic nerve or patterned visual stimuli upregulates endogenous RhoA activity while it decreases the activity of Rac and Cdc42 in the optic tectum (Li et al., 2002; Sin et al., 2002). Expressing constitutively active RhoA in individual tectal neurons blocks visual stimulation-induced dendritic arbour growth, suggesting the decrease in RhoA activity is important for promoting dendritic remodelling during visual stimulation (Sin et al., 2002). Lastly, a relationship between mechanisms underlying LTD in mature brain and developmental dendrite growth has also been established. Inhibition of calcineurin (CaN), a calcium/calmodulin-dependent serine/threonine phosphatase required for expression of NMDAR-dependent LTD results in increased dendritic arbor complexity (Schwartz et al., 2009).

1.5. Metaplasticity

Metaplasticity, the 'plasticity of plasticity', refers to the intrinsic homeostatic mechanisms that modulate neuronal susceptibility and response to plasticity-inducing stimuli based on the recent history of activity. This higher order form of synaptic plasticity is thought to modulate synaptic strength and neuronal firing to avoid reaching maximal levels, thereby maintaining values within a functional dynamic range capable of responding plastically to further stimuli (Abraham, 2008). Various neurotransmitters such as norepinephrine, dopamine, serotonin, and acetylcholine have all been shown to regulate the degree of LTP and LTD expression (Skolnick, 2002). However, one key feature that distinguishes metaplasticity from other forms of plasticity modulation is that

priming stimulus-induced changes in neuronal functions must persist even after the priming stimulus is terminated. This differs from the conventional modulation of plasticity, in which modulation often occurs in conjunction with the induction of plasticity (**Figure 1.9**). Metaplasticity also does not alter synaptic strength by itself, but instead changes the state of responsivity of a neuron to generate the subsequent LTP or LTD (Abraham, 2008; Abraham et al., 2001).

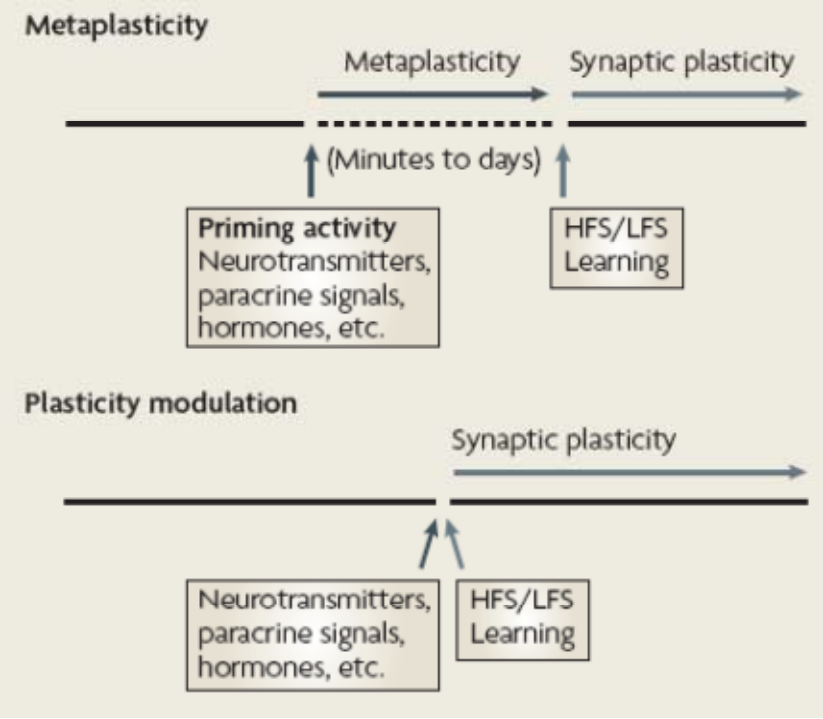

Figure 1.9 Metaplasticity and Plasticity Modulation

The standard paradigm for studying metaplasticity is to have an episode of priming activity at one point in time and then a subsequent plasticity-inducing event, such as low frequency stimulation (LFS), high-frequency stimulation (HFS) or learning, which evokes synaptic plasticity such as long-term potentiation (LTP) or long-term depression (LTD). The priming signal can entail electrical stimulation of neural activity, pharmacological activation of specific transmitter receptors, or behavioral events that might cause hormone release in addition to neural activity. An essential aspect of this protocol is that there must be a change in neural function as a result of the priming that persists after the termination or washout of the priming stimulus and that alters the response to a subsequent plasticity-inducing event (**see figure, top**). This distinguishes metaplasticity from

conventional modulation of plasticity, whereby the modulation occurs in conjunction with the induction of plasticity (see figure, bottom). There is no agreed criterion for the degree of persistence that is required to meet the definition of metaplasticity, but commonly studied effects have ranged from minutes to many days. The study of metaplasticity is facilitated when the priming stimulation does not overtly alter the strength of synaptic transmission, but instead changes only the state of readiness of synapses to generate LTP or LTD later on. Protocols that induce LTP can also trigger metaplastic mechanisms that inhibit further LTP, and LFS can evoke a metaplastic lowering of the LTD threshold early in the stimulus train that is necessary for LTD induction. This can complicate the interpretation of molecular correlates of plasticity, such as gene expression and protein synthesis, because in principle these events might be critical for synaptic plasticity, metaplasticity or both. *Reprinted with permission from (Abraham, 2008)*

1.5.1. The Bienenstock, Cooper and Munro (BCM) computational model of synaptic plasticity

The Bienenstock, Cooper and Monroe (BCM) theory is a model that was first proposed to account for experience-dependent synaptic plasticity of visual cortex synapses during development (Bienenstock et al., 1982), and this model has been soon adapted for explaining the physiological changes underlying metaplasticity. The model features two main ideas, illustrated in **Figure 1.10**. First, the model proposes that each synapse or neuron possesses a dynamic response to plasticity-inducing input, ranging from no change to depression or potentiation in synaptic strength or firing rate. The y-axis in this plot represents the plasticity outcomes, with positive values for potentiation and negative values for depression. The x-axis represents the strength of the plasticity inducing stimulus. The plot demonstrates that very low levels of stimulus elicit no plasticity, and slightly higher levels induce lasting depression. As the stimulus activity increases, neuronal response transitions from depression to no change at the modification threshold (θm) and then to lasting potentiation. The BCM profile has

demonstrated that the same activity-dependent processes may underlie both LTP and LTD, depending on the level of their activation.

The second feature of the BCM model is that the modification threshold, θm is not a fixed value, and it can shift based on the neuron's recent history of activity. This shift of θm alters the response to plasticity-inducing stimuli, and is termed 'metaplasticity' or the activity-dependent 'plasticity of plasticity' (Abraham, 2008). For instance, if a neuron's activity was maintained at a low level for a long period of time, θm will shift to the left, making LTP easier to obtain (**Figure 1.10**). Such phenomenon has been previously demonstrated in the mouse visual cortex, where binocular visual deprivation in developing animals results in the shift of the threshold to the left, thereby enhances LTP induction (Abraham et al., 2001; Chen and Bear, 2007; Kirkwood et al., 1996; Philpot et al., 2007; Philpot et al., 2003). Hence, it has been proposed that metaplasticity may function to prevent synaptic strength and firing rates from reaching plateau levels. By maintaining values within a dynamic physiological range, neurons can continue to respond plastically to future inputs.

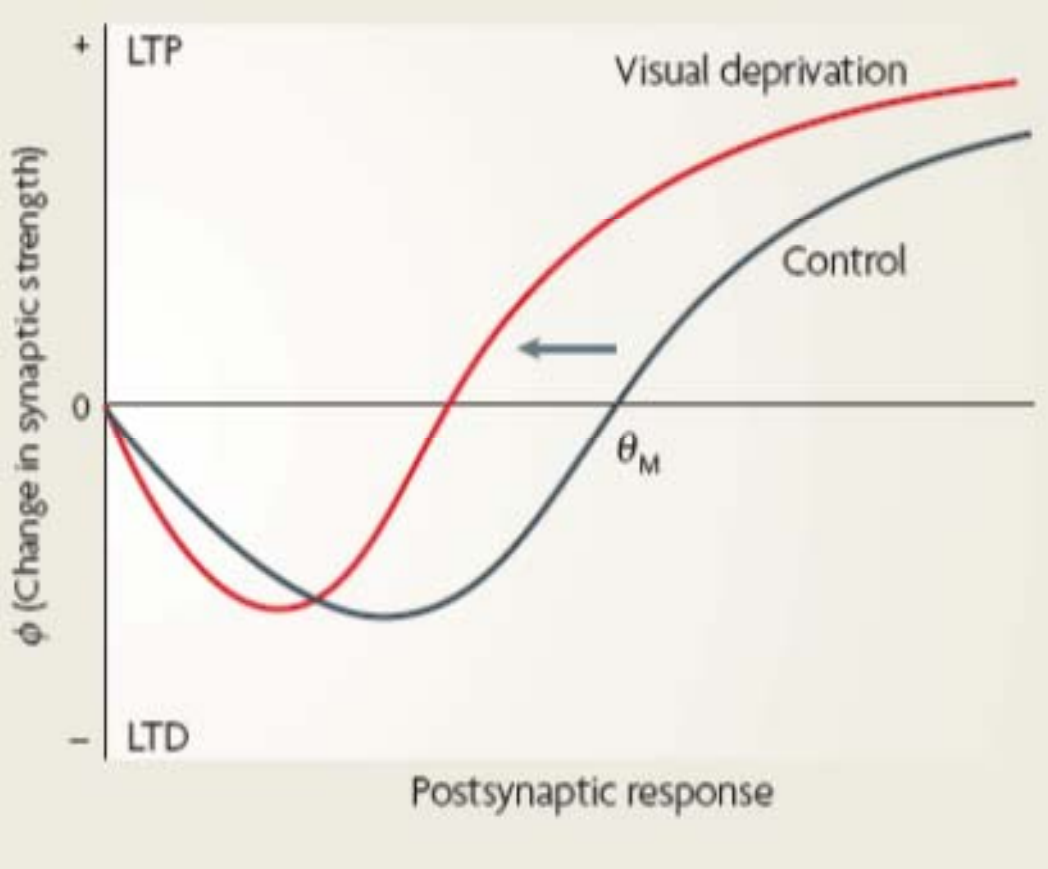

Figure 1.10 The Bienenstock, Cooper and Munro (BCM) Model

The Bienenstock, Cooper and Munro (BCM) computational model of synaptic plasticity was developed to account for experience-dependent plasticity in the kitten visual cortex. Subsequently it has been adapted to account for experience-dependent plasticity in the adult rat barrel cortex and long-term potentiation (LTP) and metaplasticity in the adult rat dentate gyrus. The model has two principal features. First, it describes the extent of LTP or LTD as a function (φ) of the degree of postsynaptic cell firing during afferent activation. If afferents are active during times of low postsynaptic activity, those inputs are depressed. Conversely, if afferents are active during high postsynaptic activity, those inputs are potentiated. To preserve stability in the network and prevent runaway potentiation or depression, the model incorporates a feature that varies the crossover point between LTD and LTP on the φ function, termed the modification threshold (θM), with the time-averaged level of postsynaptic firing. Thus, if firing levels are maintained at a high level, the modification threshold shifts to the right, making LTP harder to obtain and LTD easier to obtain. *Adapted with permission from (Abraham, 2008)*

1.5.2. Molecular mechanisms underlying metaplasticity

To date, the molecular mechanisms underlying the metaplastic shift in plasticity thresholds remains poorly understood. Interestingly, while activation of NMDARs has been well implicated in LTP and LTD induction, it is also required for inducing metaplasticity. Priming brain slice with NMDA for 60-90 minutes prior to HFS inhibits LTP (Huang et al., 1992), and the effects slowly wears down with time. However, increasing the intensity of HFS can recover LTP induction, suggesting that NMDA priming only increases the threshold of LTP rather than blocks it (Huang et al., 1992). One important thing to notice is that NMDAR priming does not induce any detectable changes in basal synaptic transmission; however, it changes the state of readiness of the synapse to potentiate or depress later on (Abraham and Huggett, 1997; Fujii et al., 1996; Huang et al., 1992).

The molecular cascades downstream of NMDARs, however remain largely unknown. One of the proposed effecters responsible for mediating the shift in plasticity response is due to the change in the ratio of NMDAR subunits, NR2A/NR2B during the priming (Philpot et al., 2007; Philpot et al., 2003). These NMDAR subunits are thought to be good candidates for regulating plasticity thresholds because NR2A and NR2B each contribute distinct biophysical properties that alter calcium influx (Paoletti and Neyton, 2007). NR2B-containing NMDARs have longer single-channel open channel duration, resulting in longer synaptic currents and increased calcium influx than NR2A-containing receptors (Laurie and Seeburg, 1994; Monyer et al., 1992). Deletion of NR2A in knockout mice abrogates the effects of visual experience-induced metaplasticity in visual cortex (Philpot et al., 2007). Hence, the model of synaptic plasticity thresholds regulated by NMDAR subunits posits that synapses with a low NR2A/NR2B ratio allow more Ca^{2+}

to enter into postsynaptic sites which is more likely to activate CaMKII and trigger LTP induction. Conversely, when NR2A-containing receptors dominate, Ca^{2+} entry is reduced, and a stronger presynaptic activation is required to activate sufficient CaMKII to trigger LTP. A greater range of weaker stimulation will now lead to activation of calcineurin (PP2B) and induction of LTD (Yashiro and Philpot, 2008). Although changes in NR2A/NR2B ratios have been extensively studied at developmental stages, they have also been reported in mature brain, supporting their roles in mediating metaplastic shifts in plasticity thresholds at all stages. An experience-dependent reduction in NR2A/B ratio in the visual cortex can be induced in adult rodents by visual deprivation for 10 days, shown by electrophysiological recordings (He et al., 2006; Yashiro et al., 2005), and by single cell RT-PCR analysis of mRNA (Tropea et al., 2006).

1.6. Experience-Driven Plasticity and Metaplasticity in The Developing Brain

1.6.1. Visual-driven synaptic plasticity

The *Xenopus laevis* tadpole has proven to be a powerful model system for investigating development of central neural circuits. The retinotectal system offers an accessible and isolatable pre- and postsynaptic population for electrophysiological studies of developmental studies of LTP and LTD. Seminal work on synapse plasticity in *Xenopus* has been carried out by Mu-Ming Poo's Lab. They first demonstrated that similar to the induction of LTP and LTD in the CA1 region of the hippocampus, both LTP and LTD can be induced at retinotectal synapses by repetitive electrical stimulation of

RGC axons, in a NMDAR-dependent manner (Zhang et al., 1998). They also showed natural visual sensory stimuli can also induce long-term synaptic modification. By applying repetitive dimming light stimuli (consisting 90, 50 msec dimming stimuli at 0.3 Hz) to the contralateral eye of the *Xenopus* tadpole and performing *in vivo* perforated whole-cell recording at the optic tectum, Zhang *et al.* demonstrated that visual stimulation, which elicits bursting activity similar to TBS electrical stimulation (Tao et al., 2001), induces a persistent enhancement in glutamatergic transmission but not GABAergic or glycinergic transmission on tectal cells (Zhang et al., 2000). In their later studies, Poo and colleagues expanded the natural visual stimulation paradigm to include moving bar stimulus and showed that tectal neurons can also be trained to become direction-sensitive to the moving bar in a particular trained direction (Engert et al., 2002; Zhou et al., 2003). These experiments demonstrate that natural sensory experience induces long-lasting synaptic modifications *in vivo* in the developing central neural circuit.

1.6.2. Visual-driven functional plasticity and metaplasticity

The Haas lab has recently developed novel experimental paradigms for studying plasticity and metaplasticity in the intact and awake developing brain in response to visual stimuli. Building upon work from the Poo Lab, we have developed specific patterns of visual stimuli that shift visual-evoked tectal responses toward either potentiation or depression in an NMDAR-dependent manner (Dunfield and Haas, 2009). Tadpole brains are loaded with the calcium-sensitive dye Oregon Green BAPTA-1 (OGB-1) for *in vivo* two-photon calcium imaging in the unanesthetized tadpole to sample action potential-associated activity in 10s-100s of neurons, with single-neuron resolution

(Dunfield and Haas, 2010) (**Figure 1.11**). Calcium imaging differs from the electrophysiological perforated whole-cell recording by allowing simultaneous recording activity in large numbers of neurons. Using wide-field OFF and ON visual stimuli, Dunfield and Haas showed that specific visual training paradigms can induce lasting potentiation - *Spaced Training (ST)*, or depression - *Invariant Training (IN)*, of evoked responses to probing visual stimuli (Dunfield and Haas, 2009). This work also demonstrated that natural experience-driven plasticity in the developing brain is metaplastically regulated. Changing the brain neurons' history of firing alters their subsequent response to plasticity-inducing stimuli. For example, Dunfield found that presenting 1 hr of *White Noise (WN)* stimulation, consisting of randomly varying wide-field OFF/ON visual stimuli that enhances endogenous firing without inducing plasticity, shifts the outcome of ST-induced plasticity from potentiation to depression (Dunfield and Haas, 2009). These findings demonstrate a role for BCM metaplasticity in regulating experience-driven plasticity in the developing brain and provide a novel model system for identifying underlying molecular mechanisms.

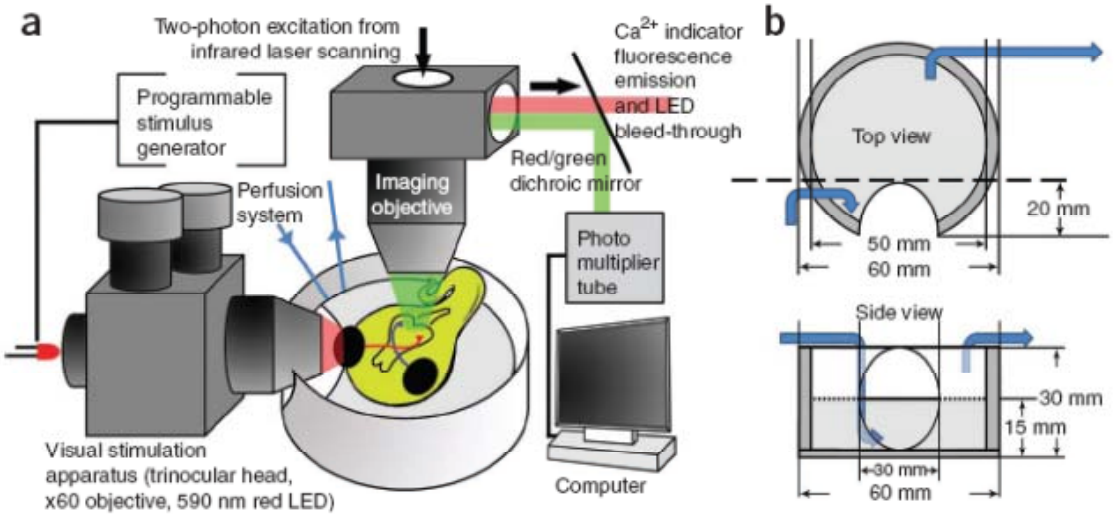

Figure 1.11 In vivo Calcium Imaging Setup in Xenopus tadpole

(**A**) A custom made imaging chamber is perfused with Steinberg's solution oxygenated at room temperature. Two photon microscopy is used to image ensemble neuronal activity with a green calcium indicator, whereas red light of varying contrasts is projected onto the tadpole's contralateral eye. (**B**) Schematic drawing of the imaging chamber (top) top view and (bottom) side view. Blue arrows indicate locations for fixation of perfusion tubes. Reprinted *with permission from (Dunfield and Haas, 2010)*

1.7. Research Aims and Hypothesis

1.7.1. Examining the role of the cell adhesion molecules, NRXs and NLGs in brain neuronal growth and function in vivo

The "synaptotropic hypothesis" of dendrite growth states that synapse formation stabilizes filopodia to prevent retraction and promotes their transition into longer and more persistent dendritic branches, culminating over time into increased complexity and size of the entire arbor. However, the role of trans-synaptic cell adhesion molecules that mediate the initial nascent contacts between growing axons and dendrites in regulating dynamic dendrite morphogenesis is unclear. Therefore, I propose to test whether ***NRX-NLG1 interactions play a critical role in directing normal dendritic arborization in the developing brain*.**

1.7.2. Determining the morphological correlates of physiological plasticity and metaplasticity in vivo.

While studies have demonstrated that visual experience can induce functional plasticity and regulate brain neuron dendritic arbor growth, direct evidence for a

relationship between functional and structural plasticity of dynamic neural circuit formation during early brain development is lacking. By employing the novel experimental paradigm to elicit potentiation, depression and metaplasticity that our laboratory has developed, I propose to ***examine the dynamic growth of individual brain neurons within the intact and awake developing brain before, during, and after the neuron is going through long-lasting plasticity induced by sensory experience***.

1.7.3. Deciphering the molecular mechanisms mediating functional and structural metaplasticity

Metaplasticity is a homeostatic mechanism that regulates synaptic, dendritic integration and neuronal firing to maintain afferent-evoked neuronal activity within useful dynamic ranges, and to avoid limits incapable of further plasticity. However, molecular mechanisms that trigger the metaplastic shift and determine a neuron's state of plasticity responsiveness are poorly understood. Identifying the proteins involved in regulating this process may offer important targets for novel therapeutics designed to modulate brain plasticity. Hence, I propose to ***investigate the molecular mechanisms underlying metaplasticity of natural sensory-evoked plasticity in the unanesthetized developing vertebrate brain.***

2. NRX-NLG CELL ADHESION COMPLEXES CONTRIBUTE TO SYNAPTOTROPIC DENDRITOGENESIS VIA GROWTH STABILIZATION MECHANISMS IN VIVO

Cell adhesion molecules are well characterized for mediating synapse initiation, specification, differentiation and maturation, yet little is understood of their contribution to directing dendritic arborization during early brain circuit formation. Using two-photon time-lapse imaging of growing neurons within intact and awake embryonic *Xenopus* brain, I examined roles of β-neurexin (NRX) and neuroligin-1 (NLG1) in dendritic arbor development. Employing novel methods of dynamic morphometrics for comprehensive 3D quantification of rapid dendritogenesis, I find initial trans-synaptic NRX-NLG1 adhesions confer transient morphologic stabilization independent of NMDA receptor activity, while persistent stabilization requires NMDA receptor-dependent synapse maturation. Disrupting NRX-NLG1 function destabilizes filopodia while reducing synaptic density and AMPA receptor mEPSC frequency. Altered dynamic growth culminates in reduced dendritic arbor complexity as neurons mature over days. These results expand the synaptotropic model of dendritogenesis to incorporate cell adhesion molecule-mediated morphological stabilization necessary for directing normal dendritic arbor

growth, and provide a potential morphological substrate for developmental cognitive impairment associated with cell adhesion molecule mutations

2.1. Specific Background

2.1.1. Neurexin and Neuroligin

Neuroligins (NLGs) are postsynaptic cell adhesion molecules that bind to presynaptic neurexins (NRXs) to form trans-synaptic complexes that induce pre- and postsynaptic differentiation (Graf et al., 2004; Ichtchenko et al., 1995; Scheiffele et al., 2000). NRX-NLG1 complexes promote postsynaptic differentiation and maturation by recruiting PSD-95 (Irie et al., 1997) and NMDA receptors (Barrow et al., 2009; Chih et al., 2005) through interactions with an intracellular C-terminal PDZ binding domain. Upon stimulation of glutamate, AMPARs are then recruited to PSD-95/NMDAR scaffolds (Nam and Chen, 2005). Blocking NRX-NLG1 interactions by application of a soluble fragment of NRX blocks the effects of NLG1 on synapse formation (Levinson et al., 2005), and expression of a dominant negative form of NLG1 lacking the PDZ-binding domain, preventing it from binding to PSD-95, also results in reduced clustering of postsynaptic proteins (Chih et al., 2005; Nam and Chen, 2005). These results confirm a specific role of NRX and NLG1 in the assembly of glutamatergic synapses.

Mice express four different neuroligin isoforms (NLG1-4), and they share ~60% identical amino acid sequence with each other. NLG1 has four variants, NLG1(-), NLG1A, NLG1B, and NLG1AB (Chih et al., 2006). The extracellular sequences of NLGs include a domain that is homologues with acetylcholinesterase, but is not functional due

to lack of the crucial residues in the active site. The ectodomain contains two sites (designated A and B) for insertion of short exons to form splice forms (**Fig. 2.1**) (Ichtchenko et al., 1995; Song et al., 1999; Sudhof, 2008). Recombinant NLG1B and NLG1AB are most expressed in glutamatergic synapses, whereas NLG1A is sparsely expressed in GABAergic synapses (Chih et al., 2006). NRXs, on the other hand, are even more diverse than NLGs. Mammalian NRXs are made from three genes, referred to as NRX1, 2, 3, and NRXs are expressed in two forms, a long α- (α-NRX) and a shorter β- form (β-NRX). NRXs can undergo extensive alternate splicing and generate thousands of isoforms (Boucard et al., 2005; Sudhof, 2008). Conceptually, these isoforms are believed to serve as a specific code of interactions at synapses. For example, the splice site 4 of NRX1β is a critical regulator for binding correct postsynaptic neuroligins (Boucard et al., 2005; Graf et al., 2006). It has been shown that NRX1β4(+) from axonal terminals efficiently binds to NLG1A to recruit GABAergic postsynaptic proteins, such as gephryin. In contrast, NRX1β4(-) binds to NLG1B and promotes glutamatergic postsynaptic differentiation by recruiting postsynaptic proteins, such as PSD95 (Boucard et al., 2005; Graf et al., 2006; Graf et al., 2004). The alternative splicing of NRX1 is also temporally and spatially controlled, in which neuronal activity can trigger a shift in NRX1 alternative splicing choice via calcium/calmodulin-dependent kinase IV signaling (Iijima and Scheiffele 2011).

In the past few years, generation of NRX and NLG knockout mice has helped us to further understand about the roles of NRXs and NLGs in synapse development. Mice with αNRX1, αNRX2, αNRX3 triple knockout, while leaving the three βNRX intact, leads to prenatal death due abnormalities in presynaptic Ca^{2+} channels (Missler et al., 2003). Detailed electrophysiological recordings showed that the neurotransmitter release that is

dependent on the N-type and P/Q-type Ca^{2+} channels is severely impaired in these knockout animals (Zhang et al., 2005). On the other hand, mice lacking NLG1, NLG2, and NLG3 also die shortly after birth due to respiratory failure, but interestingly, these mice exhibit normal density of synaptic contacts and spine morphology in the hippocampal and cortical neurons (Varoqueaux et al., 2006). However, while the synapse number is normal, there are marked functional defects in synaptic function. In some areas in the brain, the frequency of spontaneous inhibitory current was found to be reduced by ~90%, and the frequency of spontaneous excitatory transmission was reduced by ~75% (Varoqueaux et al., 2006). Mice with NLG1 or NLG2 knockout are viable, but they also demonstrate significant impairments in synaptic transmission, in which NLG1 knockout mice exhibit dysfunctions in NMDA receptor signaling, and NLG2 knockout mice has deficits in inhibitory synaptic transmission (Chubykin et al., 2007). One major discrepancy between *in vivo* gene-knockout studies and *in vitro* co-culture assays is that synaptic density does not change in the knockout animals. Hence, it is proposed that the major function of NLGs might be in the maturation of synaptic junctions, rather than the initial formation (Sudhof, 2008).

Genetic mutations of NLG family, *NLG-3* (a point mutation in arginine 451, Arg451→Cys451) and *NLG4* (a nonsense mutation at aspartate 396, D396X), have been identified in patients with Autism Spectrum Disorders (ASDs) (Jamain et al., 2003; Yan et al., 2005). ASDs are severe neurodevelopmental disorders that affect approximately 1 in every 150 children. All of the disorders encompassed by ASDs, including classical idiopathic autism, Asperger's syndrome, Rett's syndrome, and fragile-X mental retardation share impairments in social interactions, communication deficits, restricted patterns of interest, and repetitive behaviors. While the causes of ASDs are

enigmatic, the early age of onset and shared developmental deficits imply common errors in early brain development (Zoghbi, 2003). Hence, identifications of gene mutations in CAMs associated with familial ASDs were important breakthroughs in finding discrete origins of this disorder, as well as in clearly linking ASDs to disruption in early brain circuit development. In cultured neurons, expression of rat NLG3-R451C was found to induce partial retention of both exogenous and endogenous NLG proteins within the endoplasmic reticulum (Chih et al., 2004; Comoletti et al., 2004), thus in turn decreases the delivery of functional NLG3 to the cell surface. Mice with NLG3 point mutation (R451C mutant mice) showed impaired social interactions and enhanced learning abilities with increased inhibitory synaptic transmission but not excitatory synaptic transmission (Tabuchi et al., 2007). However, another group has reported that these R451C mutant mice only display minimal aberrant behavioral phenotypes (Chadman et al., 2008). Interestingly, different NLG mutant mice have also been shown with abnormal behaviors. Transgenic mice with enhanced expression or deletion of NLG2 display anxiety behaviors with repetitive jumping stereotypes (Blundell et al., 2009; Hines et al., 2008). Mice with enhanced expression of NLG2 show enlarged synaptic contact size, vesicle reserve pool, and enhanced frequency of miniature inhibitory synaptic currents (Hines et al., 2008), while the NLG2 KO mice have impairments in inhibitory synaptic function without altering the synapse number (Blundell et al., 2009). Hence, one proposed cellular mechanism underlying ASDs is that the ability of NLGs to regulate excitatory and inhibitory synapse formation is also important for maintaining the excitatory/inhibitory (E/I) ratio in the brain. Thus, ASD-associated mutations that result in altered NLG levels may disrupt the E/I balance and result in behavioral deficits (Hines et al., 2008; Levinson et al., 2005; Lise and El-Husseini, 2006).

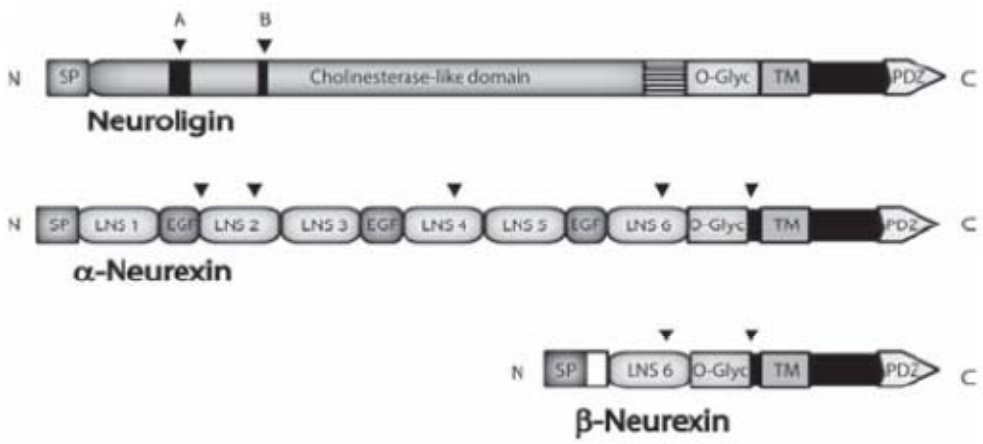

Figure 2.1 Structure of Neuroligin and Neurexin

Neuroligins are composed of a large N-terminal extracellular domain, followed by a single transmembrane region and a short cytoplasmic sequence containing a type I PDZ-recognition motif. The extracellular region of neuroligins is composed of a signal peptide (SP), followed by a cholinesterase-like domain, which mediates binding to neurexin LNS domains. The extracellular region of neuroligins contains two alternatively spliced sites (A and B), an oligomerization domain (hatched box) and a carbohydrate attachment region for O-linked glycosylation (O-Glyc). Neurexins are composed of an N-terminal extracellular sequence containing a signal peptide, 6 LNS domains separated by 3 EGF-like sequences, followed by an O-glycosylation region (O Glyc), a single transmembrane domain and a short cytoplasmic region containing a type II PDZ-interaction site. β-Neurexins contain only one LNS domain, which is preceded by a β-neurexin-specific sequence (white box). Arrowheads indicate the location of the five alternative splice sites present in α-neurexins, and the two present in β-neurexins. *Reprinted with permission from (Lise and El-Husseini, 2006)*

2.2. Introduction

Formation of functional neural circuits during critical periods of embryonic brain development requires correct neuronal morphological growth and formation of appropriate synaptic connections. Mounting evidence suggests interplay between dendritic morphogenesis and synaptogenesis, since the size and shape of dendritic arbors determine the number and types of synapses formed, and synapse formation confers structural stabilization to growing dendritic processes (Cline and Haas, 2008; McAllister, 2000; Wong and Ghosh, 2002). The 'synaptotropic hypothesis' of dendrite growth posits that activity-dependent synaptogenesis directs dendrite growth by preferentially stabilizing processes in regions of appropriate innervations while destabilizing growth in regions with sparse or incorrect input (Niell et al., 2004; Vaughn, 1989). The molecular mechanisms proposed to mediate synaptotropic stabilization of nascent dendrites, to date, include glutamatergic synaptic transmission and subsequent downstream activation of plasticity-associated kinases and Rho GTPases (Haas et al., 2006; Liu et al., 2009; Rajan and Cline, 1998; Sin et al., 2002; Wu and Cline, 1998). Lacking from this model of dendritic arbor pattern formation, however, is the role of trans-synaptic cell adhesion molecules that mediate the initial nascent contacts between growing axons and dendrites.

Neurexin (NRX) and neuroligin (NLG) are cell adhesion molecules expressed on growing axons and dendrites, respectively (Ichtchenko et al., 1995; Song et al., 1999). A critical role of these cell adhesion molecules in functional neural network formation arises from the recent identification of mutations in members of the NLG family and their associated binding partners, including NRX and SHANK3, in human autism spectrum

disorders (ASDs) (Durand et al., 2007; Feng et al., 2006; Jamain et al., 2003). NLGs consist of a family of proteins including NLG1 – NLG4, with NLG1 predominantly localized to glutamatergic synapses (Bolliger et al., 2001; Philibert et al., 2000; Song et al., 1999). Trans-synaptic NRX-NLG binding induces pre- and postsynaptic differentiation by triggering bi-directional intracellular signaling and recruitment of synaptic proteins (Graf et al., 2004; Scheiffele et al., 2000). At nascent dendritic sites of axo-dendritic contact, NLG1 promotes postsynaptic differentiation and maturation by recruiting PSD-95 (Irie et al., 1997) and NMDA receptors (Barrow et al., 2009; Chih et al., 2005) through interactions with an intracellular C-terminal PDZ (PSD-95/Dlg/ZO-1) binding domain. Manipulation of NLG1 expression levels dramatically alters synapse number and function in cultured neurons (Chih et al., 2005; Chubykin et al., 2007; Dean et al., 2003; Graf et al., 2004). Combined with results from NLG knockout (KO) mice (Chubykin et al., 2007; Varoqueaux et al., 2006), these studies suggest a role for NLGs in synapse specification and maturation. However, no studies have yet investigated the relationship between NRX and NLG in regulating patterning of dendritic arborization, which occurs concomitantly with synaptogenesis during early brain development and is critical to network function.

To examine the role of NRX-NLG1 interactions in regulation of dendritogenesis, our laboratory has developed novel methods for imaging and analyzing rapid dendrite growth within the intact and awake developing vertebrate brain. These techniques, termed '*dynamic morphometrics*', involve *in vivo* rapid two-photon time-lapse imaging of brain neurons in the intact and awake *Xenopus* tadpole and comprehensive 3D quantification of growth behaviors of all dendritic processes on the entire dendritic arbor at 5 min intervals over hours. Measures of dynamic dendritic growth including rates of

filopodial addition and elimination, lifetimes, and motility describe the morphological plasticity underlying searching of extracellular space for appropriate axons, and stabilization associated with contact formation. While dendritic filopodia in some mature neurons are precursors of spines, during early dendritic morphogenesis, filopodia develop into longer branches; hence, their growth dynamics are critical for establishing appropriate and persistent circuit structures. Long interval imaging spanning days captures the cumulative effects of altered dynamic growth behaviors on the mature neuron's dendritic arbor morphology.

Using these sensitive measures, I identify NRX-NLG1 interactions in mediating a multi-step process involving initial activity-independent formation of trans-synaptic adhesions followed by activity-dependent postsynaptic development. Imaging at 24 h intervals over periods spanning neuronal morphological maturation demonstrates cumulative effects of NRX-NLG-mediated regulation of rapid growth behavior on persistent dendritic arbor size and complexity. Furthermore, whole-cell patch clamp recording of glutamatergic synaptic transmission, and time-lapse imaging of neurons expressing fluorescently tagged PSD-95 reveals that NRX-NLG mediated arbor growth and synapse formation are tightly connected. Gain- or loss-of-function of NLG1 affects both synapse number and function as well as dendrite arbor structure. Hence, this chapter provides new insights to the roles of cell adhesion molecules in directing neuronal structural growth, critical to development of functional brain circuits.

2.3. Material and Methods

2.3.1. Animals

Freely swimming albino *Xenopus laevis* tadpoles were reared in 10% Steinberg's solution (Hewapathirane et al., 2008) at 22°C on a 12h light/dark cycle. Experiments were performed on Stage 47 tadpoles (Nieuwkoop and Faber, 1967). All experimental procedures were conducted according to the guidelines of the Canadian Council on Animal Care, and were approved by the Animal Care Committee of the University of British Columbia.

2.3.2. Plasmids and morpholinos

Xenopus laevis neuroligin 1 (NLG1) was cloned from brain by RT-PCR, and the PCR product was inserted into a pcDNA expression vector for over-expression studies. The *Xenopus laevis* NLG1 cDNA sequence predicts an amino acid sequence containing all identified functional motifs, and high overall homology (91%) compared to mouse. Structure-function studies of NLG1 function employed the following constructs: hemaglutinin (HA)-tagged NLG1 containing splice insertions A and B (WT-NLG1); a dominant-negative form in which the extracellular neurexin-binding domain was exchanged with acetylcholinesterase (AChE) (NLG1-swap, amino acids 48-630 of neuroligin-1ab were replaced with amino acid 31-565 of mouse AChE); and a dominant negative version with an intercellular C-terminal deletion lacking a PSD-95-binding motif (NLG1-ΔC1, a stop codon was inserted after amino acid 803) (Scheiffele et al., 2000). All three constructs were generous gifts from Dr. Peter Scheiffele (University of Basel,

Switzerland). In order to test the suitability of employing mouse NLG1-swap and NLG1-ΔC1 in *Xenopus*, I compared effects of expressing *Xenopus* NLG1 (*Xen*-NLG1) with mouse NLG1 and found no significant differences in any dynamic morphometric measures (data not shown). To knockdown endogenous NLG1, lissamine-tagged Morpholino antisense oligonucleotides against *Xen*-NLG1 (MO-NLG1: AAGAGCCTCCATGAATATACACCAT) and control Morpholino oligonucleotides (MO-control: CCTCTTACCTCAGTTACAATTTATA) that do not correspond to any known *Xenopus laevis* sequence were purchased from GeneTools (Philomath, OR). Lissamine-tagged Morpholinos allowed fluorescent detection of loading into neurons *in vivo*.

2.3.3. Immunoblotting

Tadpoles were anesthetized with 0.02% 3-aminobenzoic acid ethyl ester (MS222, Sigma), sacrificed, and brains were dissected and homogenized in lysis buffer (50 mM Tris-HCL, 1X protease inhibitor cocktail (Roche Products, Welwyn Garden City, UK), 1% Triton X-100, pH 7.4). Protein homogenates were separated on a 8% Bis-Tris acrylamide gel (Invitrogen, Carlsbad, CA) and transferred to nitrocellulose membrane. Blots were blocked in 5% nonfat milk with 0.1% Tris-buffered saline (TBS) and incubated with primary antibodies diluted in blocking solution (mouse monoclonal NLG1 antibody; 1:1000, Synaptic System, Goettingen, Germany). Blots were rinsed and incubated with HRP-linked mouse IgG, and imaged using chemiluminescence (Biorad, Hercules, CA).

2.3.4. Immunohistochemistry

Tadpoles were anesthetized with 0.02% MS222, sacrificed, and fixed with 4% paraformaldehyde (PFA) in phosphate-buffered saline (PBS) for two hours at room

temperature and cryoprotected in 30% sucrose solution at 4°C overnight followed by cutting the whole tadpole into 30 μm horizontal cryosections. Slices were blocked in 5% normal goat serum for 1 h and incubated in primary antibodies at 4°C overnight. After washing with PBS, sections were incubated in Alexa Fluor-conjugated secondary antibodies (Invitrogen, Eugene, OR) for 1 h at room temperature, mounted and imaged with an Olympus FV-1000 confocal microscope, using a PlanApo N 60X oil immersion objective (1.42NA, Olympus). The primary antibodies and dilution used were as follows: pan-NLG antibody (mouse monoclonal, 1:500, Synaptic Systems), SNAP-25 (rabbit polyclonal, 1:400, Stressgen, Ann Arbor, MI), and PSD-95 (mouse IgG, 1:200, Millipore, Billerica, MA). For secondary antibodies, Alexa 568-conjucated goat-to-rabbit antibody (1:200) and Alexa 633-conjucated goat-to-mouse antibody (1:200) were used. For the measurement of the density of immunostained SNAP-25 and PSD-95 puncta, all fluorescent puncta larger than 0.2 - 3 μm^2 were included (Lim et al., 2008; Ruthazer et al., 2006; Sanchez et al., 2006) and density was determined using NIH ImageJ software.

2.3.5. Neurexin-neuroligin binding assay

Soluble form of mouse neurexin-1β lacking splice site 4 fused to Fc-IgG (NRX-Fc) and a mutation version (D137A NRX-Fc) (Graf et al., 2006), were generated in HEK293T cells (ATCC CRL-1573). NRX-Fc and D137A NRX-Fc were generous gifts from Dr. Ann Marie Craig (University of British Columbia). Protein was purified on Agarose Ni-NTA columns (Qiagen, Germantown, MD) using imidazol gradient elution and dialyzed with column buffer. Protein concentration was quantitatively determined by anti-myc clone 9E10 (Dev. Studies. Hyb. Bank, University of Iowa) by immunoblot. HEK293T cells were plated on poly-l-lysine treated glass coverslips and were left either untransfected or transfected with *Xenopus* NLG1 using Fugene 6 (Roche Basel, Switzerland). Soluble

NRX-Fc and D137A NRX-Fc were diluted to 30 µg/mL in conditioned media, applied to coverslips containing live untransfected and transfected HEK293T cells, and incubated at 37°C, with 5% CO_2 for 30 min. Coverslips were washed 6x every 2 min in warm MEM media (Invitrogen, Carlsbad, CA) prior to fixation in 4% PFA for 15 min at room temperature. After blocking in 10% bovin serum albumin (BSA), cells were stained with anti-myc clone 9E10 detected by Alexa 568-conjugated mouse IgG1 secondary antibody (Invitrogen).

2.3.6. *In vivo single cell transfection and loading with dyes and morphlinos*

Individual growing neurons within the *Xenopus* optic tectum were transfected using *in vivo* single-cell electroporation (Bestman et al., 2006; Haas et al., 2001) for expression of membrane-targeted farnesylated enhanced green fluorescent protein (EGFP), alone or in combination with NLG1 constructs. Stage 47 *Xenopus* tadpoles were anesthetized with 0.02% MS-222 and individual neurons in the optic tectum were electroporated using plasmid DNA (2 µg/µl) and an Axoporator 800A stimulator (Molecular Devices, Sunnyvale, CA) to deliver electric pulses (stimulus parameters: pulse intensity = 1.5 µA; pulse duration = 1 msec; pulse frequency = 300 Hz; train duration = 300 msec). To visualize postsynaptic specializations and tectal neuron morphology simultaneously, individual neurons were electroporated with expression plasmids encoding PSD-95 conjugated to cyan fluorescent protein (PSD-95-CFP, a gift from Dr. Ann Marie Craig, University of British Columbia), yellow fluorescent protein (YFP), and with or without NLG1 constructs. Single-cell electroporation was also used to co-deliver synthetic Morpholino oligonucleotides (pipette concentration: 0.5mM) and the

space-filling dye Alexa Fluor 488, 3000MW (1.5mM, Invitrogen, Eugene, OR), using the stimulation parameters: pulse intensity = 2 μA; pulse duration = 700 μsec; pulse frequency = 700 Hz; train duration 20 msec. Loading of lissamine-tagged Morpholinos was confirmed by fluorescence and confocal microscopy. Co-electroporation of Morpholinos and Alexa Fluor 488 yielded 100% co-loading.

2.3.7. In vivo time-lapse imaging of dendrite growth dynamics

Images of growing neurons within intact and awake embryonic brain were captured using a custom-built two-photon laser-scanning microscope constructed by modification of an Olympus FV300 confocal microscope (Olympus, Center Valley, PA), and addition of a Chameleon XR laser light source (Coherent, Santa Clara, CA). Optical sections through the optic tectum were captured using a 60x, 1.1 NA, water immersion objective (LUMPlanFI, Olympus), and images were recorded using Fluoview software (Olympus). For rapid time-lapse experiments, un-anesthetized tadpoles were immobilized for imaging using brief (~5 min) exposure to the reversible paralytic pancuronium dibromide (PCD, 2mM, Tocris), and embedded under a thin layer of agarose (1.0%, prepared with 10% Steinberg's solution) in a Sylgard imaging chamber continuously perfused with oxygenated 10% Steinberg's solution at room temperature (22°C). Tadpoles were not anesthetized during imaging to avoid the confounding effects of altered synaptic transmission on endogenous activity-dependent synaptogenesis and growth. Entire dendritic arbors of individual tectal neurons were imaged *in vivo* using optical sectioning with a z-axis step size of 1.5μm, every 5 min over 1 or 2 h. The two-photon fluorescence microscopy point-spread function is inherently broader in the z- than x-y axes. Given that dendritic arbors from neurons in all groups were imaged and

analyzed in 3D, the potential distortion in length values in the z-axis were consistent across groups. For tectal infusions, a solution containing recombinant NRX-Fc (30 µg/ml), D137A NRX-Fc (30 µg/ml) or D-APV (50µM, Tocris) was slowly delivered from a micropipette into the optic tectum using low pressure (<10psi) over 3-5 min using a Picospritzer III (General Valve Corporation, Fairfield, NJ). For 8 h imaging experiments, single time point images were taken three times every 4 h. For measures of long-term dendritic arbor growth, neurons were imaged at 24 h intervals over 4 days. For daily imaging, tadpoles were briefly anesthetized with MS-222, imaged over 5 min and returned to their chambers where they recovered from anesthesia within 1-2 min.

2.3.8. Morphometric analysis

Dynamic growth behavior of dendritic filopodia and branches was analyzed from rapid time-lapse imaging data sets using a custom-written IGOR-based program (developed by Dr. Jamie Boyd, University of British Columbia). All filopodia (processes with length less than 10 µm) were identified, tracked and measured across multiple time point image stacks providing comprehensive and precise 3D measures of growth dynamics. Measures of total dendritic arbor structure for analysis of long-term changes over days were achieved using 3D rendering of single time point images reconstructed using the computer-assisted drawing software Neurolucida (MicroBrightfield, Williston, VT). For puncta analysis, individual puncta were identified in single optical sections, using our custom-written IGOR-based program. PSD-95-CFP clusters of 0.5 – 1.5 µm in size and located within dendritic processes were considered to be single synaptic puncta (Niell et al., 2004; Sanchez et al., 2006).

2.3.9. Statistical tests

Data were tested with the Student t-test to compare between groups unless otherwise stated. Data were present as mean ± SEM. Significance were labeled as * $p < 0.05$, ** $p < 0.01$, *** $p < 0.001$.

2.4. Results

2.4.1. Endogenous NLG1 expression in developing Xenopus brain

To determine the function of NRX-NLG1 interactions on dendritogenesis in the *Xenopus* optic tectum, I first characterized NLG1 expression by isolating cDNAs encoding NLG1 from tadpole brain. Sequencing analysis reveals that *Xenopus laevis* NLG1 shares a high degree of homology across species ranging from birds to mammals, with 79% identity at the nucleotide level and 91% identity at the predicted amino acid level, while exhibiting complete conservation throughout all known protein binding motifs (**Figure 2.2A**) (Ichtchenko et al., 1996). Western blot analysis using NLG1- and NRX-specific antibodies found developmental regulation with low expression in brain at Stage 35 and a gradual increase to Stage 50 (**Figure 2.2B**), corresponding to the progressive developmental increase in retinal ganglion cell (RGC) axonal innervations of the tectum, tectal neuron dendritogenesis, and the establishment and refinement of retino-tectal synapses (Holt and Harris, 1993). Co-immunoprecipitation using pull-down antibodies against endogenous *Xenopus* NLG1 identified close association with the endogenous postsynaptic protein PSD-95 (**Figure 2.2C**); and *in vivo* single-cell co-expression (Haas

et al., 2001) of NLG1 tagged with YFP (NLG1-YFP), and PSD-95 tagged with CFP (PSD-95-CFP) demonstrated colocalization of NLG1 with PSD-95 (**Figure 2.2F and 2.2H**), supporting NLG1 localization at synapses in *Xenopus*. In order to selectively interfere with NLG inter-molecular interactions, two mutants of wild-type mouse NLG1 (WT-NLG1) were used (Chih et al., 2005; Scheiffele et al., 2000). I employed NLG1-swap, in which the NLG extracellular cholinesterase domain is exchanged with a homologous sequence from acetylcholinesterase that is unable to bind to β-NRX, to selectively disrupt extracellular interactions between NRX and NLG1 (Chih et al., 2005; Chubykin et al., 2007; Scheiffele et al., 2000). Furthermore, to interfere with the intracellular association between NLG1 and PSD-95, I expressed NLG1-ΔC, a NLG1 mutant lacking the C-terminal PSD-95 binding domain, which has been shown to disrupt NRX-induced PSD-95 clustering and synapse formation *in vitro* (Chih et al., 2005; Dresbach et al., 2004; Nam and Chen, 2005; Scheiffele et al., 2000). Here, using bulk electroporation (Haas et al., 2002) for widespread tectal expression of HA-tagged versions of WT-NLG1, NLG1-swap, or NLG1-ΔC, and co-immunoprecipitation with antibodies against HA, I demonstrated that WT-NLG1 and NLG1-swap associate with endogenous PSD-95 *in vivo*, but NLG1-ΔC does not (**Figure 2.2E**). Furthermore, co-immunoprecipitation with the same antibodies detects association between exogenously expressed WT-NLG1 and NLG1-ΔC with endogenous NRX, but NLG1-swap does not (**Figure 2.2E**).

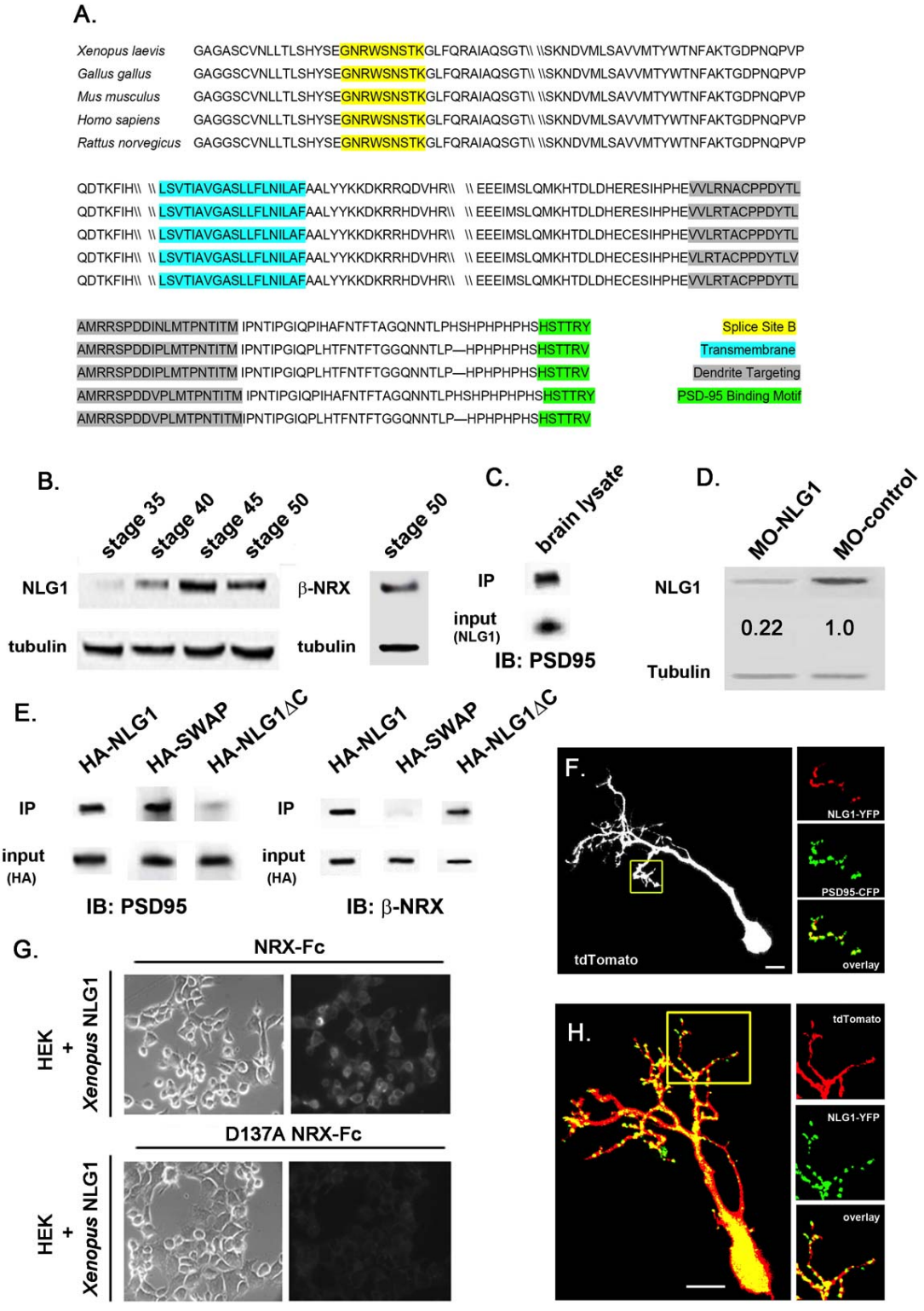
A.
Xenopus laevis GAGASCVNLLTLSHYSEGNRWSNSTKGLFQRAIAQSGT\\ \\SKNDVMLSAVVMTYWTNFAKTGDPNQPVP
Gallus gallus GAGGSCVNLLTLSHYSEGNRWSNSTKGLFQRAIAQSGT\\ \\SKNDVMLSAVVMTYWTNFAKTGDPNQPVP
Mus musculus GAGGSCVNLLTLSHYSEGNRWSNSTKGLFQRAIAQSGT\\ \\SKNDVMLSAVVMTYWTNFAKTGDPNQPVP
Homo sapiens GAGGSCVNLLTLSHYSEGNRWSNSTKGLFQRAIAQSGT\\ \\SKNDVMLSAVVMTYWTNFAKTGDPNQPVP
Rattus norvegicus GAGGSCVNLLTLSHYSEGNRWSNSTKGLFQRAIAQSGT\\ \\SKNDVMLSAVVMTYWTNFAKTGDPNQPVP
QDTKFIH\\ \\ LSVTIAVGASLLFLNILAFAALYYKKDKRRQDVHR\\ \\ EEEIMSLQMKHTDLDHERESIHPHEVVLRNACPPDYTL
QDTKFIH\\ \\ LSVTIAVGASLLFLNILAFAALYYKKDKRRHDVHR\\ \\ EEEIMSLQMKHTDLDHERESIHPHEVVLRTACPPDYTL
QDTKFIH\\ \\ LSVTIAVGASLLFLNILAFAALYYKKDKRRHDVHR\\ \\ EEEIMSLQMKHTDLDHECESIHPHEVVLRTACPPDYTL
QDTKFIH\\ \\ LSVTIAVGASLLFLNILAFAALYYKKDKRRHDVHR\\ \\ EEEIMSLQMKHTDLDHECESIHPHEVLRTACPPDYTLV
QDTKFIH\\ \\ LSVTIAVGASLLFLNILAFAALYYKKDKRRHDVHR\\ \\ EEEIMSLQMKHTDLDHECESIHPHEVVLRTACPPDYTL
AMRRSPDDINLMTPNTITM IPNTIPGIQPIHAFNTFTAGQNNTLPHSHPHPHPHSHSTTRY
AMRRSPDDIPLMTPNTITM IPNTIPGIQPLHTFNTFTGGQNNTLP—HPHPHPHSHSTTRV
AMRRSPDDIPLMTPNTITM IPNTIPGIQPLHTFNTFTGGQNNTLP—HPHPHPHSHSTTRV
AMRRSPDDVPLMTPNTITM IPNTIPGIQPIHAFNTFTAGQNNTLPHSHPHPHPHSHSTTRY
AMRRSPDDVPLMTPNTITMIPNTIPGIQPLHTFNTFTGGQNNTLP—HPHPHPHSHSTTRV
Splice Site B
Transmembrane
Dendrite Targeting
PSD-95 Binding Motif
B.
stage 35
stage 40
stage 45
stage 50
stage 50
NLG1
β-NRX
tubulin
tubulin
C.
brain lysate
IP
input (NLG1)
IB: PSD95
D.
MO-NLG1
MO-control
NLG1
0.22
1.0
Tubulin
E.
HA-NLG1
HA-SWAP
HA-NLG1ΔC
HA-NLG1
HA-SWAP
HA-NLG1ΔC
IP
input (HA)
IP
input (HA)
IB: PSD95
IB: β-NRX
F.
tdTomato
NLG1-YFP
PSD95-CFP
overlay
G.
NRX-Fc
HEK + Xenopus NLG1
D137A NRX-Fc
HEK + Xenopus NLG1
H.
tdTomato
NLG1-YFP
overlay

***Figure 2.2. Characterization of Xenopus laevis* NLG1**

(A) NLG1 amino acid sequence alignment between *Xenopus laevis* and other species with protein binding motifs highlighted. **(B)** Western blot demonstrates developmental expression pattern of endogenous NLG1, and β-NRX expression in tadpole brain. **(C)** Co-immunoprecipitation using pull-down antibodies against endogenous NLG1 identifies close association with endogenous PSD-95 **(D)** Morpholino oligonucleotides specific for *Xenopus* NLG1 (MO-NLG1) reduce expression of NLG1 in HEK293T cells exogenously expressing *Xenopus* NLG1 compared to MO-control (top band) on Western blot. **(E)** Immunoprecipitation using anti-HA antibody to pull down HA-tagged WT-NLG1, NLG1-swap, and NLG1-ΔC demonstrates WT-NLG1 and NLG1-swap interaction with PSD-95, while NLG1-ΔC does not, and demonstrates association of WT-NLG1 and NLG1-ΔC, but not NLG1-swap with endogenous NRX. **(F)** Co-expression of NLG1-YFP and PSD-95-CFP in individual tectal neurons show co-localization of NLG1 with PSD-95 *in vivo*, supporting NLG1 localization at post-synaptic sites. **(G)** Binding assay shows mouse soluble NRX-Fc binds HEK293T cells expressing *Xenopus* NLG1 (top panel), but control soluble D137A NRX-Fc does not (bottom panel). **(H)** Expressing NLG1-YFP in individual neurons demonstrate discrete NLG1 puncta localized to both dendritic branches and filopodia.

To determine whether NRX-NLG1 interactions regulate dendrite growth in brain neurons undergoing morphogenesis *in vivo*, I selectively interfered with the formation of trans-synaptic cell adhesions by intra-tectal infusion of a soluble form of mouse neurexin-1β lacking splice site 4, fused to Fc-IgG (NRX-Fc). Application of this recombinant protein to immature neurons in culture has been shown to block glutamatergic synapse formation by competing with endogenous presynaptic NRX binding to postsynaptic NLG1 (Levinson et al., 2005; Nguyen and Sudhof, 1997; Scheiffele et al., 2000). Kevin She from Dr. Ann Marie Craig's Lab performed binding assays to demonstrate that mouse soluble NRX-Fc, but not a mutated version (D137A NRX-Fc) (Graf et al., 2006), binds to *Xenopus* NLG1 expressed in HEK293T cells (**Figure 2.2G**). To test the effects of blocking NRX-NLG1 interactions *in vivo*, immature

tectal neurons were labeled with EGFP using single-cell electroporation (Haas et al., 2001) and imaged using rapid and long-interval two-photon time-lapse microscopy in the intact and unanaesthetized brain. Complete 3D images of dendritic arbors were captured every 5 min over 2 h, with the initial 1 h baseline period serving as an internal control, followed by infusion of soluble NRX-Fc into the tectum and continued imaging for an additional hour (N = 6 cells, n = 272 filopodia). Controls were infused with the non-binding D137A NRX-Fc (N = 5 cells, n = 227 filopodia). Post-imaging analysis of filopodial growth behavior was conducted by tracking all filopodia from all branches on the entire dendritic arbor in 3D across every 5 min time point over 1 h epochs for accurate measurements of length, motility, lifetime, and density. For all similar measures throughout this study, 'N' represents the number of neurons examined, in which the entire dendritic arbor of each neuron was analyzed, and 'n' refers to the total number of dendritic filopodia examined on all neurons within that group. Imaging smaller portions of dendritic arbors at 30 sec intervals found that 5 min interval imaging captured similar rates of addition and retraction as 30 sec interval imaging because 88.5% of filopodia had lifetimes greater than 5 minutes. However, motility measures were sensitive to sample rate with 5 min under-sampling compared to 30 sec imaging. This under-sampling would be consistent across all groups imaging under-estimates measures of motility, however this bias is shared across groups.

Dendritic filopodia were separated into 2 groups to distinguish older filopodia potentially containing synapses from newly extended nascent filopodia lacking presynaptic contacts. Filopodia present at the initial imaging time point are categorized as '*pre-existing*' and represent a mixture of younger and older processes, while those added during the 1 h imaging session are termed '*new'*. *Pre-existing* filopodia were

further characterized as either '*stable'* if maintained for the 1 h imaging session, or '*lost'* if they retract within that time. *In vivo* imaging of fluorescently tagged postsynaptic protein PSD-95 demonstrates an inverse relationship between the establishment of postsynaptic specializations and filopodial dynamics (**Figure 2.3A and 2.3B**) (Washbourne P 2002, Prange O 2001, Niell 2004, Sanchez 2006). Consistent with previous studies (Niell 2004, Sachez 2006), I find no effects of exogenous expression of PSD-95 on filopodial dynamics and dendritic growth (**Figure 2.3C and 2.3D**), yet I find a correlation in the *pre-existing* population between expression of PSD-95 puncta, and motility and lifetimes (**Figure 2.3E and 2.3F**). Most *pre-existing* filopodia possess PSD-95 puncta and are stable, exhibiting low motility and longer lifetimes, while filopodia lacking PSD-95 puncta are unstable and extremely motile, tending to have higher motility and shorter lifetimes. In contrast, PSD-95 puncta are not present on newly extended filopodia, but appear after tens of minutes and are associated with stabilization by decreasing motility and increasing lifetimes (Niell et al., 2004).

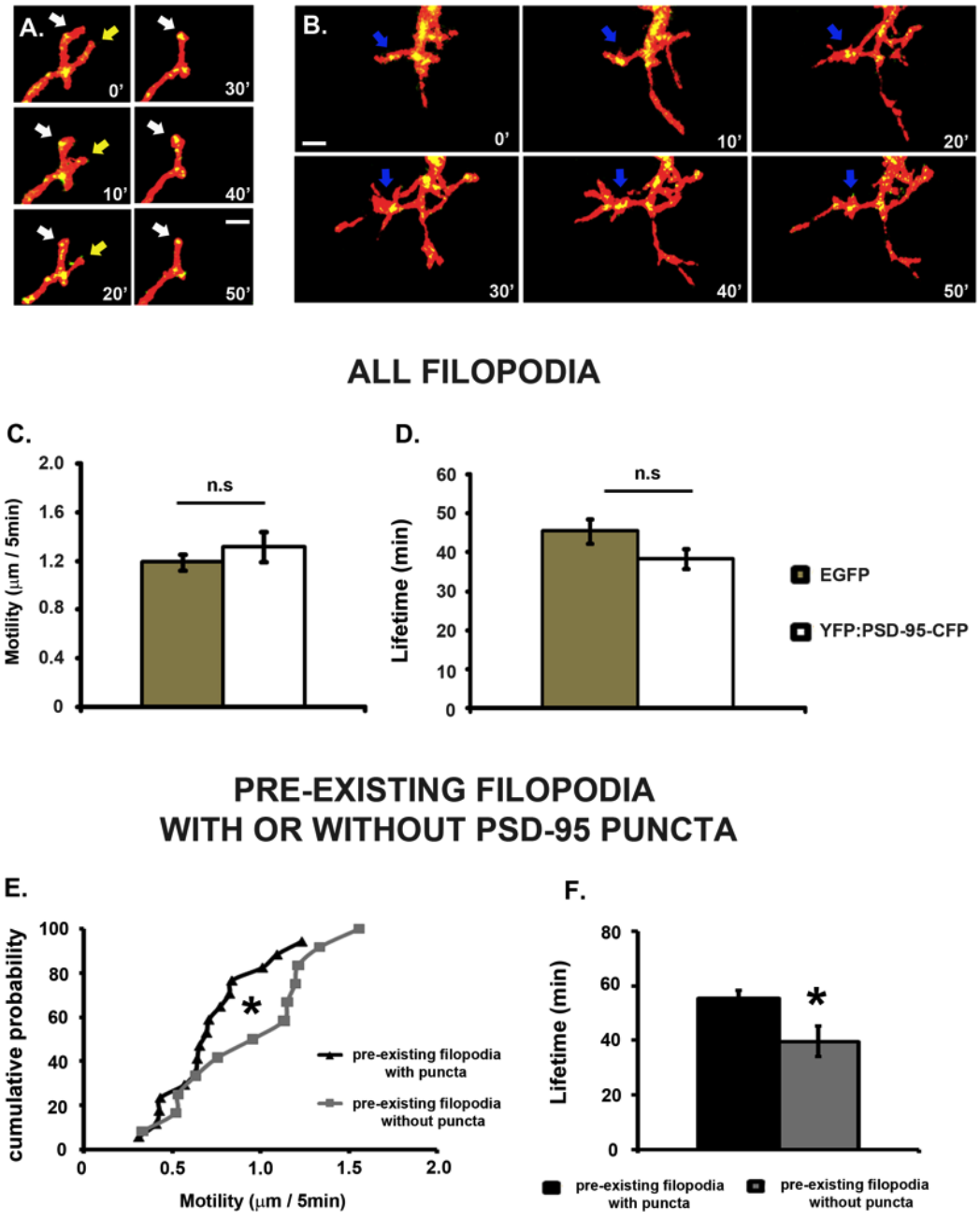

Figure 2.3 Dual Imaging of PSD-95 Puncta and Dendritic Filopodia.

In vivo rapid time-lapse imaging of individual tectal neurons expressing YFP and PSD-95 CFP every 5 min for 1 h. **(A)** Series of images showing a filopodium with a PSD-95 punctum (white open arrowhead) exhibits low motility and long lifetime. Scale bar = 5 μm, while a filopodium without a PSD-95 punctum (yellow open arrowhead) exhibits high motility and retracts within 30 min. **(B)** A series of time-lapse images show PSD-95 puncta at stabilized points from which *new*

filopodia protrude. Scale bar = 5 μm. **(C-F)** Morphometric analysis of dendritic filopodial dynamics of EGFP neurons (n = 54 filopodia) and neurons expressing PSD-95-CFP (n = 43 filopodia) demonstrating that expression of PSD-95-CFP does not affect filopodial motility **(C)**, and lifetimes **(D).** *Pre-existing* filopodia present at the first time point of a rapid time-lapse series differ in their **(E)** motility, and **(F)** lifetime based on whether they express PSD-95 puncta. *Pre-existing* filopodia with puncta (n = 21 filopodia) are more stable and have longer lifetimes, whereas *pre-existing* filopodia that do not possess PSD-95 puncta are more motile and have shorter lifetimes (n = 27 filopodia). *p < 0.05, **p < 0.01, ***p < 0.001. Error bars indicate SEM. Cumulative probability plot was analyzed by two-sample Kolmogorov-Smirnov comparison.

Intra-tectal infusion of soluble NRX-Fc led to a 30% reduction in overall filopodial density (**Figure 2.4A and 2.4D**), due primarily to a dramatic increase in the rate of elimination of *pre-existing* filopodia with only 35% remaining after 1 h (Control = 70 ± 2.8% remaining, NRX-Fc = 35 ± 3.2% remaining; p < 0.05; Fig. 2B, 2C). Furthermore, soluble NRX-Fc also dramatically increases elimination rates of *new* filopodia by 90% compared to D137A NRX-Fc-treated neurons (**Figure 2.4C**). Fewer *new* filopodia are stabilized in the presence of soluble NRX-Fc, evident from decreased average filopodial lifetimes (Fig. 2E) and a shift towards increased motility (**Figure 2.4F**). These results suggest a model in which soluble NRX-Fc interferes with synapse formation, thus preventing filopodia from stabilizing and promoting filopodial elimination.

To investigate the long-term physiological consequences of losing dendritic filopodia due to blocking NRX-NLG1 interactions, I examined dendritic arbor growth, synapse number and synaptic transmission 4 h after tectal infusion of soluble NRX-Fc. Individual growing tectal neurons were imaged over two sequential 4 h intervals, with the growth rate over the first 4 h period used as an internal baseline. Soluble NRX-Fc or D137a NRX-Fc was infused into the tectum following the first 4 h period. Dendritic arbor

size and filopodia density were quantified in 3D. I observed similar arbor growth rates during the first 4 h across all neurons with a mean of 10% increase in both total dendritic arbor length and number of dendritic filopodia (NRX-Fc: N = 9 cells, D137A NRX-Fc: N = 8 cells; **Figure 2.4G and 2.4H**). However, while neurons treated with D137A NRX-Fc continue to grow at the same rate for the second 4 h period, neurons treated with NRX-Fc exhibit a dramatic decrease in overall arbor size (-9.8 ± 2.9%; Fig. 2H). This stunting of arborization results from loss of dendritic filopodia over 4 h without significant changes in dendritic branch length (**Figure 2.4I and 2.4J**). Imaging of PSD-95-CFP finds puncta density increases by 20% during the first 4 h, but significantly decreases 4 h following intra-tectal infusion of NRX-Fc (**Figure 2.4K**). In order to confirm whether this decrease in PSD-95 puncta density represents a loss of functional synapses, I performed immunostaining of the pre- and postsynaptic markers SNAP-25 and PSD-95 to determine changes in synapse density. I find that the density of SNAP-25 puncta is unaltered following 4 h of NRX-Fc treatment, but the density of endogenous PSD-95 puncta is significantly reduced by 25% compared to control brains treated with D137A NRX-Fc. Furthermore, I find a significant reduction in the number of colocalized SNAP-25 and PSD-95 puncta (**Figure 2.4P**), not solely caused by the decrease in PSD-95 puncta number, but by the significant reduction in the probability of colocalization (**Figure 2.4Q**). These results are confirmed by whole-cell patch clamp electrophysiology of tectal neurons, which demonstrates a significant decrease in the frequency, but not amplitude, of AMPA receptor-mediated mEPSCs after 4 h of NRX-Fc treatment (**Figure 2.4L – 2.4N**), evidence supporting a decrease in synapse number.

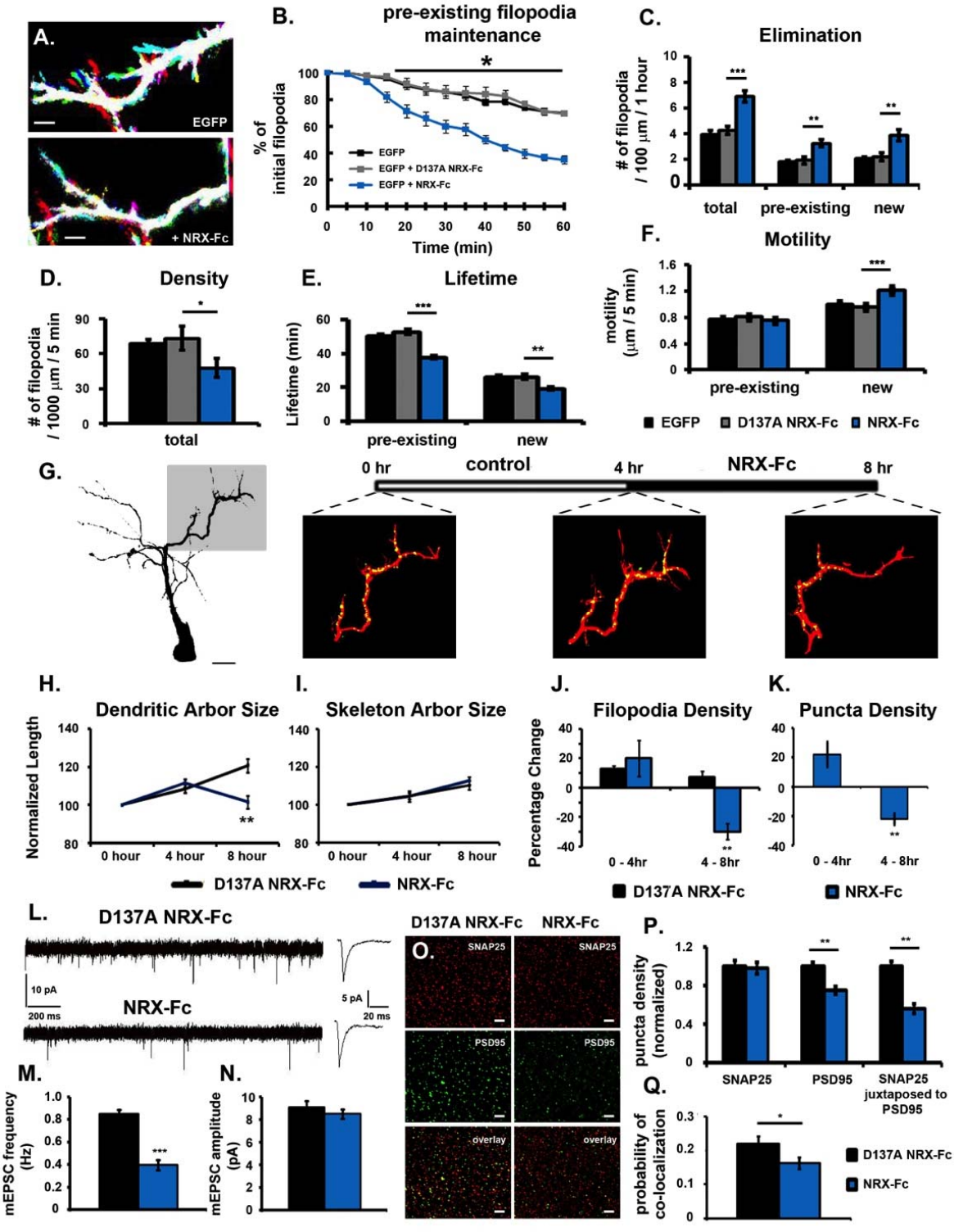
A.
EGFP
+ NRX-Fc
B.
pre-existing filopodia maintenance
% of initial filopodia
EGFP
EGFP + D137A NRX-Fc
EGFP + NRX-Fc
Time (min)
C.
Elimination
# of filopodia / 100 μm / 1 hour
total
pre-existing
new
D.
Density
# of filopodia / 1000 μm / 5 min
total
E.
Lifetime
Lifetime (min)
pre-existing
new
F.
Motility
motility (μm / 5 min)
pre-existing
new
EGFP
D137A NRX-Fc
NRX-Fc
G.
0 hr
control
4 hr
NRX-Fc
8 hr
H.
Dendritic Arbor Size
Normalized Length
0 hour
4 hour
8 hour
I.
Skeleton Arbor Size
J.
Filopodia Density
Percentage Change
0 - 4hr
4 - 8hr
K.
Puncta Density
D137A NRX-Fc
NRX-Fc
L.
D137A NRX-Fc
10 pA
200 ms
5 pA
20 ms
NRX-Fc
M.
mEPSC frequency (Hz)
N.
mEPSC amplitude (pA)
D137A NRX-Fc
NRX-Fc
O.
SNAP25
PSD95
overlay
P.
puncta density (normalized)
SNAP25
PSD95
SNAP25 juxtaposed to PSD95
Q.
probability of co-localization
D137A NRX-Fc
NRX-Fc

Figure 2.4 Blocking NRX-NLG1 Interactions Prevents Dendritic Filopodial Stabilization, Dendritic Arbor Growth, and Reduces Synapse Number.

(A) *In vivo* two-photon imaging of single tectal neuron expressing EGFP before and after NRX-Fc treatment. Superimposed images of six successive time-points at 10 min intervals (each time point a separate color; white = overlap). Scale bar = 5 μm **(B-F)** Morphometric analysis of dendritic filopodial dynamic growth behavior prior to, and after NRX-Fc treatment (EGFP = 11 cells, n = 407 filopodia; EGFP + NRX-Fc = 6 cells, n = 272; EGFP + D137A NRX-Fc = 5 cells, n = 227 filopodia). Filopodial growth behavior was analyzed by tracking all filopodia from all branches from each dendritic arbor in 3D across every 5 min time point over 1 h epochs **(B)** Survival plot of percentage of *pre-existing* filopodia remaining at each time point. **(C)** Average number of filopodia eliminated within 5 min in all groups (*total*); only of filopodia present at the initial imaging time point (*pre-existing)*; or only filopodia added during the 1 h imaging period (*new)*. **(D)** Average density of filopodia from 5 min interval imaging over 1 h. **(E)** Average lifetime of *pre-existing* and *new* filopodia. **(F)** Average absolute motility (mean |Δ length|) of *pre-existing* and *new* filopodia. **(G-K)** Tectal neurons expressing YFP and PSD-95-CFP imaged at 4 h intervals over 8 h. NRX-Fc (N = 9 cells) or D137A NRX-Fc (N = 8 cells) was infused into the tectum after the first 4 h. Scale bar = 20 μm **(H)** NRX-Fc reduced total dendritic arbor size. **(I-J)** Arbor size change was not due to alterations in dendritic branch length, but due to reduction in dendritic filopodia number. **(K)** NRX-Fc reduced PSD-95 puncta density. **(L)** Representative traces of AMPA receptor mEPSCs from tectal cells 4 h following tectal infusion of NRX-Fc (N = 10 cells) or D137A NRX-Fc (N = 12 cells). At *right*: mean mEPSC traces. **(M-N)** NRX-Fc significantly reduces AMPA receptor mEPSC frequency but not amplitude. **(O)** Immunostaining of tectal neuropil from horizontal brain sections probed with antibodies against SNAP-25 (red) and PSD-95 (green) 4 h following tectal infusion of NRX-Fc or D137A NRX-Fc (control). Colocalized SNAP-25 and PSD-95 puncta are shown in yellow. Scale bar = 1 μm. **(P)** Average densities of SNAP-25, PSD-95, and juxtaposed puncta (n = 3 sections/tadpole; 5 tadpoles per group). **(Q)** Quantitative analysis of the colocalization probability [(number of juxtaposed puncta)^2 / (number of SNAP-25 puncta x number of PSD-95 puncta)]. *p < 0.05, **p < 0.01, ***p < 0.001. Error bars indicate SEM.

2.4.2. Cell-autonomous NRX-NLG1 disruption prevents dendritic filopodia stabilization

In order to identify the cell-autonomous effects of interference with NRX-NLG1 interactions, I employed single-cell electroporation to express the NLG1-swap mutant in

individual immature growing brain neurons. I found neurons expressing NLG1-swap are extremely plastic and unstable (**Figure 2.5A**), evident from plots of filopodial absolute vs. relative motility (**Figure 2.5B**). The 'absolute' motility (Y-axis) is the mean length change during successive 5 min imaging intervals regardless of extension or retraction, while the 'relative' motility (X-axis) depicts the mean movement per 5 min using extension as positive values and retractions as negative values. Thus, absolute motility reflects average distance extended or retracted, and relative motility denotes the average net change in length. Plotting absolute and relative motility values are useful to differentiate distinct filopodia dynamic behavior. In control neurons, *stable pre-existing* filopodia with lifetimes of at least 1 h exhibit a range of motilities yet little net change in length, while *lost pre-existing* filopodia that retracted within 1 h were highly motile and exhibited negative relative motility values, and *new* filopodia primarily exhibit high motility and positive values for growth (**Figure 2.5B**). In contrast, NLG1-swap neurons (N = 11 cells, n = 524 filopodia) demonstrated high filopodial motility across all filopodial groups, with both *lost* and *new* populations exhibiting predominantly large negative growth (Fig. 3B). Morphometric analysis also revealed that NLG1-swap neurons exhibit short average lifetimes (**Figure 2.5C**) and high motility (**Figure 2.5D**) similar to the *new* filopodia from neurons treated with soluble NRX-Fc (**Table 2.1**). In addition, NLG1-swap expression significantly increases filopodia turnover, evident from the high filopodial density (**Figure 2.5F**), addition, and elimination rates (**Figure 2.5E**).

To test the potential role of altered synaptogenesis in NLG1-swap mediated dendritic filopodial instability, I co-expressed PSD-95-CFP and NLG1-swap in individual tectal neurons. Analysis reveals that although dendritic filopodia number is increased, PSD-95 densities are significantly decreased (**Figure 2.5G and 2.5H**). Moreover, only

20% of the remaining PSD-95 puncta are present on dendritic filopodia (**Figure 2.5I**), suggesting that dendritic filopodia are incapable of stabilization due to the inability to recruit postsynaptic PSD-95. These results support the synaptotropic hypothesis that synapse formation confers morphological stabilization, and demonstrates the importance of NRX-NLG1 interactions in regulating this process.

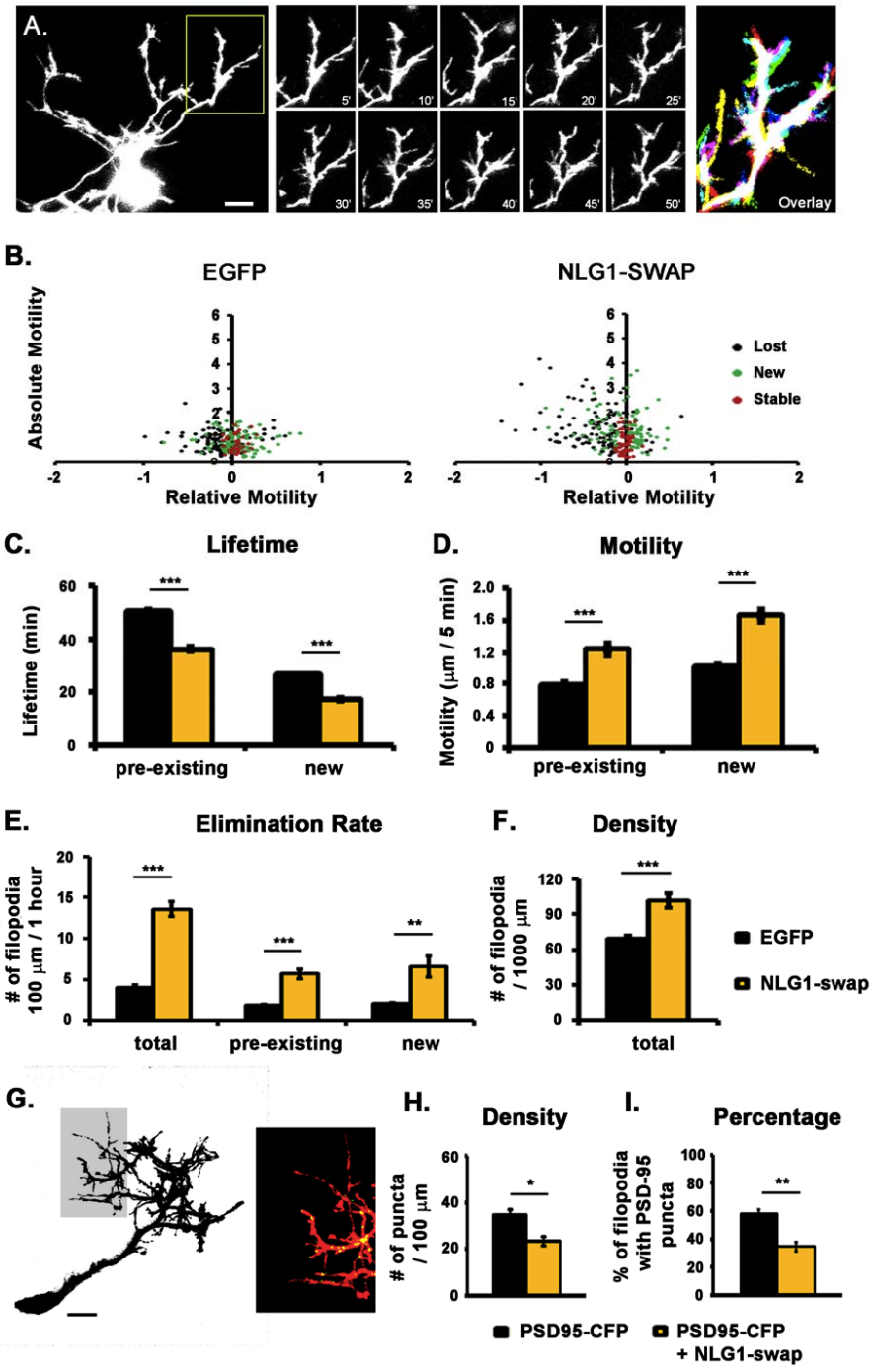
A.
5'
10'
15'
20'
25'
30'
35'
40'
45'
50'
Overlay
B.
EGFP
NLG1-SWAP
Absolute Motility
Relative Motility
Lost
New
Stable
C.
Lifetime
Lifetime (min)
pre-existing
new
D.
Motility
Motility (μm / 5 min)
pre-existing
new
E.
Elimination Rate
# of filopodia 100 μm / 1 hour
total
pre-existing
new
F.
Density
# of filopodia / 1000 μm
total
EGFP
NLG1-swap
G.
H.
Density
# of puncta / 100 μm
I.
Percentage
% of filopodia with PSD-95 puncta
PSD95-CFP
PSD95-CFP + NLG1-swap

Figure 2.5 Expression of NLG1-swap Increases Filopodia Turnover and Decreases Postsynaptic Specializations.

(A) *Left*: Representative neuron expressing dominant-negative NLG1-swap. *Middle*: multiple enlargements of boxed region of dendritic arbor every 5 min for 10 consecutive images. *Right*: overlay of six successive images at 10 min intervals. Scale bar = 20 μm **(B-G)** Morphometric analysis of dendritic filopodial dynamics of NLG1-swap neurons (N = 11 cells, n = 524 filopodia) and EGFP controls (N = 11 cells, n = 407 filopodia). **(B)** Plots of each filopodium's absolute motility (mean |Δ length|) vs. relative motility (mean Δ length) over 1 h. Positive values = filopodial extension; negative values = retraction. Filopodia that fluctuate without extending or retracting show no net change in relative motility. Filopodia are separated into 3 groups based on lifetimes; '*stable*' = filopodia present over the entire 1 h imaging period (red); '*new*' = filopodia not present at initial image, but emerging within 1 h (green); and '*lost*' = filopodia present at the initial image but eliminated within 1 h (black). **(C)** Average lifetimes of *pre-existing* and *new* filopodia. **(D)** Average absolute motility of all filopodia. **(E)** Number of filopodia eliminated every 5 min. **(F)** Average density of filopodia throughout 1 h. **(G)** *Left:* Representing neuron expressing YFP, PSD-95-CFP, and NLG1-swap. *Right:* enlargement of boxed region of dendritic arbor showing PSD-95 puncta. Scale bar = 20 μm **(H)** Puncta analysis reveals a decrease in PSD-95 puncta in neurons expressing NLG1-swap (N = 3 cells) compared to control neurons (N = 5 cells). **(I)** Percentage of total filopodia possessing PSD-95 puncta. *p < 0.05, **p < 0.01, ***p < 0.001. Error bars indicate SEM.

2.4.3. Increased NLG1 function hyper-stabilizes dendritic filopodia

I next monitored the cell-autonomous effects of enhancing NRX-NLG1 interactions by over-expressing NLG1 in individual tectal neurons (N = 5 cells, n = 227 filopodia). Neurons expressing either mouse NLG1 (WT-NLG1) or *Xenopus NLG1 (Xen*-NLG1) exhibited compact and complex dendritic arbors (**Figure 2.6A**), and no significant difference was found between the two groups (data not shown). Morphometric analysis showed a 36% increase in filopodial densities compared to EGFP controls (**Figure 2.6A**) due to increased filopodial lifetimes (**Figure 2.6C**) and reduced elimination rates (**Figure**

2.6E). Furthermore, NLG1-mediated hyper-stabilization of dendritic filopodia is evident from decreased filopodial motility (**Figure 2.6D**) and changes in dynamic behavior of both *pre-existing* and *new* filopodia, evident in plots of absolute vs. relative motility showing low absolute and relative motility in both *stable* and *new* groups (**Figure 2.6B**). Neurons co-expressing PDS-95-CFP and *Xen*-NLG1 exhibit an increase in PSD-95 density (**Figure 2.6G and 2.6H**), and a significant increase in the proportion of filopodia exhibiting postsynaptic specializations (**Figure 2.6I and Table 2.1**). These results suggest that enhancing NRX-NLG1 interactions promotes rapid PSD-95 recruitment and potentially synaptogenesis, which hyper-stabilizes dendritic filopodia and reduces dynamic searching behavior.

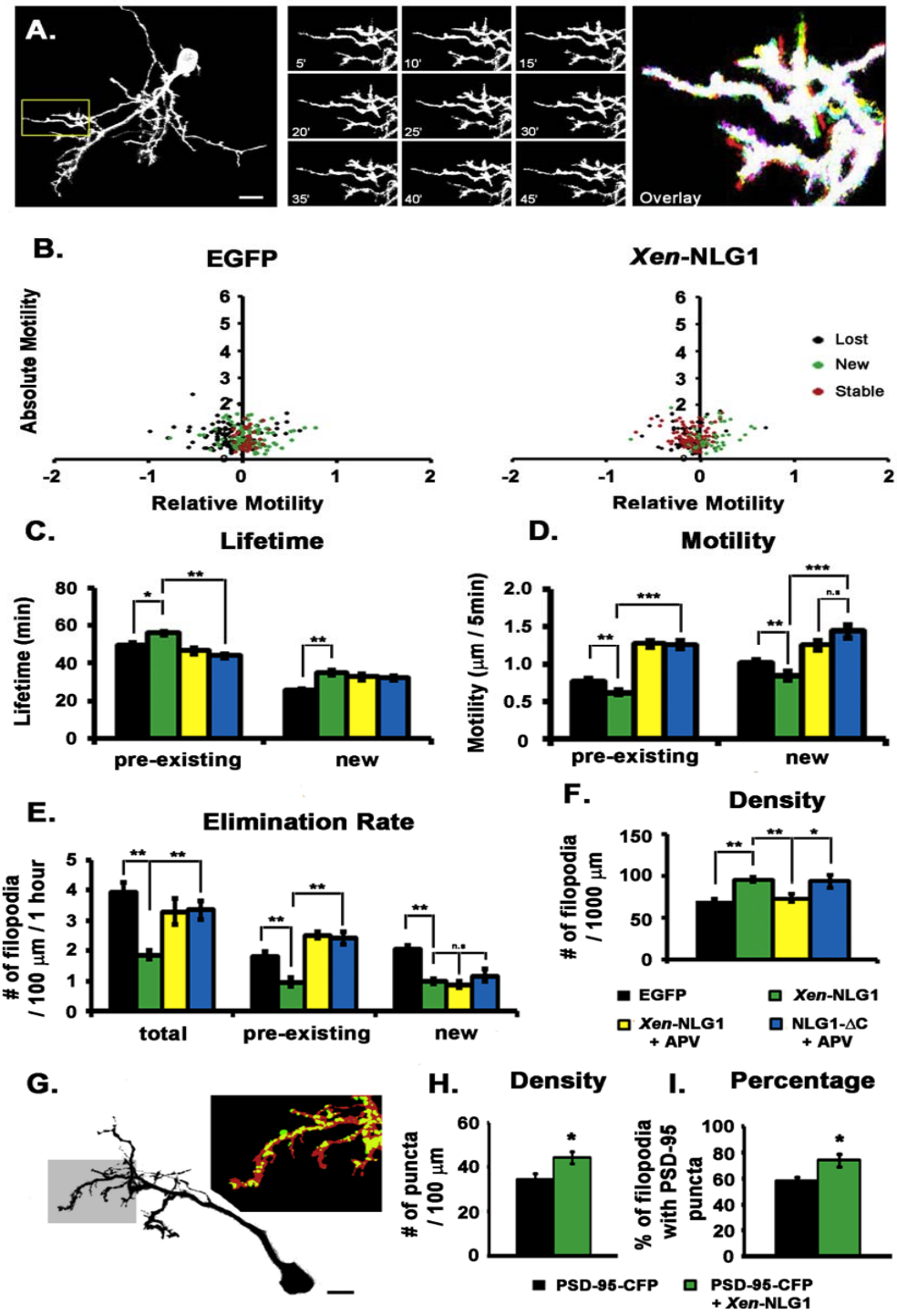
A.
5'
10'
15'
20'
25'
30'
35'
40'
45'
Overlay
B.
EGFP
Xen-NLG1
Absolute Motility
Relative Motility
Lost
New
Stable
C.
Lifetime
Lifetime (min)
pre-existing
new
D.
Motility
Motility (μm / 5min)
pre-existing
new
E.
Elimination Rate
# of filopodia / 100 μm / 1 hour
total
pre-existing
new
F.
Density
# of filopodia / 1000 μm
EGFP
Xen-NLG1
Xen-NLG1 + APV
NLG1-ΔC + APV
G.
H.
Density
# of puncta / 100 μm
PSD-95-CFP
I.
Percentage
% of filopodia with PSD-95 puncta
PSD-95-CFP + Xen-NLG1

Figure 2.6 Over-Expression of NLG1 Hyper-Stabilizes Dendritic Filopodia and Increases Postsynaptic Specializations.

(A) *Left*: Projection of tectal neuron imaged *in vivo* over-expressing *Xen*-NLG1.*Middle*: enlargement of boxed region of dendritic arbor showing images at 5 min intervals. *Right*: overlay of six successive images at 10 min intervals. Scale bar = 20 µm. **(B-I)** Morphometric analysis of dendritic filopodial dynamics of EGFP controls, neurons over-expressing *Xen*-NLG1 prior to, and after APV treatment, and NLG1-ΔC neurons treated with APV (EGFP = 11 cells, n = 407 filopodia; *Xen*-NLG1 = 5 cells, n = 227 filopodia; *Xen*-NLG1+APV = 5 cells, n = 170 filopodia; NLG1-ΔC+APV = 5 cells, n = 204). **(B)** Plots of absolute motility (mean |Δ length|) vs. relative motility (mean Δ length) for each filopodia. Positive relative motility values = extension; negative values = retraction. Filopodia are separated into 3 groups: '*stable*' = filopodia present over the entire 1 h imaging period (red); '*new*' = filopodia not present at initial image, but emerging within 1h (green); and '*lost*' = filopodia present at the initial image but eliminated within 1h (black). **(C)** Average lifetimes, **(D)** absolute motility, **(E)** number of filopodia eliminated every 5 min, and **(F)** filopodial density of *pre-existing* and *new* filopodia. **(G)** *Left:* Representative neuron expressing YFP, PSD-95-CFP, and *Xen*-NLG1. *Right:* enlargement of boxed region of dendritic arbor demonstrating high density of postsynaptic specializations. Scale bar = 20 µm **(H)** Puncta analysis reveals an increase in PSD-95 puncta in neurons expressing *Xen*-NLG1 (N = 4 cells) compared to control neurons (N = 5 cells). **(I)** Percentage of dendritic filopodia possessing PSD-95 puncta. *p < 0.05, **p < 0.01, ***p < 0.001. Error bars indicate SEM

2.4.4. Knock-down of NLG1 blocks dendritic filopodia stabilization

Morpholino oligonucleotides (MO) were designed to selectively reduce expression of *Xenopus* NLG1 (MO-NLG1) and as controls (MO-control) whose sequence does not correspond to any known *Xenopus* mRNA (Fig. 1D). Single-cell electroporation was used to introduce the fluorescent dye Alexa Fluor 488 along with lissamine–tagged MO into individual immature neurons. I first examined filopodia

dynamics in MO-labeled neurons using *in vivo* rapid time-lapse imaging every 5 min for 1 h. I found that delivery of MO-NLG1 targeting NLG1 mRNA produced simple dendritic arbors compared to MO-control neurons (**Figure 2.7A and 2.7B**; MO-control: N = 6 cells, n = 182 filopodia; MO-NLG1: N = 6 cells, n = 100 filopodia). Detailed analysis showed that MO-NLG1 neurons had significantly lower filopodial density (**Figure 2.7C**), and rates of addition (**Figure 2.7F**) and elimination (**Figure 2.7G**). Moreover, filopodia in MO-NLG1 neurons demonstrate reduced stabilization, similar to filopodia on NLG1-swap neurons, evident by high motility (**Figure 2.7E**) and short average lifetimes (**Figure 2.7D and Table 2.1**). Whole-cell patch clamp recordings of the MO-NLG1 neurons have also revealed a significant decrease in both the frequency and amplitude of AMPA receptor-mediated mEPSCs, demonstrating reduced synapse number and impaired synaptic transmission in these simple-arbor neurons (**Figure 2.7H – 2.7J**).

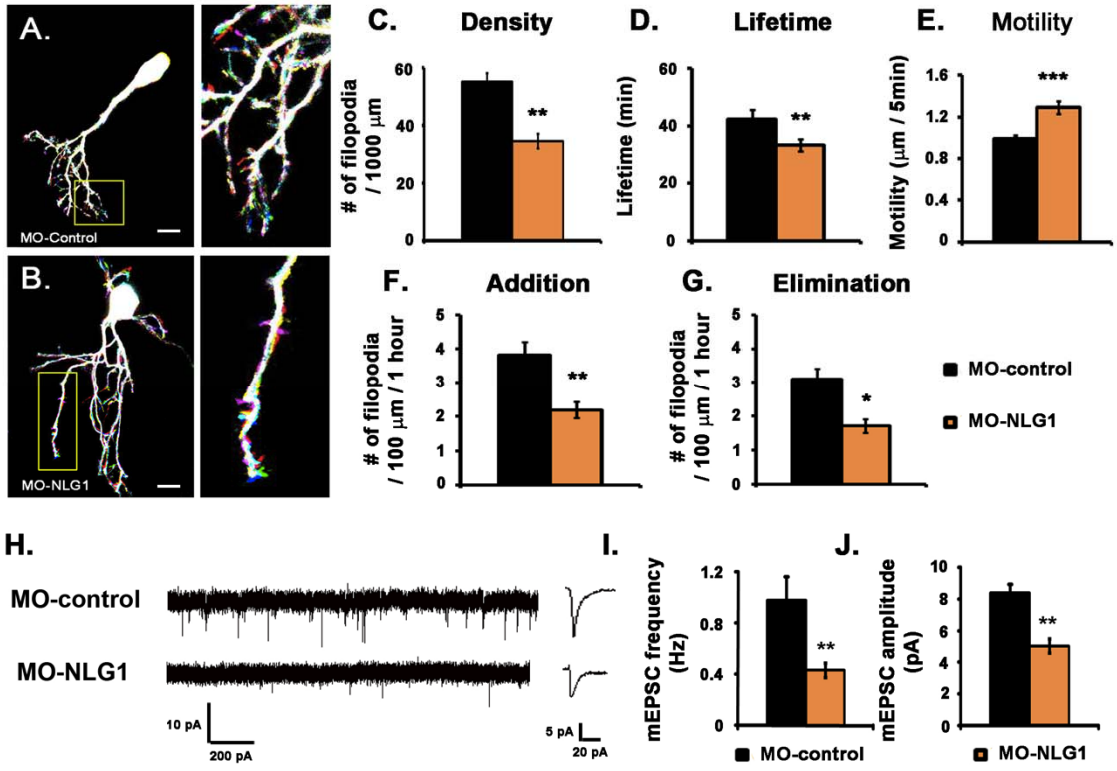

Figure 2.7 Morpholino-Mediated Knockdown of NLG1 Inhibits Dendrite Growth and Impairs Synaptic Transmission

(A-B) *Left*: Single neurons imaged *in vivo* filled with Alexa Fluor 488 dextran and the Morpholino oligonucleotides MO-control or MO-NLG1. Scale bar = 20 m. *Right*: overlays of boxed region of 6 successive images at 10 min intervals. **(C-G)** Morphometric analysis of dendritic filopodial dynamics of MO-control or MO-NLG1 neurons (MO-control = 6 cells, n = 182 filopodia; MO-NLG1 = 6 neurons, n = 100 filopodia). **(C)** Average density, **(D)** lifetime, **(E)** absolute motility, **(F)** addition rates, and **(G)** elimination rates of filopodia from 5min interval imaging over 1 h. **(H)** Representative raw and averaged traces of AMPA receptors mEPSCs from MO-control (N = 10 cells) or MO-NLG1 (N = 11 cells). **(I-J)** MO knock-down of NLG1 decreases both AMPA receptors mEPSC frequency and amplitude. *p < 0.05, **p < 0.01, ***p < 0.001. Error bars indicate SEM.

2.4.5. NRX-NLG1 adhesion creates transient stabilization

To determine whether NLG1-mediated stabilization of dendritic filopodial dynamics are due to formation of NRX-NLG1 trans-synaptic adhesion complexes or via postsynaptic protein clustering and synapse formation, I employed a NLG1 mutant able to bind NRX but unable to recruit PSD-95. I find that NLG1-ΔC neurons (N = 11 cells, n = 397 filopodia) exhibit high absolute filopodial motility, yet exhibit little net change in relative motility indicating large length fluctuation without net extension or retraction (**Figure 2.8B**). This effect is prominent in both the *stable* and *new* populations, (**Figure 2.8A and 2.8B**). Morphometric analyses show both *pre-existing* and *new* filopodia from neurons expressing NLG1-ΔC exhibited high motility, similar to NLG1-swap neurons (**Figure 2.8D**). Surprisingly, no difference was observed in the overall elimination rates between NLG1-ΔC and control neurons (**Figure 2.8E**), unlike the high elimination rates in NLG1-swap neurons (NLG1-ΔC = 3.66 ± 0.18 filopodia eliminated / 100μm / 1 hour, NLG1-swap = 13.6 ± 0.88 filopodia eliminated / 100μm / 1 hour; $p < 0.001$). Detailed analysis reveals that *pre-existing* filopodia from NLG1-ΔC neurons exhibit higher

elimination rates (**Figure 2.8E**) with shorter average lifetimes (**Figure 2.8C**), whereas *new* filopodia show reduced elimination rates (**Figure 2.8E**) and longer average lifetimes (**Figure 2.8C**). Interestingly, although *pre-existing* filopodia in NLG1-ΔC neurons had similar elimination rates to those on NLG1-swap neurons, their lifetimes were significantly longer (NLG1-swap = 36.3 ± 1.5 min, n = 197 filopodia; NLG1-ΔC = 44.4 ± 2.1 min, n = 224 filopodia; $p < 0.001$). *New* filopodia in NLG1-ΔC neurons have similar lifetimes to *Xen*-NLG1 over-expression neurons, but with significantly higher motility (NLG1-ΔC = 1.35 ± 0.04 μm / 5min, n = 127 filopodia; *Xen*-NLG1 = 0.84 ± 0.06 μm / 5min, n = 95 filopodia; $p < 0.001$). These results demonstrate that filopodia in NLG1-ΔC neurons, in general, have relatively longer average lifetimes with high motility, yet exhibit reduced capacity for stabilization. Interestingly, neurons co-expressing both NLG1-ΔC and PSD-95-CFP demonstrate an increase in filopodia number, but decreased PSD-95 density, with the majority of dendritic filopodia not possessing puncta (**Figure 2.8G – 2.8I**), suggesting that the increased lifetime phenotype does not result from the recruitment of postsynaptic scaffold proteins. Therefore, I propose a model in which upon initial contact between growing axons and dendrites, NRX and NLG1 form inter-cellular adhesion complexes that transiently stabilize the membrane to limit process elimination, but do not affect cytoskeletal dynamics necessary to provide persistent stabilization.

To test the validity of this hypothesis, I treated NLG1-ΔC neurons with soluble NRX-Fc (N = 5 cells, n = 162 filopodia) to examine whether the enhanced lifetime phenotype could be reversed. I imaged NLG1-ΔC neurons every 5 min for 2 h, in which the first hour served as an internal baseline, followed by tectal infusion of soluble NRX-Fc and imaged for another hour. Infusion of NRX-Fc increases the elimination rates of

new filopodia (**Figure 2.8E**) and decreases their average lifetimes when compared to untreated NLG1-ΔC neurons, supporting the findings in the previous section (**Figure 2.8C**). However, NRX-Fc does not affect the lifetimes or the elimination rates of *pre-existing* filopodia (**Figure 2.8C and 2.8E**), consistent with the findings that NRX-Fc preferentially interferes with the formation of new adhesion complexes between nascent axonal and dendritic filopodia.

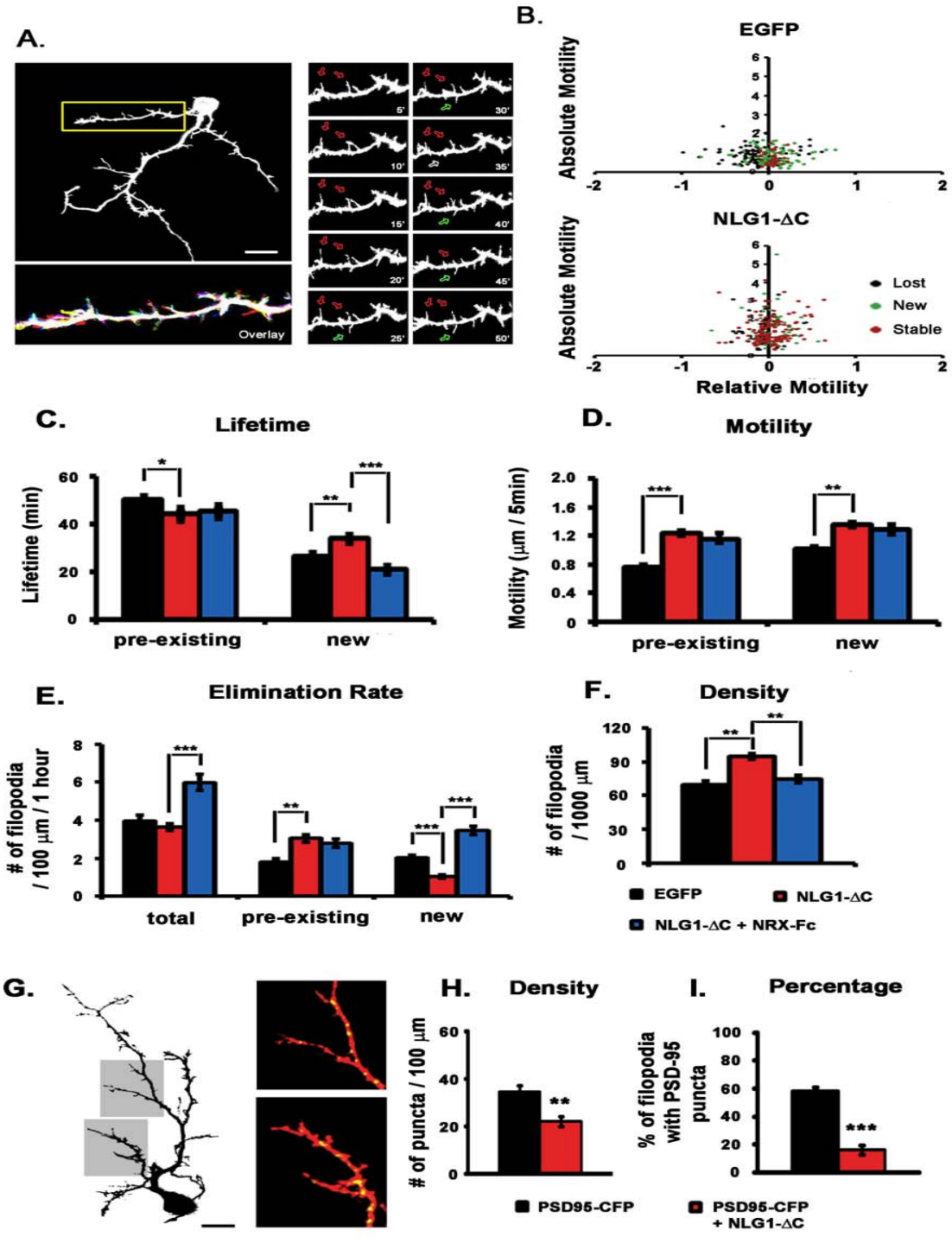
A.
Overlay
5'
10'
15'
20'
25'
30'
35'
40'
45'
50'
B.
EGFP
NLG1-ΔC
Absolute Motility
Relative Motility
Lost
New
Stable
C.
Lifetime
Lifetime (min)
pre-existing
new
D.
Motility
Motility (μm / 5min)
pre-existing
new
E.
Elimination Rate
# of filopodia / 100 μm / 1 hour
total
pre-existing
new
F.
Density
# of filopodia / 1000 μm
EGFP
NLG1-ΔC
NLG1-ΔC + NRX-Fc
G.
H.
Density
# of puncta / 100 μm
PSD95-CFP
I.
Percentage
% of filopodia with PSD-95 puncta
PSD95-CFP + NLG1-ΔC

Figure 2.8 Expressing of NLG1-ΔC Increases Filopodia Lifetime Without Persistent Stabilization and Decreases Postsynaptic Specializations

(A) *Top left*: *In vivo* image of tectal neuron expressing dominant-negative NLG1-ΔC. *Right*: enlargements of boxed region showing consecutive images every 5 min. Red open arrowheads track *stable* filopodia present throughout 1 h imaging. *Bottom left*: Overlay of 6 images at 10 min imaging interval. Scale bar: 20 μm. **(B-I)** Morphometric analysis of dendritic filopodial dynamics of EGFP controls and NLG1-ΔC neurons prior to, and after treatment with NRX-Fc (EGFP = 11 cells, n = 407 filopodia; NLG1-ΔC = 10 cells, n = 397 filopodia, NLG1-ΔC+NRX-Fc = 5 cells, n = 162 filopodia). **(B)** Plots of each filopodium's absolute motility (mean |Δ length|) vs. relative motility (mean Δ length). Filopodia are separated into 3 groups: '*stable*' = filopodia present over the entire 1 h imaging period (red); '*new*' = filopodia not present at initial image, but emerging within 1h (green); and '*lost*' = filopodia present at the initial image but eliminated within 1h (black). **(C)** Average lifetimes, **(D)** absolute motility, **(E)** number of filopodia eliminated every 5 min, and **(F)** filopodial density of *pre-existing* and *new* filopodia. **(G)** *Left:* Representative neuron expressing YFP, PSD-95-CFP, and NLG1-ΔC. *Right:* enlargements of boxed regions of dendritic arbor demonstrating low density of postsynaptic specializations. Scale bar = 20 μm **(H)** Puncta analysis reveals a decrease in PSD-95 puncta in neurons expressing NLG1-ΔC (N = 3 cells) compared to control neurons (N = 5 cells). **(I)** Percentage of dendritic filopodia possessing PSD-95 puncta. *p < 0.05, **p < 0.01, ***p < 0.001. Error bars indicate SEM.

2.4.6. NLG1 over-expression mediated filopodial stabilization requires NMDA receptor transmission

Previous studies in *Xenopus* tectum have demonstrated the importance of synaptic activity and synapse maturation in regulating dendritic growth (Haas et al., 2006; Liu et al., 2009; Rajan and Cline, 1998; Sin et al., 2002). To investigate whether NLG1-mediated dendritic filopodial stabilization is solely depended on NLG1-induced postsynaptic protein recruitment or also requires glutamatergic synaptic activity, I treated *Xen*-NLG1 neurons with the NMDA receptor antagonist APV (N = 5 cells, n = 170 filopodia). NLG1-ΔC neurons were also treated with APV as a negative control (N = 5 cells, n = 204 filopodia) since NLG1-ΔC cannot recruit PSD-95 to promote synapse

formation (Scheiffele et al., 2000; Chih et al., 2005; Nam and Chen, 2005). I imaged *Xen*-NLG1 neurons every 5 min over 2 h, in which the first hour served as an internal baseline, followed by bath application of APV (50 μM) and imaged for another hour. Strikingly, application of APV transformed hyper-stabilized *Xen*-NLG1 neurons into dynamically motile neurons (**Figure 2.6D**). APV increases the elimination rate of *pre-existing* filopodia by 77% (**Figure 2.6E**) and significantly reduces their lifetimes (**Figure 2.6C**). These data demonstrate that NLG1-mediated filopodial stabilization requires synaptic activity through NMDA receptors. Furthermore, APV does not affect the lifetimes or the elimination rates of *new* filopodia in *Xen*-NLG1 neurons (Fig. 4C, 4E), as would be expected for immature processes lacking synapses. These filopodia behave similarly to *new* filopodia on NLG1-ΔC neurons in that they were highly motile and have relatively longer lifetimes, but are not persistently stabilized (**Figure 2.6I**). I found no significant effects of APV on filopodial dynamics in NLG1-ΔC neurons, supporting the increased lifetime in immature processes being solely mediated by enhancing NRX-NLG1 adhesions, and the requirement of synapse formation and maturation for persistent filopodial stabilization. Taken together, these findings suggest a series of distinct events underlying filopodial stabilization in which the initial NRX-NLG trans-synaptic adhesion complexes provide a transient, activity-independent interaction that prevents nascent axo-dendritic contacts from separating. Subsequent synaptic protein clustering and NMDA receptor-dependent synapse maturation then confers persistent stabilization to the filopodia cytoskeleton restricting elimination.

2.4.7. NRX-NLG1 interactions influence long-term dendritic arbor patterning

To assess the long-term effects of altered NRX-NLG1 interactions on larger and persistent dendritic arbor morphology, I monitored arbor growth at 24 h intervals over 4 days. Previous studies demonstrate that newly differentiated tectal neurons grow by dramatically expanding arbor size over 4 days, after which a mature stabilized stage is reached in which no further net increase in branch length or number occur (Haas et al., 2006; Liu et al., 2009). Here, I find that over 4 days, control neurons increase arbor size and complexity, while neurons over-expressing *Xen*-NLG1 exhibit restricted arbor growth (**Figure 2.9A and 2.9B**). Although the arbor size of *Xen*-NLG1 neurons was smaller than controls, the number of filopodia in *Xen*-NLG1 was significantly higher (**Figure 2.9C**), resulting in the formation of spatially restricted, but more complex arbors (**Figure 2.9D**). Long-term imaging demonstrates that filopodial hyper-stabilization restricts filopodial transitions into longer branches. In order to identify structural changes in neurons lacking endogenous NLG1, I monitored long-term structural changes in MO-NLG1 neurons at 24 h intervals over 4 days (**Figure 2.9E**). MO-NLG1 neurons develop simple arbors with significantly reduced total dendritic branch length and filopodia density (**Figure 2.9F and 2.9G**), with reduced arbor complexity evident from 3D Sholl analysis (**Figure 2.9H**).

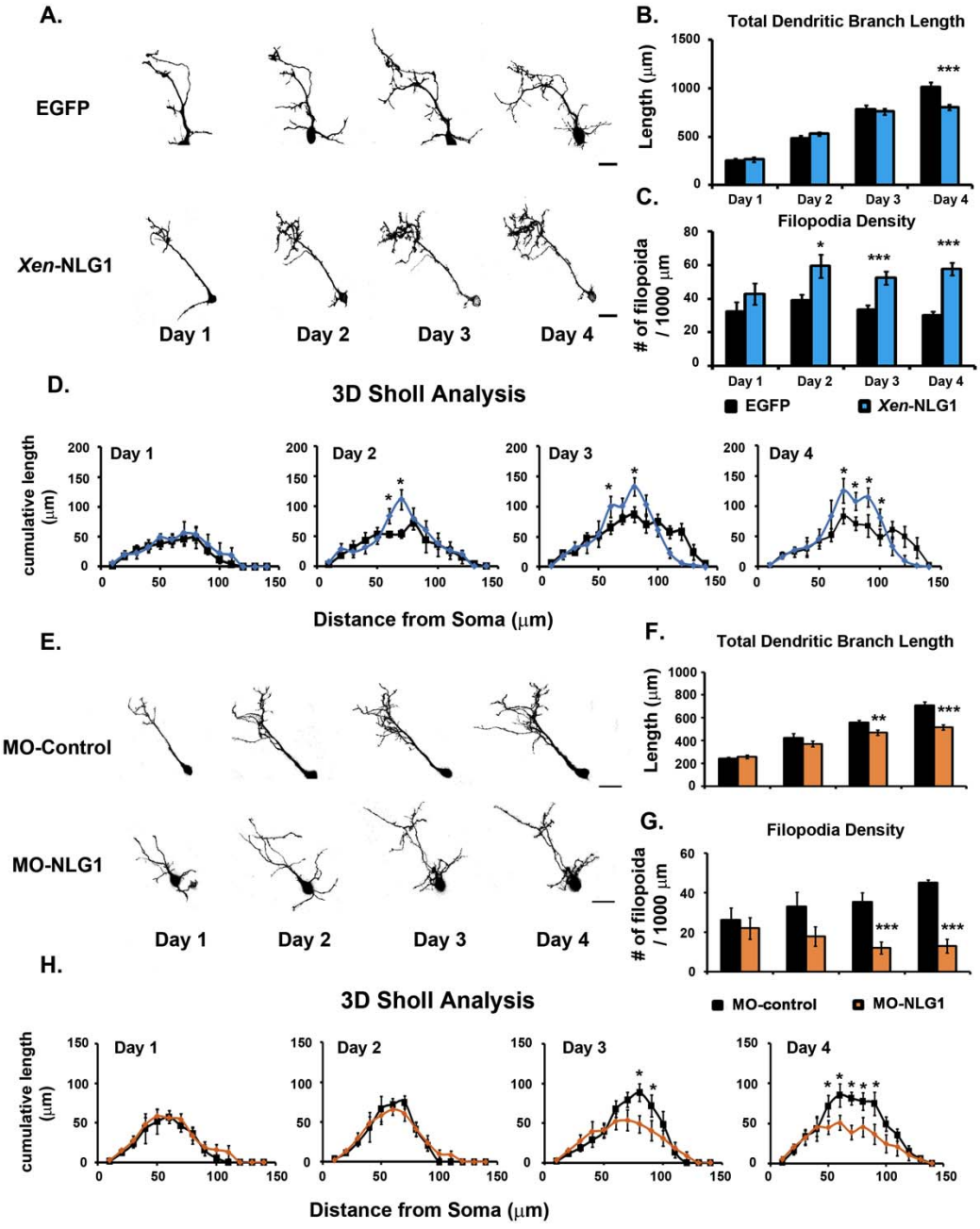

Figure 2.9 NRX-NLG1 Interactions Influence Long-Term Dendritic Arbor Patterning.

(A) *In vivo* time-lapse images of neurons expressing EGFP (control, N = 7 cells) and *Xen*-NLG1 (N = 8 cells) acquired at 24 h intervals over 4 days. Scale bar = 40 m **(B-D)** 3D morphometric analysis shows over-expressing *Xen*-NLG1 decreases total dendritic branch length **(B),** but increases dendritic filopodial density **(C),** and local complexity shown with 3D Sholl analysis **(D)**.

(E) *In vivo* time-lapse images of MO-control (N = 6 cells) and MO-NLG1 neurons (N = 7 cells) acquired at 24 h intervals over 4 days. Scale bar = 40 m. **(F-H)** 3D morphometric analysis shows that MO knock-down of NLG1 inhibits dendrite growth by decreasing both total dendritic branch length **(F)** and filopodia density **(G)**, resulting in formation of simple dendritic arbors with decreased 3D Sholl complexity **(H)**. *p < 0.05, **p < 0.01, ***p < 0.001. Error bars indicate SEM.

2.5. Discussion

In this chapter, I have examined the contribution of the cell adhesion molecules NRX and NLG1 to synaptotropic dendritic arborization. Genetic deletion of NLG1 in mice (NLG1-KO) has been shown to reduce glutamatergic synapse maturation and inhibit long-term synaptic plasticity in CA1 pyramidal neurons of the hippocampus (Blundell et al.; Chubykin et al., 2007), as well as producing behavioral deficits and reduced spatial learning and memory (Blundell et al.). It remains untested, however, whether altered neuronal morphogenesis contributes to these functional abnormalities. Neuronal morphology is a critical component of brain development with important impact on mature brain circuit function. Direct *in vivo* imaging of brain neuron growth within unanaesthetized vertebrate embryos provides unpredicted insights into neuronal structural development within intact native tissue environments (Liu et al., 2009). Rapid time-lapse imaging reveals that dendritic arbor growth involves a remarkable degree of turnover, with rapid extension and retraction of short filopodia and longer branches, suggesting searching of the local environment for scarce factors required for stabilization. During early neuronal morphogenesis, dendritic filopodia are precursors of persistent branches; hence, quantification of these dynamic filopodial behaviors and identification of molecular mechanisms underlying filopodial stabilization are required to

understand how filopodia probe for optimal synapse formation and how they contribute to mature dendritic arbor patterning. Here, using novel methods of dynamic morphometrics for comprehensive 3D quantification of rapid and long-term dendritogenesis, I have characterized a multi-step process by which the cell adhesion molecules NRX and NLG1 regulate filopodia dynamic behavior with long-term consequences to dendritic arbor morphogenesis.

Dendritic filopodia mediating dendritic branch formation demonstrate a range of behaviors that shift over time as they make contact with axons and form synapses. Upon first emerging from dendritic shafts, nascent filopodia lack synapses and display rapid extension and retraction (**Figure 2.3B**). The results in this chapter demonstrate that upon first contact between dendritic filopodia with axons, trans-synaptic NRX-NLG1 binding rapidly creates adhesions. Blocking adhesion formation with extracellular soluble NRX-Fc or postsynaptic expression of NLG1-swap dramatically destabilizes nascent dendritic filopodia, evident from increased elimination rates and decreased lifetimes. Expression of NLG1-ΔC enhances NRX-NLG1 adhesions without allowing synapse formation, resulting in high filopodial motility, yet with increased lifetimes. The elimination of NLG1-ΔC-induced enhanced lifetimes by application of soluble NRX-Fc supports endogenous NRX interactions with NLG mediating this effect, rather than non-specific binding. Furthermore, the NLG1-ΔC phenotype resembles expression of *Xen*-NLG1 in the presence of NMDA receptor blockade, consistent with both manipulations enhancing adhesions without postsynaptic development. From these results, I postulate that NRX-NLG1 adhesions create membrane-based stabilizations that provide tension and traction forces to temporarily restrict rapid filopodial retraction and elimination, yet are insufficient to stabilize the cytoskeleton necessary for altered motility. Similar phenomena have

been observed in studies of cell migration where filopodia from adjacent cells form adhesion complexes following initial contact creating short-lived support independent of cytoskeletal stabilization that provides traction for further movement (Mattila and Lappalainen, 2008; Zamir and Geiger, 2001).

In addition to forming trans-synaptic adhesions, cell adhesion molecules can function as nucleators to recruit and cluster proteins associated with synaptogenesis. A role for NRX-NLG interactions in synaptogenesis *in vivo* in the developing *Xenopus* retinotectal system is supported by endogenous interactions between NLG1 and PSD-95 identified by co-immunoprecipitation, and localization of NLG1 at postsynaptic sites. Furthermore, decreases in synapse density and AMPA receptor-mediated mEPSC frequency following tectal infusion of soluble NRX-Fc are consistent with previous findings that NRX-NLG1 interactions are critical for excitatory synapse formation and function in mammalian neurons (Levinson et al., 2005; Nguyen and Sudhof, 1997; Scheiffele et al., 2000). However, triple knockout of NLG1/2/3 in mice produced no change in synapse density in cortex, potentially suggesting compensation not possible with acute NRX-Fc exposure or transfection of post-differentiated neurons in developing tectum. The roles of NRX-NLG1 interactions in pre- and postsynaptic differentiation and synaptic functions have also been shown in *Drosophila*, suggesting that the fundamental aspects of NRX and NLG are widely conserved across species (Banovic et al.). Hence, I further tested the roles of NRX-NLG-mediated coalescence of postsynaptic proteins and synapse formation in filopodial growth dynamics by comparing effects of expression of NLG1-ΔC to over-expression of *Xen*-NLG1. Exogenous expression of *Xen*-NLG1, which increases both adhesions and downstream synapse formation, produces abnormal hyper-stabilization of dendritic filopodia and increased PSD-95 puncta density. However,

expression of NLG1-ΔC, which increases adhesion formation but restricts development of postsynaptic specializations, does not induce hyper-stabilization and reduces density of postsynaptic specializations.

Strikingly, *Xen*-NLG1 induced filopodial hyper-stabilization can be reversed by inhibition of NMDA receptor-mediated transmission. Thus, I conclude that NRX-NLG1-mediated persistent filopodial stabilization requires activity-dependent synapse maturation. Although PSD-95 binds to both NLG1 (Irie et al., 1997) and scaffolding proteins (Kim and Sheng, 2004), providing a link between NLG1 and the actin cytoskeleton, this association is insufficient to promote transition from motile and short-lived filopodia to non-motile and persistently stabilized processes. The findings here agree with previous studies in *Xenopus* tectum that synaptic activity and synapse maturation regulate dendrite growth by conferring morphological stabilization. Natural visual experience that enhances tectal afferent innervations increases tectal synapse number and strength (Aizenman and Cline, 2007), which in turn promotes dendritic branch stabilization (Sin et al., 2002). Conversely, blocking synapse maturation by NMDA receptor blockade or interfering with AMPA receptor trafficking into synapses reduces filopodial stabilization and dendritic arbor elaboration, and blocks visual stimulation-induced dendrite growth (Haas et al., 2006; Rajan and Cline, 1998; Sin et al., 2002).

The synaptotropic hypothesis of dendrite growth states that synapse formation stabilizes filopodia to prevent retraction and promotes transition into longer and more persistent dendritic branches, culminating over time into increased complexity and size of the entire arbor. The work here further expands this model by identifying three distinct mechanisms by which the cell adhesion molecules NRX and NLG contribute to dendritic

filopodial stabilization (**Figure 2.10**). In the initial step, upon nascent axonal-dendritic contact, NRX and NLG1 create membrane-based adhesions that confer transient stabilization to prevent rapid filopodial retraction. Subsequently, NLG1 clustering promotes recruitment and coalescence of postsynaptic proteins through its intracellular PDZ domain. These nascent synapses may be 'silent' synapses containing only NMDA receptors (Nam and Chen, 2005). Neuronal transmission is then necessary to drive activity-dependent synapse maturation likely involving insertion of AMPA receptors into the developing synapses (Heine et al., 2008; Wu et al., 1996). Synapse maturation then confers local stabilization to the cytoskeleton, preventing filopodial retraction and promoting further elongation and transition into branches (Haas et al., 2006; Niell, 2006; Niell et al., 2004; Rajan and Cline, 1998; Sin et al., 2002).

Moreover, an unforeseen result was observed when *Xen*-NLG1 neurons were monitored at 24h intervals over 4 days. While MO knockdown of NLG1 expression results in formation of simple dendritic arbors, consistent with α-NRX double knockout mice that exhibit shortened dendritic branches in hippocampal pyramidal neurons (Dudanova et al., 2007), over-expressing *Xen*-NLG1 results in stunted dendritic arbors with increased complexity. Although a simple interpretation of the synaptotropic model would predict that manipulations that increase synapse formation would promote formation of larger dendritic arbors, excessive NRX-NLG1 mediated synaptogenesis results in hyper-stabilization of the cytoskeleton and loss of growth plasticity. These findings are consistent with excessive stabilization of dendritic growth produced by PKMz enhancement of synaptogenesis (Liu et al., 2009), and suggest a graded effect relating synapse maturation to morphological stabilization. In this modification of the synaptotropic model, immature synapses confer sufficient stabilization to prevent

process retraction and elimination, while allowing continued dynamic extension from the site of the synapse. Mature synapses, however, further stabilize to prevent all morphological plasticity. This model explains the loss of dendritic arbor plasticity as neurons mature and excitatory synapses undergo maturation.

An important implication inherent to the synaptotropic hypothesis is that activity-dependent competition-based synaptogenesis directs elaboration of the dendritic arbor, promoting structures optimized for processing patterned activity experienced during growth. Since deletion of NLG1, both *in vitro* and *in vivo*, alters synaptic function (Blundell et al., 2010; Chih et al., 2005; Chubykin et al., 2007), cell-autonomous interference with NLG1 is expected to reduce glutamatergic synapse function leading to altered synaptogenesis and synaptotropic growth due to competition with surrounding normal neurons, resulting in simplified mature arbor patterns. However, different cell-autonomous molecular perturbations of synaptic function yield distinct morphological phenotypes, demonstrating specific contributions by each molecular component to growth rather than a simple effect based on altered glutamatergic synapse function. Manipulations that reduce CaMKII or PKMz activity, or prevent the delivery of AMPA receptors to synapses lead to different patterns of abnormal branch elaboration (Haas et al., 2006; Liu et al., 2009; Zou and Cline, 1999), suggesting that synaptotropic-driven dendritic arborization is a complex and multi-step process and interference with synaptogenesis at different stages results in distinct dendritic growth patterns. Hence, results in this chapter add another layer of complexity to the synaptotropic model of dendritogenesis and demonstrate how cell adhesion molecules play a critical role in brain circuit structural development. Disruption of normal cell adhesion interactions,

therefore, may produce persistent abnormal neural circuit structures leading to lasting dysfunction.

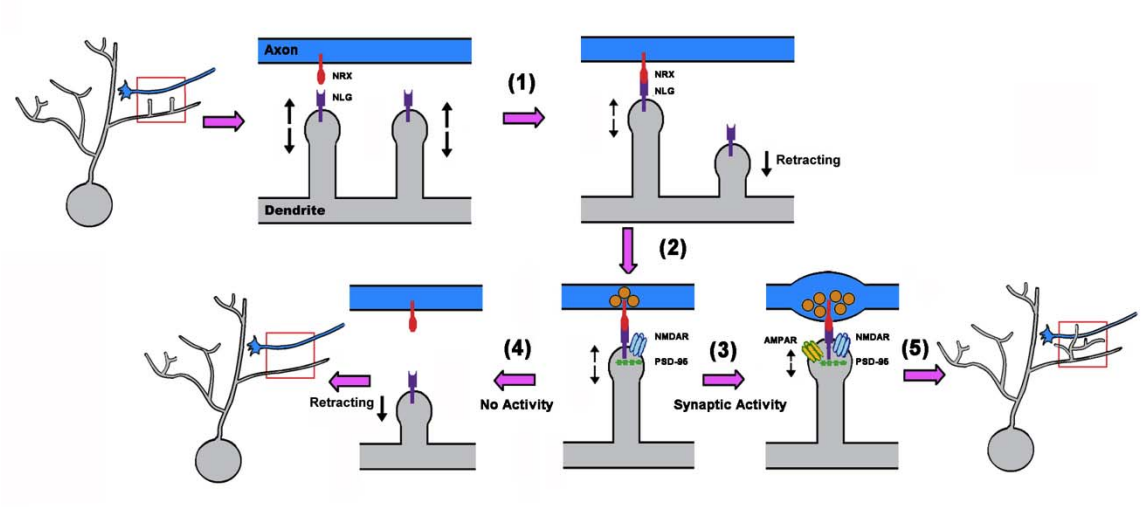

Figure 2.10 Model of NRX-NLG1 Regulation of Dendritogenesis

NRX-NLG1 interactions regulate dendritic filopodial stabilization through a multi-step process: **(1)** Upon nascent axonal-dendritic contact, NRX and NLG1 create adhesions that confer transient membrane stabilization to prevent rapid filopodial retraction; **(2)** NLG1 clustering then promotes coalescence of postsynaptic proteins, including PSD95 and NMDA receptors, through its intracellular PDZ domain; **(3)** filopodia receiving strong neuronal transmission become stabilized, and **(4)** those that do not receive sufficient input disassemble. **(5)** Synapse maturation confers local stabilization of cytoskeleton, which promotes further elongation.

Fast Imaging	Density	Addition Rate	Filopodial Elimination Rate			Filopodial Lifertime			Filopodial Motility		
			Total	Pre-existing	New	Total	Pre-existing	New	Total	Pre-existing	New
NRX-Fc	↓	NC	↑↑	↑	↑		↓	↓		NC	↑
NLG1-SWAP	↑	↑↑	↑↑	↑	↑		↓	↓		↑	↑
NLG1-ΔC	↑	↑	NC	↑	↓		↓	↑↑		↑	↑
NLG1-ΔC + NRX-Fc	↓	NC	↑↑	↑	↑		NC	↓		NC	NC
WT-NLG1	↑	NC	↓↓	↓	↓		↑	↑		↓	↓
WT-NLG1 + APV	↓	NC	↑	↑	NC		↓	NC		↑	↑
NLG1-ΔC + APV	NC	NC	NC	NC	NC		NC	NC		NC	NC
MO-NLG1	↓	↓	↓			↓			↑		

PSD-95 puncta imaging	PSD-95 puncta density	Percentage of dendritic filopodia with PSD-95 puncta
NLG1-swap	↓	↓
WT-NLG1	↑	↑
NLG1-ΔC	↓	↓

8-hour Imaging	TDBL	Skeletal TDBL	Filopodial Density	PSD-95 puncta density
NRX-Fc	↓	NC	↓	↓
D137A NRX-Fc	NC	NC	NC	NC

Immuno	SNAP-25	PSD-95	Colocalization	Probability of Colocalization
NRX-Fc	NC	↓	↓	↓
D137A NRX-Fc	NC	NC	NC	NC

Electrophysiology	mEPSC frequency	mEPSC amplitude
NRX-Fc	↓	NC
D137A NRX-Fc	NC	NC
MO-NLG1	↓	↓

4-day Imaging	TDBL	Branch length	Filopodial Density	Arbor Complexity
WT-NLG1	↓	↓	↑	↑
MO-NLG1	↓	↓	↓	↓

Table 2.1. Summary of the Effects of Different NLG1 Constructs on Filopodial Dynamics, Arbor Growth, and Synapses.

3. THE TRANSCRIPTIONA FACTOR MEF2 IS A MASTER REGULATOR OF VISUAL EXPERIENCE-DRIVEN FUNCTIONAL AND STRUCTURAL METAPLASTICITY IN THE DEVELOPING BRAIN

Natural sensory input shapes both structure and function of developing neurons, but how early experience-driven morphological and physiological plasticity are inter-related remains unclear. Using rapid time-lapse two-photon calcium imaging of network activity and single neuron growth within the unanesthetized developing brain, I demonstrated that natural visual stimulation induces coordinated changes to neuronal responses and dendritogenesis. Further, we identify the transcription factor MEF2A/2D as a major regulator of neuronal response to plasticity-inducing stimuli directing both structural and functional changes. Unpatterned sensory stimuli that changes plasticity thresholds induces rapid degradation of MEF2A/2D through a classical apoptotic pathway requiring NMDA receptors and caspases-9 and 3/7. Knockdown of MEF2A/2D alone is sufficient to induce a metaplastic shift in threshold of both functional and morphological plasticity. These findings demonstrate how sensory experience acting

through altered levels of the transcription factor MEF2 fine-tunes the plasticity thresholds of brain neurons during neural circuit formation.

3.1. Specific Background

3.1.1. Transcription Factor MEF2

MEF2 (myocyte enhancer factor 2) belongs to a family of MADS (MCM1, Agamous, Deficiens, and Serum Response Factor) box transcription factors (Olson et al., 1995; Shalizi and Bonni, 2005). Through evolution, *C. elegans* and *D. melanogaster* only contain with one isoform of MEF2, and vertebrates express four different MEF2 isoforms (MEF2A, 2B, 2C, and 2D). The N-terminus of MEF2 contain a MADS box, which is conserved between species, and it is located adjacent to the MEF2 domain. The MEF2 domain is important for dimerization, DNA binding, and co-factor interactions (Black and Olsen 1998, McKinsey 2002). The C-terminal region of MEF2 is the transcription activation domain, where it became extremely diverse between species and it can undergo extensive alternate splicing to create complex pattern of gene transcription (Black and Olson, 1998; McKinsey et al., 2002). MEF2 is known for regulating genes involved in cellular differentiation and development, and is well characterized in both rodent and *Xenopus* for its role in directing muscle cell differentiation by working in coordination with other MyoD family proteins (della Gaspera et al., 2009; Molkentin et al., 1995). Conditional knockout of MEF2C after skeletal muscle differentiation results in disorganized sacromeres in muscle fibers (Potthoff et al., 2007).

MEF2 factors also play important roles in the central nervous system. Different MEF2 family members (MEF2A, 2C, and 2D) were detected in the mouse brain using *in situ* hybridization and immunohistochemistry, and found to be expressed in unique but overlapping patterns in different areas in the brain (Lyons et al., 1995). The transcriptional activity of MEF2 is activity-regulated, in which membrane depolarization in cultured neurons using KCl stimulation increases MEF2 transcriptional activity through calcium influx via L-type voltage-gated calcium channels (Mao et al., 1999) and calcineurin activation (Mao and Wiedmann, 1999). The Greenberg Lab has shown that in response to membrane depolarization, MEF2 is activated by dephosphorylation to promote the transcription of genes such as *arc* and *synGAP* and negatively regulate excitatory synapse number (Flavell et al., 2006; Flavell et al., 2008). Furthermore, MEF2 has been implicated in regulating dendritogenesis through its control over expression of a cluster of microRNAs (miR379-410), which in turn, inhibit the translational repressor Pumilio2 (Fiore et al., 2009). A link between MEF2-regulation of structural and functional plasticity has been demonstrated in mouse. Increasing MEF2-dependent transcription reduced synapse number in the anterior cingulate cortex and also blocked consolidation of contextual fear memory and subsequent memory expression (Vetere et al., 2011). MEF2 also serves as a pro-survival factor, in that upon insult, MEF2 is cleaved by caspases into fragments. The reduction in MEF2 levels and the formation of cleaved fragments, act as dominant-negative to bind to the remaining intact MEF2, are sufficient to block the prosurvival effects of MEF2 by decreasing its transcription activity and lead to apoptotic cell death. Expression of caspase-insensitive MEF2 in neurons reduces the effects of excitotoxity on cell death (Li et al., 2001; Okamoto et al., 2002).

3.2. Introduction

The developing brain is extremely plastic, undergoing both functional and structural changes to adapt to novel sensory inputs (Cline and Haas, 2008; Katz and Shatz, 1996). As neural circuits form, functional plasticity including synaptogenesis (Chen et al., 2010; Niell et al., 2004), altered synaptic strength (Wu et al., 1996; Zhou et al., 2003), and maturation of neuronal receptive fields (Dunfield and Haas, 2009; Engert et al., 2002; Sakaguchi and Murphey, 1985) coincide with extensive growth and turn-over of axonal and dendritic processes (Haas et al., 2006; Ruthazer et al., 2003; Sin et al., 2002). However, the relationship between these physiological and morphological changes and the molecular mechanisms coordinating them remain poorly understood. In the mature brain, functional neuronal plasticity has been well characterized, such as activity-dependent long-term potentiation and depression of synaptic strength (LTP/LTD). Recent evidence supports morphological correlates of LTP and LTD primarily involving changes in number or morphology of dendritic spines, without alterations of larger dendritic arbor structures (Hofer et al., 2009; Trachtenberg et al., 2002; Zhou et al., 2004). However, such direct evidence for a relationship between functional and structural plasticity of dynamic neural circuit formation during early brain development is lacking.

One hallmark of plasticity is that synapses and neurons can shift their response to plasticity-inducing stimuli based on their recent history of activity (Abraham et al., 2001; Bienenstock et al., 1982; Dunfield and Haas, 2009; Lee et al., 2010; Philpot et al., 2003). Activity-dependent regulation of neuronal plasticity, termed 'metaplasticity', may act to prevent runaway potentiation or depression leading to plateau levels. This maintains neuronal responses within a physiological range, enabling further plasticity in

response to future experience (Abraham, 2008). Such mechanisms may be especially critical in the developing brain during heightened periods of synaptic and morphological plasticity. While development of models to investigate metaplasticity has been limited, a robust shift in visual experience-driven functional plasticity can be elicited in the *Xenopus laevis* tadpole optic tectum by brief exposure to unpatterned white noise (WN) visual stimuli that increases circuit activity without inducing plasticity by itself (Dunfield and Haas, 2009). In this chapter, I used *in vivo* two-photon calcium imaging of tectal network activity and rapid time-lapse imaging of individual growing tectal neurons within the intact and unanesthetized brain to identify morphological correlates of functional potentiation, depression, and metaplasticity during critical periods of neural circuit formation. By employing novel methods of dynamic morphometrics to identify, track, and measure growth of all dendritic processes in 3D over periods of hours, I found that functional potentiation and depression are associated with stabilization and destabilization of newly formed dendritic processes, respectively. Furthermore, I found evidence for 'structural metaplasticity' analogous to functional metaplasticity since WN does not alter dendritic growth patterns by itself, but shifts the growth response to subsequent plasticity-inducing stimuli.

I also identified the transcription factor myocyte enhancer factor 2 (MEF2) as a central regulator of both functional and structural metaplasticity, employing a molecular cascade associated with apoptotic cell death pathways. The MEF2 proteins (MEF2A-D) belong to a family of MADS (MCM1, Agamous, Deficiens, and Serum Response Factor) box transcription factors that were originally identified as regulators for muscle cell differentiation and development (Olson et al., 1995; Shalizi and Bonni, 2005). MEF2 proteins are also highly expressed throughout the developing brain and have been implicated in the activity-dependent regulation of dendritic morphogenesis (Fiore et al.,

2009; Shalizi et al., 2006), synapse and spine number, and learning and memory (Barbosa et al., 2008; Flavell et al., 2006; Vetere et al., 2011), through a mechanism involving calcineurin-mediated dephosphorylation of MEF2 protein.

I identified a novel function for MEF2 in the developing brain in which its expression level establishes the metaplastic state, or plasticity threshold, dictating neuronal susceptibility to plasticity-inducing sensory stimuli. In accordance with theoretical models of metaplasticity (Bienenstock et al., 1982), MEF2 levels are regulated by sensory stimulation that increases neuronal firing in an N-methyl-D-aspartate type glutamate receptor (NMDAR)-dependent manner. Brief periods of unpatterned WN visual stimuli that induces changes in the plasticity threshold produces a rapid and temporary loss of MEF2 protein through transient activation of caspases-9, 3, and 7, with a time course matching the duration of the plasticity changes. Although activity-driven caspase degradation of MEF2 has been associated with triggering neuronal apoptosis, we see no increase in cell death. Furthermore, I found that reduction of MEF2 alone without WN stimuli is sufficient to induce a metaplastic shift in both functional and structural plasticity. Together, these findings demonstrate that enhanced neural activity driven by unpatterned sensory experience induces persistent alteration in neuronal susceptibility to subsequent sensory-driven plasticity of both functional responses and morphologic growth. This shift in plasticity threshold is initiated by NMDAR activation of a caspase-MEF2 signaling cascade previously identified as an excitotoxic apoptotic pathway.

3.3. Material and Methods

3.3.1. Animals

Freely swimming albino *Xenopus laevis* tadpoles were reared in 10% Steinberg's solution at 22°C on a 12 hr light/dark cycle. Experiments were performed on Stage 50tadpoles (Nieuwkoop and Faber, 1967). All experimental procedures were conducted according to the guidelines of the Canadian Council on Animal Care, and were approved by the Animal Care Committee of the University of British Columbia.

3.3.2. Western blotting

Tadpoles were anesthetized with 0.02% 3-aminobenzoic acid ethyl ester (MS-222, Sigma), sacrificed, and brains were dissected and the optic tectum homogenized in lysis buffer (50mM Tris-HCl, 1X protease inhibitor cocktail (Roche Products, Welwyn, Garden City, UK), 1% Triton X-100, pH 7.4). Protein homogenates were separated on a 8.0% Bis-Tris acrylamide gel (Invitrogen, Carlsbad, CA), transferred to nitrocellulose membrane, blocked in 5% non-fat milk with 0.1% Tris-buffered saline (TBS), and incubated with primary antibodies diluted in blocking solution. Blots were rinsed and incubated with HRP-linked secondary antibodies, and imaged using chemiluminescence (BioRad, Hercules, CA). Mouse pan anti-MEF2 monoclonal (Santa Cruz Biotechnology, Santa Cruz, CA), rabbit anti-MEF2A polyclonal (Santa Cruz Biotechnology, Santa Cruz, CA), mouse anti-MEF2D monoclonal (BD Biosciences, Lexington, KY), and rabbit anti-cleaved caspase-3 polyclonal antibodies (Cell Signaling, Danvers, MA) were used.

3.3.3. *In vivo two-photon calcium imaging*

Oregon Green Bapta-1 AM (Molecular Probes, Eugene, OR) was prepared in 10mM DMSO with 20% pluronic acid (Molecular Probes) and further diluted 10:1 in Ca^{2+}-free Amphibian Ringers solution (in mM): 116 NaCl, 1.2 KCl, 2.7 $NaHCO_3$. Dye solution was slowly delivered from a micropipette into the optic tectum using low pressure (<10 psi) over 5 min using a Picospitzer III (General Valve Corporation, Fairfield, NJ), and following injection tadpoles were returned to bath solution. One hour following OGB1-AM loading, tadpoles were immobilized using brief (5 min) exposure to the reversible paralytic pancuronium dibromide (PCD, 2mM, Tocris), and embedded under a thin layer of agarose (1.0%, prepared with 10% Steinberg's solution) in a Sylgard imaging chamber continuously perfused with oxygenated Steinberg's solution at room temperature (22^{o}C). Images were acquired by a custom-built two-photon laser-scanning microscope, constructed from an Olympus FV300 confocal microscope (Olympus, Center Valley, PA) and a Chameleon XR laser light source (Coherent, Santa Clara, CA). Optical sections through the tectum were captured using a 60X, 1.1NA, water immersion objective (LUMPlanFI, Olympus), and images were recorded using Fluoview software (Olympus). The optic tectum was imaged at a resolution of 640 x 480 pixels and zoom factor of 1.5X, encompassing a region of interest of 177 x 133 μm, allowing simultaneous imaging of ~100 neurons in a single X-Y scan at a rate of 1.2 sec per frame using a wavelength of 910 nm. Vivo-morpholino control or vivo-MO-MEF2A/2D were also infused by low pressure injection into the tectum 24 hr prior to imaging experiments.

3.3.4. Visual stimulation and training

Visual stimuli were applied by a diode (590 nm) placed close to tadpole's eye and whole-field light stimulation was controlled by custom written software (Matlab, The Matworks Inc., Natick, MA). Three training stimuli were employed: i) Invariant Training (IN) consists of 25 min ON light stimulation, ii) Spaced Training (ST) consists of three sets of 90 50 msec OFF stimuli at 0.3 Hz, spaced by 5 min intervals, iii) White Noise (WN) stimulation consists of 60 min of wide-field random variation of the diode voltage and duration between empirically determined maximum and minimum intensity values within the diode's linear range.

3.3.5. Fluorescence data processing

Fluorescence data stacks were X-Y aligned using Tuboreg (ImageJ, NIH). Custom-written software was used to identify and track regions of interests (ROIs) encompassing each cell body from Ca^{2+} imaging over the course of each experiment (Podgorski et al., 2011). The fluorescence time series for each cell was then calculated as $(F\text{-}F_0/F_0)$. The time-varying baseline fluorescence, $F_0(t)$ was fit using a Kalman smoother implementing the Rauch-Tung-Stribel algorithm (Podgorski et al., 2011). Neurons were included in the data set if they met the following criteria: 1) >70% of evoked responses with $\Delta F/F_0$ peak values >1.5 Standard Deviation above the mean, 2) Consistent pre-training responses, where the mean evoked responses of three out of the four 5 min epochs of stimuli (0–5, 5–10, 10–15, 15–20) did not differ significantly from the total mean evoked pre-training responses (0–20 min; unpaired heteroscedastic two-tailed t-test), 3) non-drifting evoked responses. For measures of long-term potentiation

and depression, responses during the 20 min of baseline were compared to responses during 40 and 60 min post-training (t-test, $p < 0.05$).

3.3.6. *In vivo single neuron labeling*

Individual growing neurons within the *Xenopus* optic tectum were transfected using *in vivo* single-cell electroporation (Haas et al., 2001) for expression of membrane-targeted farnesylated enhanced green fluorescent protein (EGFP). Stage 50 *Xenopus* tadpoles were anesthetized with 0.02% MS-222 and individual neurons in the optic tectum were electroporated using plasmid DNA (2 µg/µl) and an Axoporator 800A stimulator (Molecular Devices, Sunnyvale, CA) to deliver electric pulses (stimulus parameters: pulse intensity = 1.5 µA; pulse duration = 1 msec; pulse frequency = 300 Hz; train duration = 300 msec). Single-cell electroporation was also used to co-deliver synthetic Morpholino oligonucleotides (pipette concentration: 0.05 mM) and the space-filling dye Alexa Fluor 488, 3000 MW (1.5 mM, Invitrogen, Eugene, OR), using the stimulation parameters: pulse intensity = 2 µA; pulse duration = 700 µsec; pulse frequency = 700 Hz; train duration 20 msec. Loading of lissamine-tagged Morpholinos was confirmed by fluorescent and confocal microscopy. Co-electroporation of Morpholinos and Alexa fluor 488 yielded 100% co-loading.

3.3.7. *In vivo time-lapse imaging of dendrite growth dynamics*

Images of growing neurons within intact and awake embryonic brain were captured using a custom-built two-photon laser-scanning microscope. Tadpoles were paralyzed, embedded in a thin layer of agarose, and placed in the imaging chamber as described in the Ca^{2+} imaging section. Entire dendritic arbors of individual tectal neurons

were imaged using optical section with a Z-axis step of 1.5 μm, every 5 min over 145 min.

3.3.8. Dynamics morphometric analysis

Dynamic growth behavior of dendritic filopodia and branches was analyzed from rapid time-lapse imaging data sets using a custom-written IGOR-based programs (developed by Dr. Jamie Boyd, University of British Columbia). All filopodia (processes with length <10 μm) were identified, tracked, and measured across multiple time point image stacks providing comprehensive and precise 3D measures of growth dynamics. Data were tested with the Student t-test to compare between groups unless otherwise stated. Data were present as mean ± SEM. Significance were labeled as * $p < 0.05$, ** $p < 0.01$, *** $p < 0.001$.

3.4. Results

3.4.1. Sensory experience drives simultaneous morphological and functional plasticity

While previous experiments have demonstrated that sensory experience influences neuronal growth during early brain development (Coleman and Riesen, 1968; Haas et al., 2006; Katz and Shatz, 1996; Ruthazer et al., 2003; Sin et al., 2002; Volkmar and Greenough, 1972a), evidence from specific stimuli shown to induce well-defined functional plasticity is lacking. In the *Xenopus laevis* tadpole optic tectum, specific patterns of visual stimuli induce lasting functional plasticity, indicated by persistent

alterations in the amplitude of visual-evoked synaptic responses and action potential firing (Dunfield and Haas, 2009; Engert et al., 2002; Zhou et al., 2003). The optic tectum receives direct innervations from the retina and corresponds to the superior colliculus in mammals. *In vivo* two-photon calcium imaging of the tadpole brain loaded with the cell-permeant calcium-sensitive fluorescent dye Oregon Green BAPTA-1 (OGB-1) allows direct monitoring of the activity of 100s of brain neurons with single-neuron resolution (Dunfield and Haas, 2009, 2010). In each neuron, somatic calcium transients reflect action potential firing (Podgorski et al., 2011), and visual stimulation with brief, 50 msec wide-field OFF stimuli evokes robust firing of stable amplitude when presented at 60 sec intervals over 145 min (Dunfield and Haas, 2009, 2010).

Specific visual training paradigms induce potentiation or depression of brain neuronal responses to probing OFF stimuli. A '*Spaced Training*' (ST) paradigm, consisting of repeated trains of high-frequency 50 msec OFF stimuli (3X 90 OFF stimuli of 50 msec duration at 0.3 Hz, spaced by 5 min intervals for 25 min) induces long-lasting potentiation of the amplitude of tectal neuron responses to OFF probing (**Figure 3.1A and 3.1B**). A second plasticity-inducing visual experience paradigm, termed '*Invariant Training*' (IN), consisting of 25 min of continuous non-varying ambient light, produces lasting depression (**Figure 3.2A and 2B**) (Dunfield and Haas, 2009). These paradigms provide tools to evoke plasticity of sensory evoked brain responses driven by visual sensory experience within the intact and unanesthetized developing vertebrate brain.

I applied these plasticity-inducing visual stimuli to investigate morphological correlates of functional plasticity during early neural circuit formation. Brain neuron growth was monitored using *in vivo* rapid time-lapse two-photon imaging of newly differentiated tectal neurons fluorescently labeled by single-cell electroporation of plasmid encoding EGFP (Haas et al., 2001). Image stacks of tectum encompassing the

3D volume of each neuron's entire dendritic arbor were captured every 5 min over 145 min, including an initial 60 min baseline period serving as an internal control, followed by 25 min plasticity-inducing visual experience (ST or IN), and 60 min post-training. Throughout baseline and post-training periods, 50 msec OFF visual probing stimuli was presented at 60 sec intervals to mimic the conditions of the functional plasticity experiments. Controls were exposed to continuous 50 msec OFF stimuli at 60 sec intervals for the entire 145 min experiment.

Analysis of dendritic growth behavior was conducted using dynamic morphometrics by tracking and measuring all filopodia on the entire dendritic arbor in 3D across 5 min time points throughout the 145 min imaging session to accurately measure growth behaviors including length, motility, lifetime, and density. These dynamic behaviors are influenced by factors that affect cytoskeletal and membrane dynamics (Chen et al., 2010; Cline and Haas, 2008; Niell et al., 2004; Vaughn, 1989). Synapse formation has been demonstrated to confer morphological stabilization to growing dendritic processes, resulting in reduction in filopodial motility and concomittant increase in lifetime. Destabilizing factors, such as weakening or loss of synapses produces the opposite phenotype, with increased motility and decreased lifetime. Imaging of growth of neurons expressing a GFP-tagged version of the postsynaptic protein PSD-95, demonstrate that most filopodia at the first time point imaged possess PSD-95 puncta and are stable, while PSD-95 puncta are absent on newly extended unstable filopodia, and only appear after tens of minutes (Chen et al., 2010; Niell et al., 2004). In order to understand how ST and IN plasticity-inducing visual experience affects dendritic growth, filopodia were separated into three groups: those present at the initial imaging time point - "*pre-existing*"; filopodia that emerged during the baseline - "*pre-training*"; and filopodia

added during and after training "*training and post-training*". Neurons from tadpoles exposed to ST exhibited a gradual increase in filopodial density starting during training and reaching an 86% increase after 85 min (**Figure 3.1C and 3.1D**). Morphometric analysis revealed that while ST had no effect on *pre-existing* filopodia, it caused enhanced stabilization of *pre-training* filopodia, evident from an increase in filopodial lifetime (**Figure 3.1E**) and decrease in motility (**Figure 3.1F and 1H**). ST also induced increased filopodial turnover, with elevated filopodial addition and retraction rates (**Figure 3.1G**). These results suggest that the primary effect of ST neural activity is to strengthen nascent synapses on newly formed filopodia.

Since NMDAR inhibition has been shown to block ST-induced functional potentiation (Dunfield and Haas, 2009), we tested whether ST-induced morphological changes are also mediated through NMDARs. The competitive NMDAR antagonist 2-amino-phosphonovaleric acid (APV, 50 μM) was infused into the tectum and applied to the tadpole bath directly prior to ST stimulation, and washed out of the bath directly following training. Strikingly, application of APV blocked ST-induced stabilization of *pre-training* filopodia and the increase in filopodial turnover during and after training (**Figure 3.1E – 1H**).

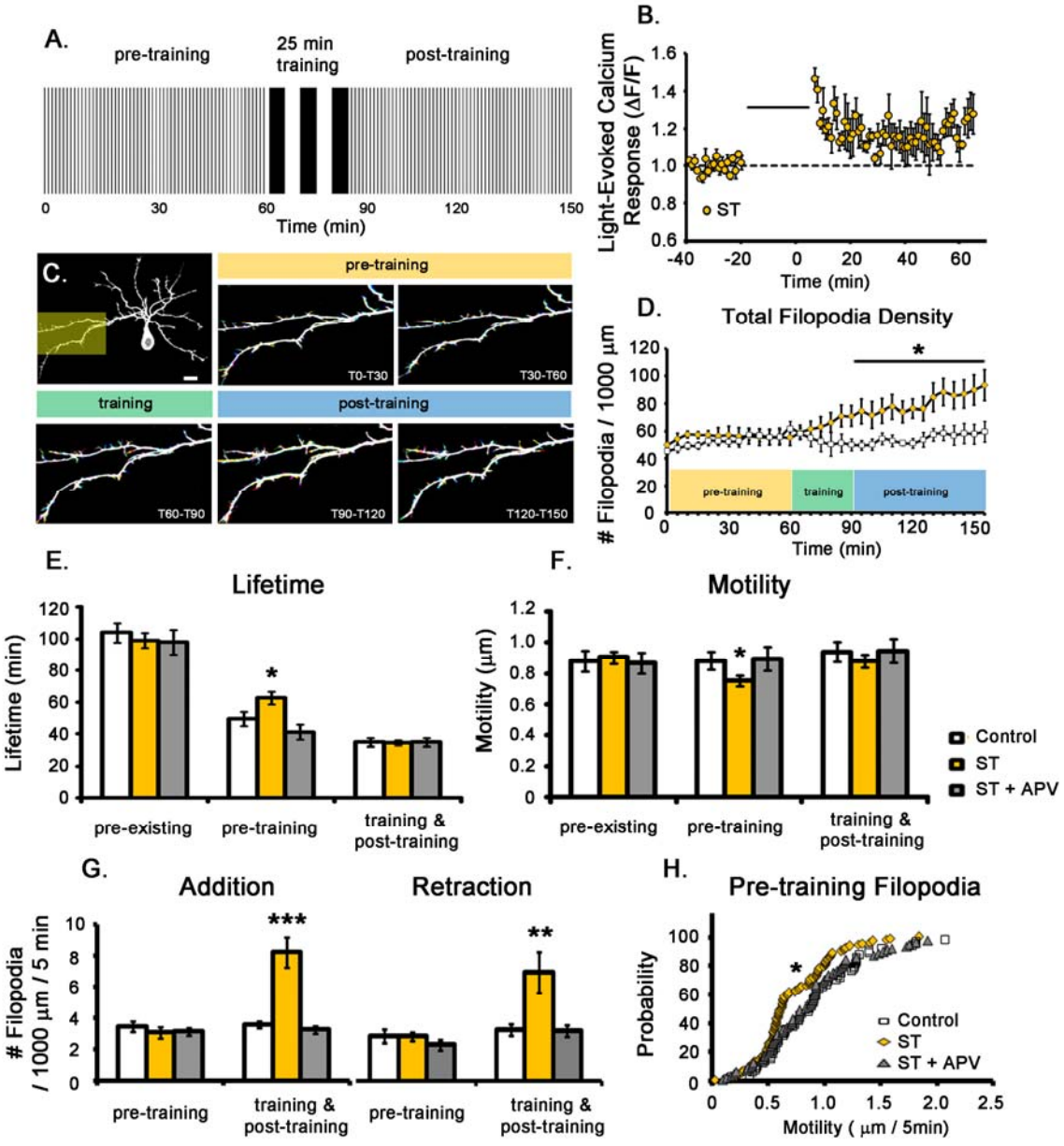

Figure 3.1 Visual-Experience Driven Potentiation is Associated with Morphological Stabilization and Sprouting

(A) Schematic of the Spaced Training (ST) visual stimulation paradigm. **(B)** Mean tectal neuron evoked Ca^{2+} responses (±SEM) show ST-induced potentiation (N = 4 tadpoles, n = 222 cells, $p < 0.001$, 40-60 min post-training, t-test). Bar denotes training period. **(C)** Individual growing tectal neurons were imaged *in vivo* every 5 min for 145 min throughout experiment. Pictures show overlay of 6 consecutive time points at 5 min intervals during each period (each time point a separate color; white = overlap). Scale bar = 20 µm. **(D-H)** Morphometric analysis of all dendritic

filopodial growth (Control: N = 5 cells, n = 251 filopodia; ST = 5 cells, n = 467 filopodia). **(D)** Total filopodial density at each time point. **(E)** Average filopodial lifetimes. **(F)** Average absolute motility (mean |Δ length|). **(G)** Average number of filopodia added or eliminated within all 5 min epochs. **(H)** Cumulative probability plot showing the distribution of motility of *pre-training* filopodia (*p < 0.001, two sample Kolmogorov-Smirnov comparison). * p < 0.05, **p < 0.01, ***p < 0.001 student t-test. Error bars indicate SEM.

Next I applied the same dynamic morphometrics imaging and analysis to determine the growth affects of IN visual training that induces lasting functional depression (Dunfield and Haas, 2009). Brain neuron morphology was imaged *in vivo* at 5 min intervals over 145 min, included 60 min baseline, 25 min IN training, and 60 min post-training. As in ST experiments and functional studies, 50 msec OFF probing stimuli were presented at 60 sec intervals throughout baseline and post-training periods (**Figure 3.2A and 2B**), and Control tadpoles were exposed to continuous probing with 50 msec OFF stimuli at 60 sec intervals. Analysis of all dendritic filopodia across 5 min intervals for 145 min found that IN prevents stabilization of labile processes. Interestingly, the same population of filopodia that emerged during the pre-training period, that were affected by ST, were also influenced by IN. IN resulted in the selective decrease in lifetime (**Figure 3.2D**) and increase in motility (**Figure 3.2E and 2F**) of *pre-training* filopodia, suggesting a reduction in synapse formation in this population. IN had no effect on filopodial turnover (**Figure 3.2G**). However, IN induced an enhanced rate of retraction of 'stable' *pre-existing* filopodia that were present for the entire 60 min baseline, suggesting breakdown of previously stable synapses (Control = 72.2 ± 13.7%, IN = 26.8 ± 9.3% remaining, P<0.01, Figure 2H). These findings demonstrate that functional potentiation is associated with stabilization of labile filopodia, and functional depression with destabilization of both labile and stable filopodia.

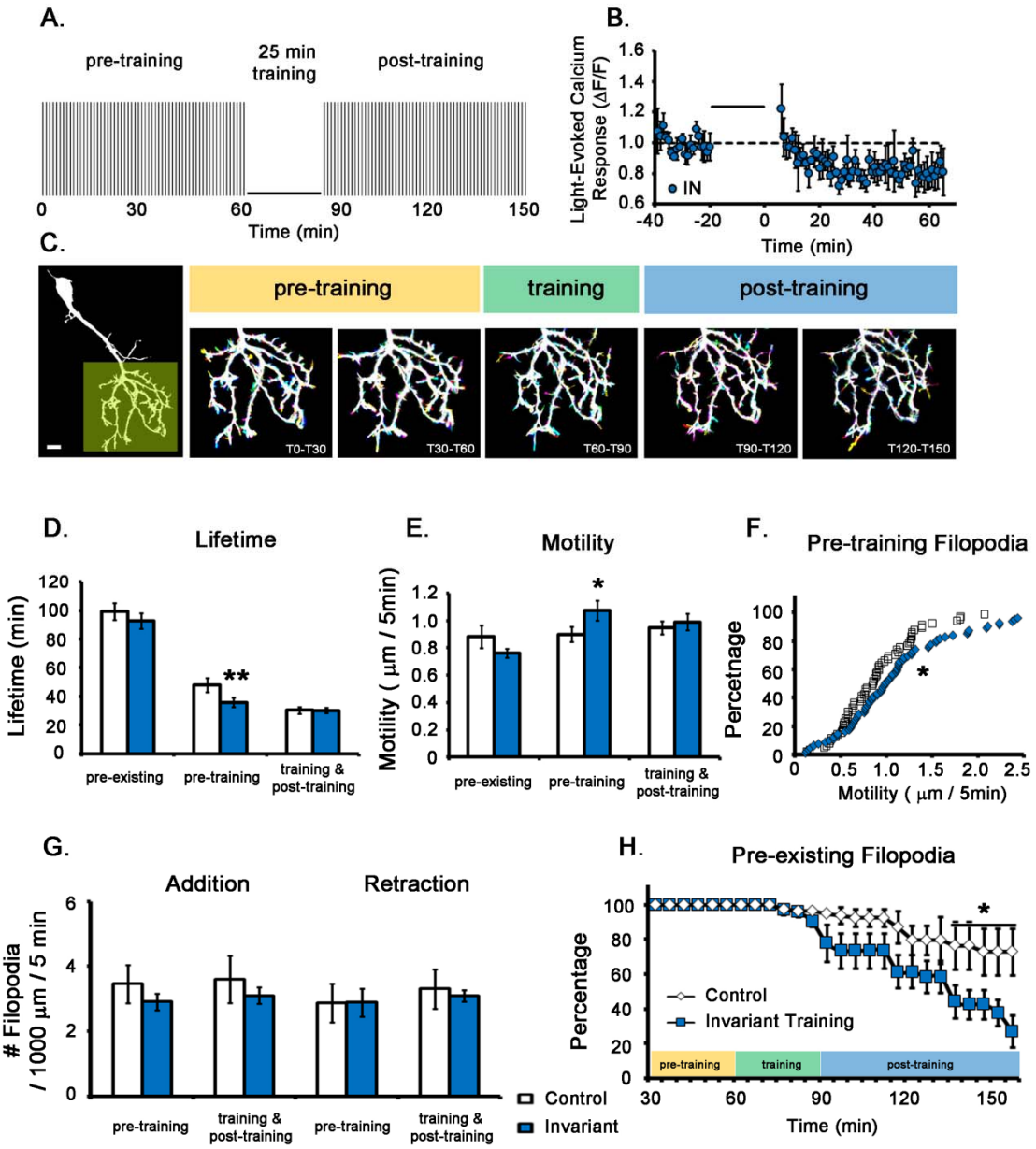

Figure 3.2 Visual-Experience Driven Depression Destabilizes Dendritic Growth

(A) Schematic of Invariant Training (IN) visual stimulation paradigm. **(B)** Mean tectal neuron Ca^{2+} responses (±SEM) showing IN-induced lasting depression (N = 5 tadpoles, n = 273 cells, $p < 0.001$, 40-60 min post-training, t-test). **(C)** Pictures show overlay of 6 consecutive time points at 5 min intervals during each period (each time point a separate color; white = overlap). Scale bar = 20 μm. **(D-H)** Morphometric analysis of dendritic filopodia prior to, during, and after IN (Control = 5 cells, n = 251 filopodia; IN = 5 cells, n = 261 filopodia). **(D)** Average lifetime. **(E)** Average

absolute motility. **(F)** Cumulative probability plot showing the distribution of motility of *pre-training* filopodia (*p < 0.001, two sample Kolmogorov-Smirnov comparison). **(G)** Average number of filopodia added or eliminated within each 5 min epoch. **(H)** Survival plot of percentage of *pre-existing* filopodia remaining at each time point. * p < 0.05, **p < 0.01, ***p < 0.001 student t-test. Error bars indicate SEM.

3.4.2. White noise priming induces functional and structural metaplasticity

Our lab has previously demonstrated that visual experience-driven plasticity in the developing retinotectal system shows metaplastic regulation, such that the history of firing alters the neuronal response to plasticity-inducing stimuli (Dunfield and Haas, 2009). Unpatterned WN visual stimulation, composed of continuously varying durations and intensities of wide-field OFF and ON stimuli increases tectal neuronal firing activity, but does not induce lasting plasticity of visual-evoked responses (Dunfield and Haas, 2009; Ramdya and Engert, 2008). Presenting 1 hr of WN to unanesthetized tadpoles prior to ST induces a switch in functional plasticity outcome from potentiation to depression (**Figure 3.3A and 3.3B**).

While mounting evidence supports metaplastic regulation of synaptic plasticity (Abraham et al., 2001; Philpot et al., 2003) and neuronal firing rates (Dunfield and Haas, 2009), whether structural plasticity is also subject to metaplastic rules remains unknown. To test whether WN stimulation alters experience-driven changes in dendritic growth, I first measured whether WN stimulation alone affects dendritogenesis using dynamic morphometrics. Individual EGFP labeled tectal neurons were imaged *in vivo* every 5 min during 60 min pre-training, 25 min WN, and 60 min post-training periods. Probing stimuli (50 msec OFF pulses) at 60 sec intervals were presented during pre- and post-training

periods to match functional calcium imaging experiments. Tracing and measurement of the growth behavior of all filopodia on entire dendritic arbors found that WN alone has no effects on filopodial dynamics or dendritic growth patterns compared to Control neurons that received continuous probing (**Figure 3.3D – 3.3H**). In order to determine whether WN priming alters the effects of visual training-induced structural plasticity as it does for functional plasticity, we next imaged neuronal dendritic arbor growth in tadpoles treated with WN stimulation prior to ST (**Figure 3.3A and 3.3C**). Strikingly, WN priming dramatically altered the dynamic growth behavior of tectal neurons in response to ST. WN priming blocked the ST-induced increase in filopodial turnover (**Figure 3.3G**), and shifted the ST response to a decrease in lifetime and increase in motility of *pre-training* filopodia (**Figure 3.3D – 3.3F**). Moreover, stable *pre-existing* filopodia that were present for the entire 60 min of pre-training baseline retracted with an increased rate during and after ST, with only 29.6% remaining 60 min following ST (Control = 72.2 ± 13.6% WN = 72.8 ± 8.1, WN + ST = 29.6 ± 8.1% remaining; $p < 0.01$; **Figure 3.3H**). As with results from functional calcium imaging, we find that WN priming prior to ST, shifts the structural plasticity outcome to become similar to the effects of IN-induced depression, with reduced morphological stabilization. Together, these results demonstrate that structural and functional plasticity is coordinated during development, and that structural plasticity is also metaplastically regulated by sensory experience.

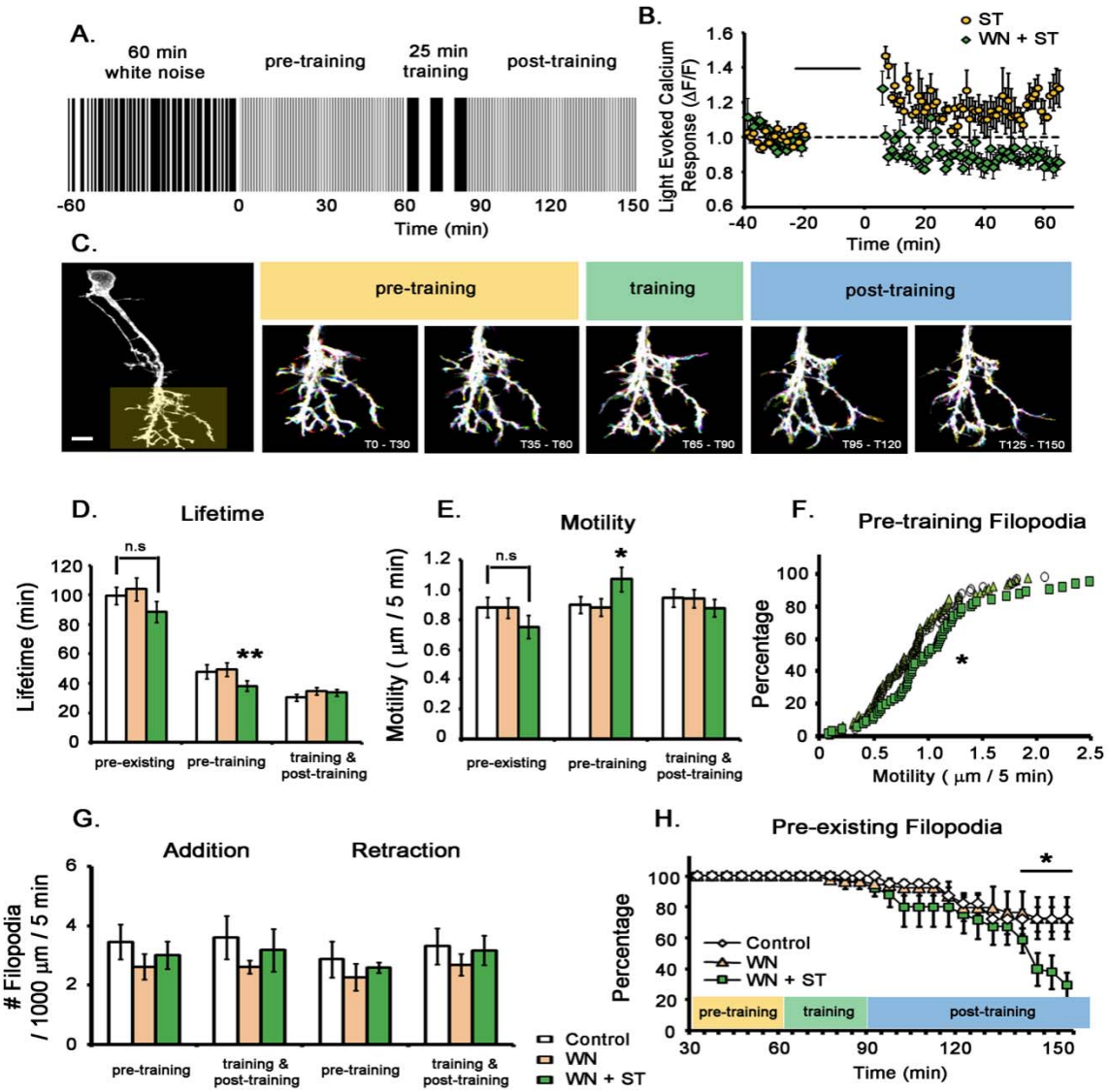

Figure 3.3 Brief Unpatterned Visual Stimulation Alters Subsequent Morphological Response to Plasticity Stimuli

(A) Schematic of White Noise (WN) + ST visual stimulation paradigm. **(B)** Mean tectal neuron Ca^{2+} responses (±SEM) in response to ST alone, and WN priming + ST (ST: N = 4 tadpoles, n = 222 cells; WN + ST: N = 5 tadpoles, n = 208 cells; $p < 0.001$, 40-60 min post-training, t-test). **(C)** Pictures show overlay of 6 consecutive time points at 5 min intervals during each period (each time point a separate color; white = overlap). Scale bar = 20 μm. **(D-H)** Dynamic morphometric analysis of all dendritic filopodia (Control = 5 cells, n = 251 filopodia; WN = 4 cells, n = 247 filopodia, WN + ST = 5 cells, n = 223 filopodia). **(D)** Average lifetime. **(E)** Average absolute motility. **(F)** Cumulative probability plot showing the distribution of motility of *pre-training* filopodia.

(G) Average number of filopodia added or eliminated during each 5 min epoch. **(H)** Survival plot of percentage of *pre-existing* filopodia remaining at each time point. * $p < 0.05$, ** $p < 0.01$, *** $p < 0.001$ student t-test. Error bars indicate SEM.

3.4.3. NMDARs are required for both functional and structural metaplasticity

I next conducted a series of experiments to examine possible molecular mechanisms mediating structural and functional metaplasticity. Our lab has previously demonstrated that NMDARs are required for the WN-induced metaplastic shift in functional plasticity outcomes to ST (**Figure 3.4B**) (Dunfield and Haas, 2009). Therefore, to determine whether structural and functional metaplasticity are regulated by the same molecular pathways, we tested whether exposing tadpoles to the NMDAR antagonist, APV (50 μM) during WN alters its effects on ST-mediated morphological growth plasticity (**Figure 3.4A**). We find that neurons in tadpoles exposed to APV during WN followed by ST showed similar growth pattern to ST alone. Since APV was infused directly into tectum, this suggests a local role for NMDAR activity. Morphometric analysis revealed an 88% increase in overall filopodial density over 145 min (**Figure 3.4F**), increased lifetime (**Figure 3.4C**) and decreased motility of *pre-training* filopodia (**Figure 3.4D**), and increased filopodial addition and retraction during the training and post-training periods (**Figure 3.4E**). Together, these results demonstrate that functional and structural metaplasticity share a requirement for NMDAR activation.

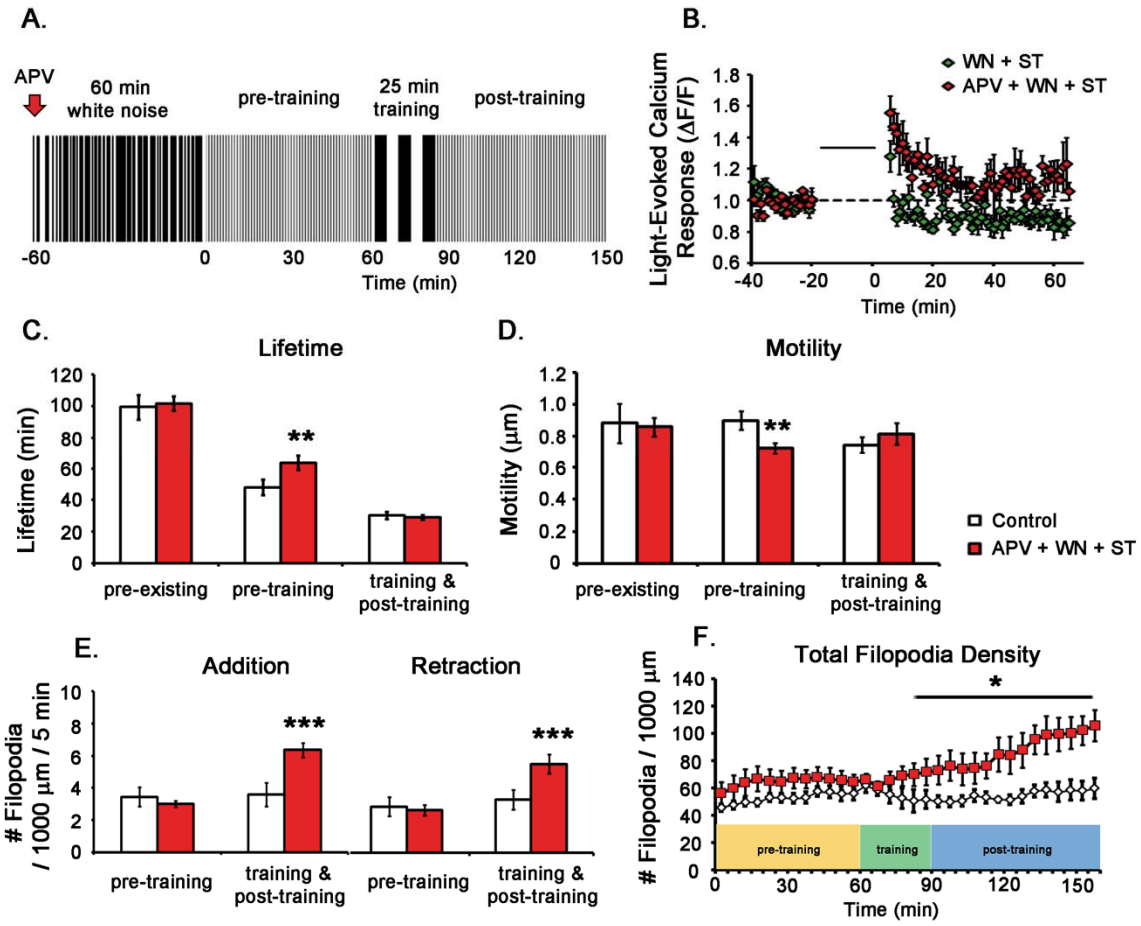

Figure 3.4 NMDAR Blockade Inhibits the WN-Mediated Metaplasticity Shift in Morphological Plasticity

(A) Schematic indicating APV (50 μM) infusion into tectum directly prior to 1 hr WN priming. **(B)** Mean tectal neuron Ca^{2+} responses (±SEM) in tadpoles exposed to WN + ST (WN + ST: N = 5 tadpoles, n = 208 cells; APV + WN + ST; N = 5 tadpoles, n = 244 cells, $p < 0.001$, 40-60 min post-training, t-test). **(C-F)** Dynamic morphometric analysis of dendritic filopodia (Control = 5 cells, n = 251 filopodia; APV + WN + ST = 5 cells, n = 449 filopodia). **(C)** Average lifetime. **(D)** Average absolute motility. **(E)** Average number of filopodia added or eliminated in each 5 min epoch. **(F)** Total filopodial density at each time point.

3.4.4. WN induces a rapid decrease in expression of the transcription factor MEF2

In order to identify components of the molecular cascades downstream of NMDARs contributing to WN-mediated metaplasticity, our lab has conducted a candidate screen for protein expression altered by WN. Focus was directed to transcription factors previously identified for roles in neuronal plasticity and with expression during developmental neural circuit plasticity. The transcription factor MEF2 was of particular interest given its role in structural and functional plasticity in the mature brain (Barbosa et al., 2008; Flavell et al., 2006), expression in the developing brain (della Gaspera et al., 2009; Shalizi et al., 2006), and neuronal growth abnormalities when knocked out during development (Fiore et al., 2009; Shalizi et al., 2006). I found that levels of the MEF2 were rapidly and dramatically reduced in brain extracts from the optic tectum following WN visual stimulation in unanaesthetized tadpoles (**Figure 3.5A**). To determine whether this change in MEF2 expression is dependent on neural circuit activity, or is specific to WN, I compared MEF2 levels in tadpoles exposed to WN, ST, IN or Control stimulation (Dunfield and Haas, 2009). Western blots of MEF2 protein expression using a pan-MEF2 antibody show a dramatic decrease in MEF2 levels following 60 min of WN stimulation, with no difference between responses to ST, IN or Control (**Figure 3.5A and 3.5B**). Since blocking NMDARs by tectal infusion of APV (50 μM) prior to WN blocks WN-induced metaplasticity, I tested whether APV also blocks WN-mediated reduction in MEF2 levels. Indeed, I found blocking NMDARs during WN stimulation prevents the complete reduction in MEF2 expression and restores the expression levels to 64 ± 12% following WN (**Figure 3.5C**), indicating that this level is sufficient to prevent a shift in plasticity thresholds.

The MEF2A and MEF2D isoforms are highly expressed in *Xenopus* tadpole brain, and WN stimulation decreased expression of both (**Figure 3.5A**). Since MEF2 phosphorylation is known to regulate its transcriptional activity (McKinsey et al., 2002), and previous studies have reported that in hippocampal neurons neural activity increases MEF2 transcriptional activity through dephosphorylation of MEF2 via calcineurin-dependent signaling pathways (Flavell et al., 2006), I examined the ratio of phosphorylated to non-phosphorylated MEF2 in Control and WN groups. Two prominent bands are detectable on Western blots, with the slower migrating band likely composed of phosphorylated MEF2 since treating brain lysate with alkaline phosphatase led to its disappearance (Figure 5E) (Flavell et al., 2006; Li et al., 2001). I found that while WN decreases overall MEF2 expression levels, it produces no change in the ratio of phosphorylated to non-phosphorylated bands (Control = 0.3 ± 0.06, WN = 0.35 ± 0.10, $p<0.01$). To determine whether calcineurin-mediated dephosphorylation of MEF2 regulates WN-mediated degradation, I treated tadpoles with a specific calcineurin inhibitor FK506, 1μM (Schwartz et al., 2009) by bath application. Blocking calcineurin activity did not inhibit WN-induced reduction in MEF2 expression, and did not alter the ratio of the phosphorylated to non-phosphorylated bands following WN (**Figure 3.5D**). These results indicate that the enhanced tectal circuit activity elicited by WN visual stimulation does not activate calcineurin-dependent signaling to produce altered phosphorylation of MEF2, but rather decreases MEF2 protein independent of its phosphorylation state.

3.4.5. The time course of metaplastic shift in plasticity outcomes matches MEF2 levels

Metaplasticity denotes the persistent alteration in neuronal susceptibility to plasticity-inducing experience in response to a history of activity. Due to a lack of models which induce shifts in plasticity responses by well-controlled periods of altered neuronal activity, little is known of the time course of metaplastic changes to the plasticity threshold following altered neuronal firing. Given the identification of MEF2 as a protein affected by a manipulation that shifts plasticity thresholds, I examined MEF2 levels in optic tectum at different time points following WN stimulation (0, 0.5, 1, 2, and 4 hr). MEF2 levels dropped immediately following WN and continued to remain at low levels after 1 hr, before gradually recovering at 4 hr (WN + 4 hr = 70% ± 5%, **Figure 3.5F**). If MEF2 levels directly contribute to experience-driven metaplasticity then MEF2 levels would correspond to the duration of the WN-mediated shift in functional plasticity evoked by ST. To test this possibility, I treated tadpoles with WN, and waited 4 hr before conducting *in vivo* calcium imaging of tectal responses to ST. We find that, similar to the return of MEF2 protein expression, the metaplasticity effects of WN sensory stimulation diminishes 4 hr following WN, indicating a close relationship between MEF2 levels and altered plasticity threshold (**Figure 3.5G**).

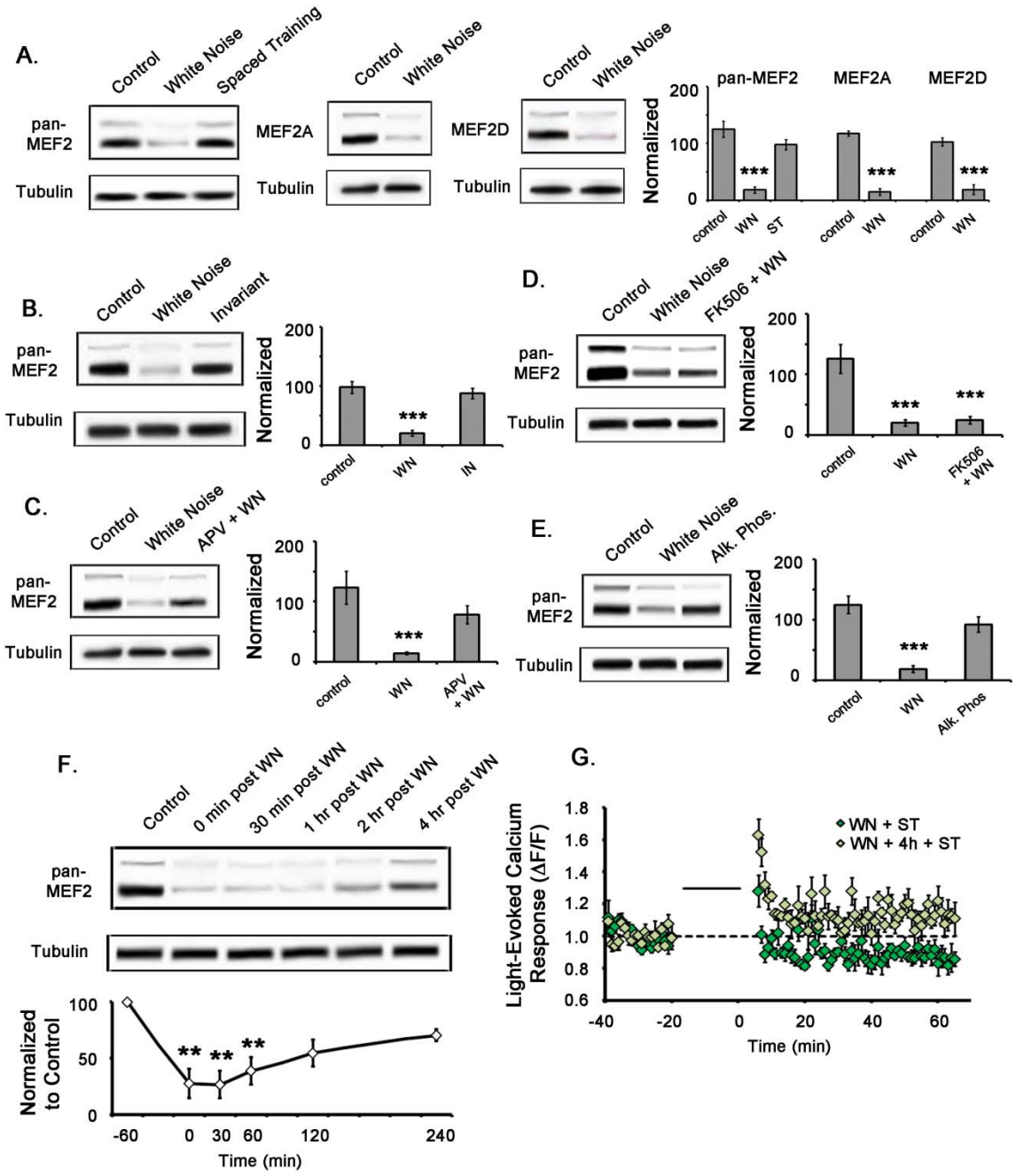

Figure 3.5 Time Course of MEF2 Reduction Following WN Corresponds to the Duration Altered Plasticity Response.

(A, B) Western blots of tectal brain lysates demonstrate reduced MEF2A/2D levels following 1h of WN compared to Controls, ST or IN. **(C)** Tectal infusion of APV (50 μM) prior to WN prevents the loss of MEF2 expression. **(D)** Tectal infusion of the calcineurin inhibitor, FK506 (1μM) before WN

does not block reduction in MEF2. **(E)** Calf Intestinal Alkaline Phosphotase (CIP, 10U/ml) treatment removes slower band. Quantification (mean ± SEM) of immunoblot band intensities (Figure 5A-E) are normalized to the tubulin band (N = 3 blots; n = 12 tadpoles). **(F)** Time course MEF2 levels following 1 hr of WN and quantification (mean ± SEM) of immunoblot band intensities normalized to Control sample (N = 3 blots; n = 12 tadpoles for each time point). **(G)** Mean tectal neuron Ca^{2+} responses (±SEM) in tadpoles receiving ST directly, or 4h following I hr WN (WN + ST: N = 5 tadpoles, n = 208 cells; 4h post WN + ST = 4 tadpoles, n = 199 cells; ; $p < 0.001$, 40-60 min post-training, t-test, compared to pre-training basline).

3.4.6. WN-induced reduction in MEF2 is mediated by digestion through caspase-9, -3/7

Previous studies in mouse cortical neurons have associated decreased MEF2 levels with neuronal apoptosis (Li et al., 2001; Okamoto et al., 2002). The canonical activation of caspase-3 occurs through two main pathways: i) the extrinsic pathway of cell death through activation of caspase-8, and ii) the mitochondrial pathway through Apaf1 apoptosome and caspase-9 (Slee et al., 1999). In neurons undergoing excitotoxic insult, caspase-3/7 are activated via a mitochondrial pathway and cleave MEF2A/2D, which contain multiple caspase target sites in their transactivation domains (Li et al., 2001; Okamoto et al., 2002). To investigate whether the WN-mediated reduction in MEF2 levels is due to degradation by activated caspases, I employed cell-permeant caspase inhibitor peptides: ZVAD-FMK (100μM; nonselective caspase inhibitor), LEHD-FMK (2μM; caspase-9-preferring inhibitor), DEVD-FMK (2μM; selective caspase-3/7 inhibitor), and WEHD-FMK (200nM; inhibitor of caspase-1/8). Tectal infusion of the pan-caspase inhibitor ZVAD-FMK, the caspase-9 inhibitor LEHD-FMK, or the caspase-3/7 inhibitor DEVD-FMK prior to WN prevented reduction in MEF2 levels, while the caspase-8 inhibitor peptide WEHD-FMK did not (**Figure 3.6A**). These results demonstrate that WN-induced reduction in MEF2 levels is likely the result of degradation through the

activation of caspases via the mitochondrial “apoptotic” pathway, involving caspase-9 digestion and activation of caspase-3/7. Since caspase-3/7 are the most downstream members of this pathway, we next tested whether blocking the activation of caspase-3/7 blocks WN-induced metaplasticity. DEVD-FMK was infused into the tectum prior to WN, followed by calcium imaging of ST-induced functional plasticity. Control tadpoles received WEHD-FMK, which did not prevent WN-mediated reduction in MEF2 levels. Inhibition of caspase-3/7 blocked the metaplastic effects of WN priming on subsequent ST plasticity, while inhibition of caspase-1/8 did not (**Figure 3.6B**),

Since caspase activation is considered to be a terminal step in the biochemical cascade leading to apoptotic cell death, I next measured levels of activated caspase-3 by Western analysis at different time points following WN. I found that activated caspase-3 levels increased by 44 ± 5.8% 1 hr following WN but subsequently decreased below baseline levels over 4 hr (**Figure 3.6C**). In contrast, staurosporine (STS), a strong inducer of activated caspase-3 and neuronal apoptosis, elicited accumulation of activated caspase-3 that remained high at 4 hr post application (**Figure 3.6D**). To determine whether this activation of caspase-3 induces brain cell death, propidium iodide (PI) was infused into the tadpole tectum 30 min or 4 hr after WN, STS treatment, or Controls exposed to continuous probing with 50 msec OFF visual stimuli presented at 60 sec intervals. While STS induced high levels of cell death, WN had no effect on the low level of cell death inherent in the developing brain, suggesting that the mode and duration of activation of caspase-3 may determine the cellular response, whether shift in plasticity threshold or death (**Figure 3.6E**). Together, findings in this section identify a non-apoptotic role of activated caspase-3, in which WN stimulation transiently activates caspase-3 leading to cleavage of MEF2 which alters neuronal plasticity thresholds.

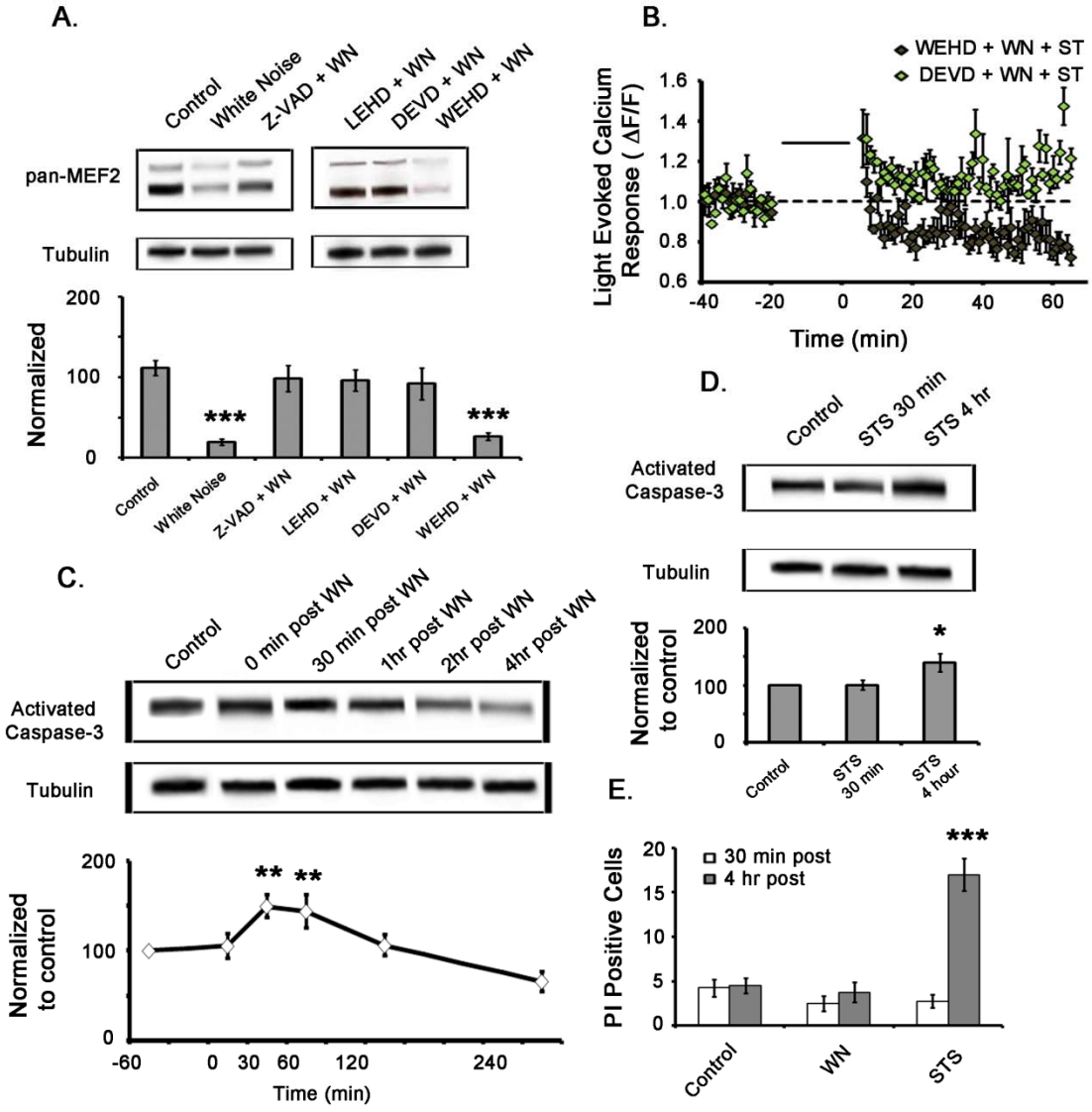

Figure 3.6 Transient Activation of Caspase-3 Leads to MEF2 Degradation and is Required for WN-mediated Shift in Plasticity Response.

(A) Western blots of tectal brain lysates demonstrate that inhibitors of pan-caspase (ZVAD), caspase-9 (LEHD), and caspase-3/7 (DEVD), but not caspase-1/8 (WEHD) prevent WN-mediated reduction of MEF2. Quantification (mean ± SEM) of immunoblot band intensities are normalized to the tubulin band (N = 3 blots; n = 12 tadpoles). **(B)** Mean tectal neuron evoked Ca^{2+} responses (±SEM) in tadpoles treated with WEHD or DEVD prior to WN + ST visual stimulation (WEHD + WN + ST: N = 4 tadpoles, n = 220 cells; DEVD + WN + ST = 5 tadpoles, n = 271 cells; ; $p < 0.001$, 40-60 min post-training, t-test, compared to pre-training baseline). **(C)** Western blots of tectal proteins showing cleaved (active) caspase-3 following 1 hr WN. **(D)** Western blots of tectal

proteins showing cleaved (active) caspase-3 following tectal infusion of staurosporine (STS, 1μM). Quantification (mean ± SEM) of immunoblot band intensities (Figure 6C and 6D) are normalized to Control sample (N = 3 blots; n = 12 tadpoles for each time point). **(E)** Propidium iodide staining to assess neuronal cell death at 30 min and 4 hr following WN or STS (N = 6 tadpoles / group).

3.4.7. MEF2A/2D knockdown is sufficient to induce a metaplastic shift in functional plasticity

The results so far have strongly indicated an important role for MEF2 in the metaplastic regulation of plasticity thresholds. I therefore examined whether a reduction in MEF2 alone is sufficient to trigger a shift in plasticity outcomes by using synthetic antisense Morpholino oligonucleotides (MO) that selectively knock down expression of *Xenopus* MEF2A (MO-MEF2A) and MEF2D (MO-MEF2D). I utilized vivo-Morpholinos, which contain a cell permeant moiety (GeneTools). Tectal infusion of vivo-MO-MEF2 (2A+2D) produced clear knockdown of MEF2 protein levels at 24 hr to a level comparable to WN (**Figure 3.7A**). Injection of control Morpholino oligonucleotides (MO-Control) whose sequence does not correspond to any known *Xenopus* mRNA did not alter MEF2 levels. I tested for possible toxic effects of vivo-MO by infusing propidium iodine into the tectum 24 hr after infusion of MO-MEF2 or MO-Control and found no significant increase in tectal cell death compared to untreated tadpoles. To test the effects of MEF2 knockdown on plasticity, I infused vivo-MO-MEF2 into tectum and performed calcium imaging of functional ST plasticity 24 hr later (**Figure 3.7B**). I found that knocking down MEF2 by itself is sufficient to shift the functional plasticity outcome of ST from potentiation to depression (**Figure 3.7C**).

3.4.8. MEF2 knockdown induces structural metaplasticity

To further investigate whether structural and functional metaplasticity share molecular mechanisms downstream of NMDARs, I tested whether MO knockdown of MEF2A/2D in individual growing tectal neurons alters structural plasticity induced by ST. Single-cell electroporation was used to deliver MO-MEF2A and MO-MEF2D along with the fluorescent dye Alexa Fluor 488 dextran as a space-filler for morphological imaging. MO-Control was introduced into separate brain neurons as a control. MO constructs were fused to the red fluorescent dye Lissamine to confirm cell loading. Twenty-four hours following single-cell electroporation, I conducted *in vivo* two-photon imaging of dendritic arbor growth in unanesthetized tadpoles following the same ST plasticity paradigm and dynamic morphometric analysis described above. MO-MEF2 neurons exhibited higher filopodial addition rates compared to MO-Controls, similar to results from MEF2 knockdown in mouse cerebellar granule neurons (Shalizi et al., 2006). Since we did not observe this effect following short duration reduction in MEF2 induced by WN, this may reflect a compensatory or secondary effect independent of metaplasticity. As with functional plasticity, MO-MEF2 neurons demonstrated a shift in the structural plasticity response to ST, evident as destabilization, with reduced lifetime and increased motility of the *pre-training* filopodia and more rapid loss of pre-existing filopodia (**Figure 3.7D-E, 7G**). Moreover, in MO-MEF2 neurons, ST failed to increase filopodial turnover (**Figure 3.7F**).

Together, these results reveal a novel pathway mediating a metaplastic shift in plasticity threshold in the developing vertebrate brain. WN visual stimulation drives glutamatergic transmission activating NMDARs, which induces caspase-9-mediated cleavage and activation of caspase-3/7. Activated caspase-3/7, in turn cleaves

MEF2A/2D, which leads to alterations in neuronal response to subsequent plasticity-inducing sensory information

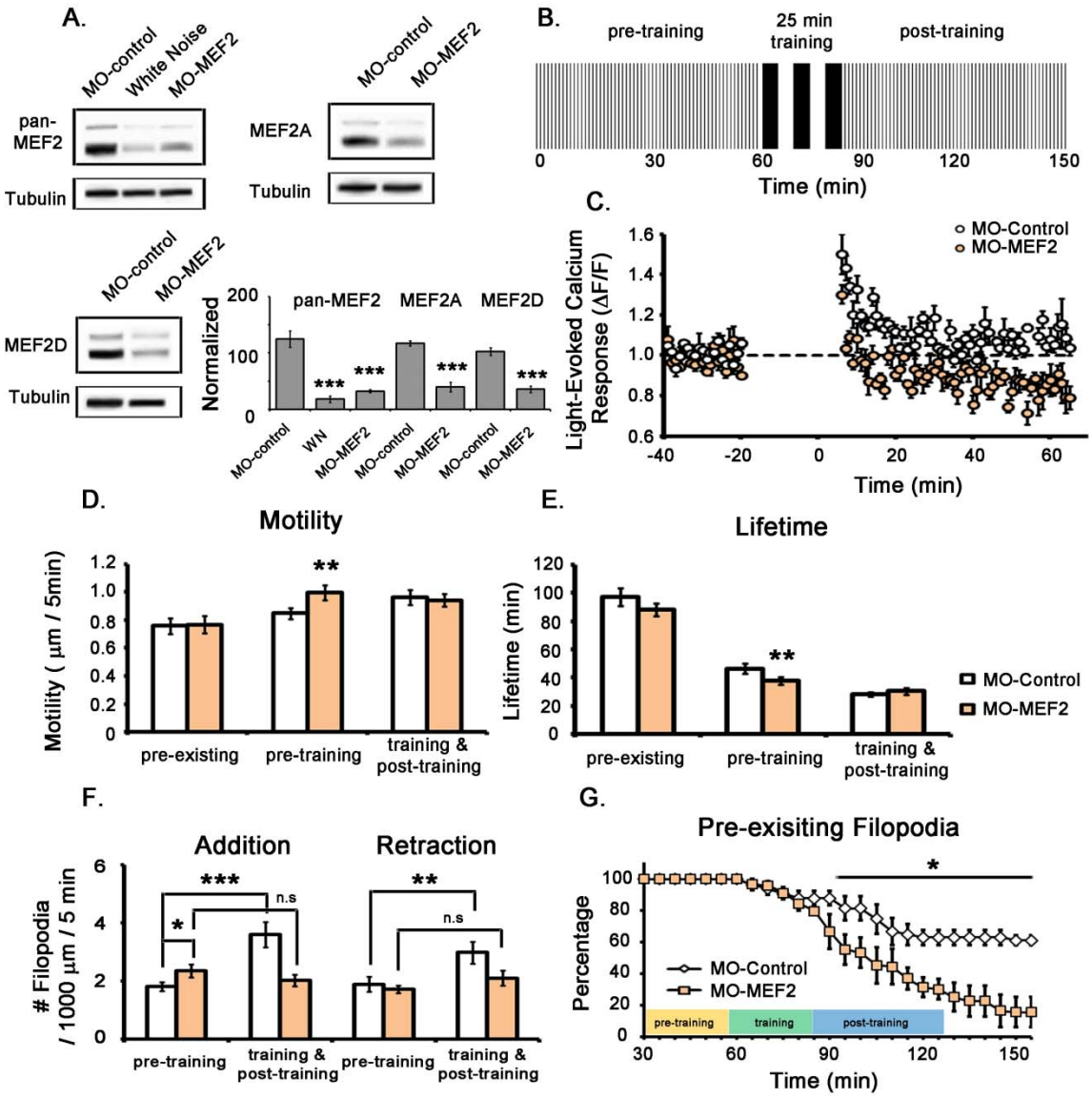

Figure 3.7 Knockdown of MEF2 Shifts Plasticity Responses.

(A) Infusion of vivo-Morpholino specific for *Xenopus* MEF2A and MEF2D (MO-MEF2) into tectum significantly reduces expression of MEF2A/2D *in vivo* after 24 hr. Quantification (mean ± SEM) of immunoblot band intensities are normalized to the tubulin band (N = 3 blots; n = 12 tadpoles). **(B)** Tadpoles received ST 24 hr after tectal infusion of MO-MEF2. **(C)** Mean tectal neuron Ca^{2+}

responses (±SEM) to ST in tadpoles treated with MO-control or MO-MEF2 (MO-control + ST: N = 5 tadpoles, n = 253 cells; MO-MEF2 + ST = 4 tadpoles, n = 213 cells; $p < 0.001$, 40-60 min post-training, t-test). **(D-G)** Dynamic morphometric analysis of dendritic filopodia prior to, during, and after ST (MO-Control = 5 cells, n = 381 filopodia; MO-MEF2 = 5 cells, n = 215 filopodia, t-test, compared to pre-training baseline).

3.5. Discussion

3.5.1. Coordination of developmental structural and functional plasticity and metaplasticity

By applying visual training that induces lasting plasticity of visual-evoked responses in networks of brain neurons while conducting *in vivo* rapid time-lapse imaging of single neuron growth, I have identified strong correlation of structural and functional plasticity during early neural circuit formation (Table S1). The findings of dendritic filopodial stabilization and destabilization associated with lasting potentiation and depression, respectively, provides evidence for coordination of morphological and physiological plasticity. During early stages of dendritogenesis, before spines develop, filopodia are precursors of longer dendritic branches (Hossain et al., 2011), and therefore, mechanisms to selectively maintain and extend or retract filopodia have profound lasting effects on larger arbor morphology and their contribution to network function. Given previous findings demonstrating a role for synaptogenesis in conferring morphological stabilization to nascent dendritic and axonal processes (Chen et al., 2010; Liu et al., 2009; Niell et al., 2004), activity-dependent synapse formation and maturation likely underlies both the functional and structural plasticity observed here. The

coordination of experience-dependent synaptogenesis underlying functional plasticity and dendritic arbor growth may enable developing neural networks to self-organize in a manner best optimized to process the specific sensory inputs encountered during maturation.

The tremendous amount of activity-dependent plasticity occurring during neural network development compared to relatively stable mature circuits likely necessitates similarly robust mechanisms of metaplasticity to maintain plasticity thresholds within a physiological range. The discovery that the application of a brief unpatterned visual experience paradigm that does not alter visual responses, yet changes brain neuronal susceptibility to subsequent plasticity-inducing sensory stimuli, has allowed further dissection of the relationship between functional and structural plasticity. The findings that morphological plasticity in response to ST can be shifted from stabilization to destabilization by priming with brief WN demonstrates that morphological growth is also metaplastically regulated and is closely correlated to functional changes.

3.5.2. MEF2 is necessary and sufficient to shift developmental plasticity thresholds

Since brief unpatterned visual stimulation elicits a shift in plasticity outcomes without inducing plasticity itself, this provides a powerful tool to identify molecular mechanisms specific to regulation of metaplasticity. The finding that WN rapidly and transiently decreases levels of the transcription factor MEF2, and that MEF2 regulates experience-driven shifts in plasticity outcomes uncovers a novel role of MEF2 during critical periods of brain circuit formation. Recently, MEF2A/2D have been reported to regulate activity-dependent excitatory synapse elimination and dendritic differentiation.

In hippocampal neurons, glutamatergic synaptic activity and calcineurin-dependent dephosphorylation of MEF2 elevates MEF2-dependent transcription resulting in spine and synapse loss (Flavell et al., 2006). In cerebellar cortex, activity-dependent calcium signaling induces calcineurin-mediated dephosphorylation of MEF2A, which inhibits formation of postsynaptic dendritic structures (Shalizi et al., 2006). In this chapter, I find that in the developing vertebrate brain, enhanced neural network activity driven by unpatterned visual stimulation induces rapid caspase-mediated digestion of MEF2A/2D independent of calcineurin dephosphorylation to produce a shift in plasticity thresholds, but without direct effects on circuit structure or function.

I further demonstrate that reduced MEF2 expression is required for the induction of experience-dependent metaplastic shift in plasticity threshold. Pharmacological approaches that block WN-mediated degradation of MEF2 also prevent a metaplastic shift in functional plasticity, and reduction in MEF2 alone using Morpholino oligonucleotides is sufficient to trigger a shift in plasticity outcomes. While it is accepted that metaplastic effects are initiated by 'the history of neuronal activity', little is known about the duration of activity necessary to initiate a change in neuronal responses or the time course of this change. Previous studies in visual cortex and hippocampus have reported that metaplastic effects can be reversed on the order of 2 to 4, and 7 to 35 days, respectively (Abraham et al., 2001; Kirkwood et al., 1996). In my studies, I was able to determine that the timeline of the metaplastic shift in plasticity due to a brief 1 hr WN corresponds to the transient reduction of MEF2 expression, returning to basal levels within 4 hr.

The finding that MEF2A/2D mediates metaplastic shifts in plasticity thresholds through its activity-dependent cleavage adds to a growing list of recently identified non-apoptotic roles for caspases in neuronal plasticity. While caspases may have originated

primarily to direct orderly cellular disassembly and death in response to external apoptotic signals (Slee et al., 1999), they have taken on additional roles to translate extrinsic signals to non-death pathways. I found that in the developing brain, unpatterned visual experience activates a novel signaling cascade regulating neuronal sensitivity to plasticity-inducing stimuli, involving NMDAR activation, caspase-9 mediated cleavage and activation of caspase-3, which in turn leads to degradation of MEF2A/2D. Pharmacological blockade of NMDARs or caspase-3/7 prevents WN-mediated reduction in MEF2 levels and blocks WN-induced shifts in plasticity outcomes in response to visual training. These results are surprising given previous finding implicating caspase-mediated MEF2 degradation in apoptotic cell death during excitotoxic neuronal stress (Li et al., 2001; Okamoto et al., 2002). However, although I showed that brief unpatterned visual stimulation provokes a rapid activation of caspase-3 and near complete loss of MEF2 from brain lysates, there is no increase in brain cell death. Recent studies by Li and colleagues have demonstrated a non-apoptotic role of the mitochondrial pathway (caspases-9 and 3) in LTD, in which NMDAR stimulation transiently activates caspase-3 and induces cleavage of Akt1 kinase, which in turn leads to AMPAR internalization and synaptic weakening (Li et al., 2010). Since WN activates caspase-3 in the developing tectum, it is possible that its effects on plasticity are due to induction of LTD. However, this is not supported by the findings that WN stimulation does not induce plasticity of visual-evoked responses (Dunfield and Haas, 2009; Ramdya and Engert, 2008), nor does it induce dendritic destabilization. Furthermore, depression-inducing IN stimuli did not cause a decrease in MEF2 levels, suggesting IN does not activate the caspase-3 pathway in tectum.

The identification of MEF2 as a master regulator of the metaplastic state or plasticity threshold suggests orchestration of downstream effectors through altered

transcriptional regulation. Genome-wide analysis of MEF2 transcription has revealed target genes with diverse actions at synapses, including proteins implicated in both decreasing (*arc, JNK,* and *SynGAP*) and increasing (*Lgi1*, adenylyl cyclase 8) excitatory postsynaptic function (Flavell et al., 2008). Moreover, activity-dependent MEF2 transcription regulates expression of a cluster of brain-specific microRNAs, which in turn mediate post-transcriptional regulation of synapse-associated mRNAs (Fiore et al., 2009). MEF2-dependent transcription may represent a mechanism in developing brain that coordinates local and global gene and miRNA transcription to modulate neuronal sensitivity and response to plasticity-inducing stimuli, without altering neuronal growth and physiology directly.

Together, findings in this chapter implicate a well known transcription factor and apoptotic pathway in the novel roles of activity-dependent regulation of developmental neuronal morphologic and functional plasticity. Involvement of caspases degradation of MEF2 in setting the metaplastic plasticity threshold adds to a growing list of non-apoptotic roles for these proteins. It is becoming clear that caspase pathways are sensitive detectors of excitatory synaptic transmission and can evoke a spectrum of responses in neurons ranging from homeostatic metaplasticity, synaptic plasticity, and excitotoxic cell death, depending on the extent of activation.

	Calcium Imaging	Filopodial Lifetime			Filopodial Motility			Filopodial Addition / Elimination	
		Pre-Existing	Pre-Training	Training & Post-Training	Pre-Existing	Pre-Training	Training & Post- Training	Pre-Training	Training & Post-Training
ST	Potentiation	NC	↑	NC	NC	↓	NC	NC	↑
ST + APV	NC (Dunfield and Haas 2009)	NC	NC	NC	NC	NC	NC	NC	NC
IN	Depression	NC	↓	NC	NC	↑	NC	NC	NC
WN	NC (Dunfield and Haas 2009)	NC	NC	NC	NC	NC	NC	NC	NC
WN + ST	Depression	NC	↓	NC	NC	↑	NC	NC	NC
WN + 4 hr + ST	Potentiation								
APV + WN + ST	Potentiation	NC	↑	NC	NC	↓	NC	NC	↑
WEHD + WN + ST	Depression								
DEVD + WN + ST	Potentiation								
MO-Control + ST	Potentiation	NC	↑	NC	NC	↓	NC	NC	↑
MO-MEF2+ ST	Depression	NC	↓	NC	NC	↑	NC	↑	NC

Table 3.1. Summary of the Effects of Different Visual Stimuli and Pharmacological Treatments on Visual-Evoked Responses and Dendrite Growth

4. CONCLUSION

4.1. Summary of Findings

The objectives of this dissertation were to

1. Examine the roles of cell adhesion molecules, NRXs and NLGs in brain neuronal growth and function *in vivo*
2. Determine the morphological correlates of functional plasticity and metaplasticity *in vivo*
3. Decipher the molecular mechanisms mediating functional and structural metaplasticity

In Chapter 2, I showed that NRX and NLG1 directly influence dendritic filopodial dynamic growth behavior with lasting effects on the arbor structure of actively growing brain neuron *in vivo*. Blocking trans-synaptic NRX-NLG1 interactions by applying extracellular soluble recombinant NRX (NRX-fc) prevents normal dendritic filopodial stabilization, while increasing NRX-NLG1 interactions by over-expression of NLG1 hyper-stabilizes filopodia. Expression of NLG1-ΔC, a NLG1 mutant lacking the PDZ domain and able to bind to NRX but unable to recruit PSD-95, prevents filopodial stabilization. However, NLG1-ΔC does induce a transient increase in filopodial lifetimes that is blocked by soluble NRX-fc, demonstrating that cell adhesion complexes transiently stabilize the membrane to limit process elimination but do not contribute to cytoskeletal changes

underlying filopodial motility needed to confer persistent stabilization. I also found that over-expression of NLG1 is insufficient to stabilize dendritic filopodia when NMDARs are blocked pharmacologically, demonstrating that although NRX-NLG1 complexes can cluster PSD-95, which binds to other cytoskeletal scaffold proteins, this interaction is insufficient to promote transition of motile filopodia into persistently stabilized dendritic branches, and that glutamatergic synaptic transmission is required. These results suggest a series of distinct events underlying filopodial stabilization in which the initial NRX-NLG trans-synaptic adhesion complexes provide a transient, activity-independent interaction that prevents nascent axo-dendritic contacts from separating. Subsequent synaptic protein clustering and NMDA receptor-dependent synapse maturation then confers persistent stabilization to the filopodia cytoskeleton restricting elimination. Work from this chapter adds another layer of complexity to the existing synaptotropic model of dendritogenesis and demonstrates how cell adhesion molecules play a critical role in brain circuit structural development

In the first half of Chapter 3, I provided evidence to show that morphological growth of brain neurons is correlated with functional plasticity *in vivo*. By employing potentiation or depression inducing visual stimuli, ST and IN respectively, I demonstrated that the growth of individual brain neurons can be influenced by specific visual experiences. ST stabilizes, and IN destabilizes recently extended filopodia. ST also increases filopodial addition and retraction rates during and after training, while IN produced no change in turnover. These effects result in a cumulative increase in filopodial density following ST and decreased density of stabilized filopodia following IN. Based on the synaptotropic model that filopodial stabilization is associated with synapse formation, I interpret these results to indicate that nascent filopodia undergo enhanced or inhibited synaptogenesis by ST or IN, respectively. Moreover, in order to determine

whether the WN visual experience, shown to induce functional metaplasticity, also has a morphological consequence, I tested growth effects of WN-induced functional metaplasticity. I found that while WN stimulation alone has no effect on dendritic filopodial dynamics and dendritic growth patterns, WN + ST induced a decrease in filopodial lifetime and increased motility of the filopodia that recently emerged. Stable pre-existing filopodia also showed an increase in their rate of retraction. Results of the morphological effects of WN + ST resemble those induced by IN, associated with lasting functional depression. These findings that morphological plasticity in response to ST can be shifted from stabilization to destabilization by priming with brief WN demonstrates, for the first time, that morphological growth is also metaplastically regulated and is closely correlated to functional changes.

In the last half of Chapter 3, I discovered a novel function of transcription factor MEF2A/D in regulating WN functional and structural metaplasticity. I found that MEF2 is rapidly degraded in response to WN visual stimulation through a classical apoptotic pathway requiring activation of NMDARs and caspases-9, 3 and 7. Interestingly, WN activation of caspases is not associated with apoptosis, suggesting that WN stimulation induces a non-apoptotic function of caspase-3 to cleave MEF2 and leading to a shift in metaplastic threshold.

4.2. Future Directions

4.2.1. Role of other NLG isoforms on dendrite growth

The “synaptotropic hypothesis” of dendrite growth states that synapse formation stabilizes filopodia to prevent retraction and promotes transition into longer and more persistent dendritic branches, culminating over time into increased complexity and size of the entire arbor. In this thesis, I expand the synaptotropic model of dendritogenesis by providing evidence to show how the cell adhesion molecules, NRX and NLG, play a critical role in regulating brain neuron structural development. However, I was mostly focused on the roles of NRX-NLG1. Mice express four different isoforms of neuroligin (NLG1-4), and different numbers of the NLG family are localized at either excitatory synapses or inhibitory synapses (Chih et al., 2005; Graf et al., 2004; Levinson et al., 2005; Song et al., 1999). NLG1 is primarily localized to excitatory synapses and promotes the formation of excitatory specializations, while NLG2 is localized to inhibitory synapses and preferentially induces the formation of inhibitory contacts (Varoqueaux et al., 2004). NLG3 has been shown to localize to both excitatory and inhibitory synapses but the roles of NLG3 on synapse formation is poorly understood (Budreck and Scheiffele, 2007). In *Xenopus* tadpoles, I cloned out NLG1, NLG2, and NLG3 by isolating cDNAs encoding these three different isoforms of NLGs from tadpole brain, but I have only characterized the expression and localization of NLG1. I found that, similar to mouse, *Xenopus* NLG1 is solely expressed at excitatory synapses and is colocalized with the postsynaptic marker, PSD-95. Future studies will examine the expression and localization of NLG2 and NLG3 in tadpole brain and test whether they are also critical for regulating dendrite growth.

Since NLG2 has been shown to regulate inhibitory synapse formation in mammalian neurons, one will have to first characterize the role of inhibitory synapse on dendrite growth in the developing brain. Evidence of how inhibitory synapses contribute to dendrite growth is lacking from the existing synaptotropic model of dendritogenesis. Time-lapsing imaging of neurons expressing PSD-95-GFP in zebrafish and *Xenopus* tadpoles has demonstrated that filopodial stabilization is associated with the presence of the PSD-95 puncta (Chen et al., 2010; Niell et al., 2004). Similar experiments, but expressing an inhibitory marker such as gephryin-GFP, will be essential to elucidate the localization of inhibitory synapses on tectal dendritic arbors and the relationship between the formation and elimination of inhibitory synapses and brain neuronal structural development.

4.2.2. Do autism-associated NLG mutants alter dendrite growth?

Genetic mutations of NLG family, *NLG-3* (a point mutation in arginine 451, Arg451→Cys451) and *NLG4* (a nonsense mutation at aspartate 396, D396X), have been identified in patients with Autism Spectrum Disorders (ASDs) (Jamain et al., 2003; Yan et al., 2005). Since NRXs and NLGs are clearly involved in regulating neural network formation, it will be important to understand whether mutations in NLG3 and NLG4 affect dendrite development. To date, research on the biological consequences produced by these mutations has largely focused on their effects on synapse development and function, yielding important evidence for altered synapse function and an imbalance between excitatory and inhibitory synapses (Chih et al., 2004; Levinson et al., 2005; Tabuchi et al., 2007). Investigating the effects of specific ASD-associated

mutations of NLGs on early brain neuron growth and functional development will add another layer of understanding to how neural circuits of ASD patients may be altered due to perturbations during brain development. I have conducted preliminary studies by expressing the rat version of NLG3-R741C and the corresponding rat version of R473C NLG1 mutant (rat NLG1-R473C) in individual neurons in the *Xenopus* optic tectum. Preliminary results show that neurons expressing autism-associated NLG mutants have simpler, and less complex dendritic arbors with significantly lower filopodial density. These neurons also exhibit low addition and retraction rates with high filopodial motility suggesting an inability to form new synapses necessary to stabilize filopodia (**Figure 4.1**). These neurons have morphological features similar to neurons with MO-mediated knockdown of NLG1. Since expression of NLG1-R473C in cultured neuron causes partial retention of NLG proteins within the endoplasmic reticulum and impairs synaptic function (Chih et al., 2004; Chubykin et al., 2007; Chubykin et al., 2005; Comoletti et al., 2004), one possible explanation may be attributed to NLG1-R473C heterodimerization with endogenous NLGs and result in loss of functional NLG1 at the membrane surface. Future studies will be needed to clarify the effects of human ASD-associated mutations on neuronal morphological development.

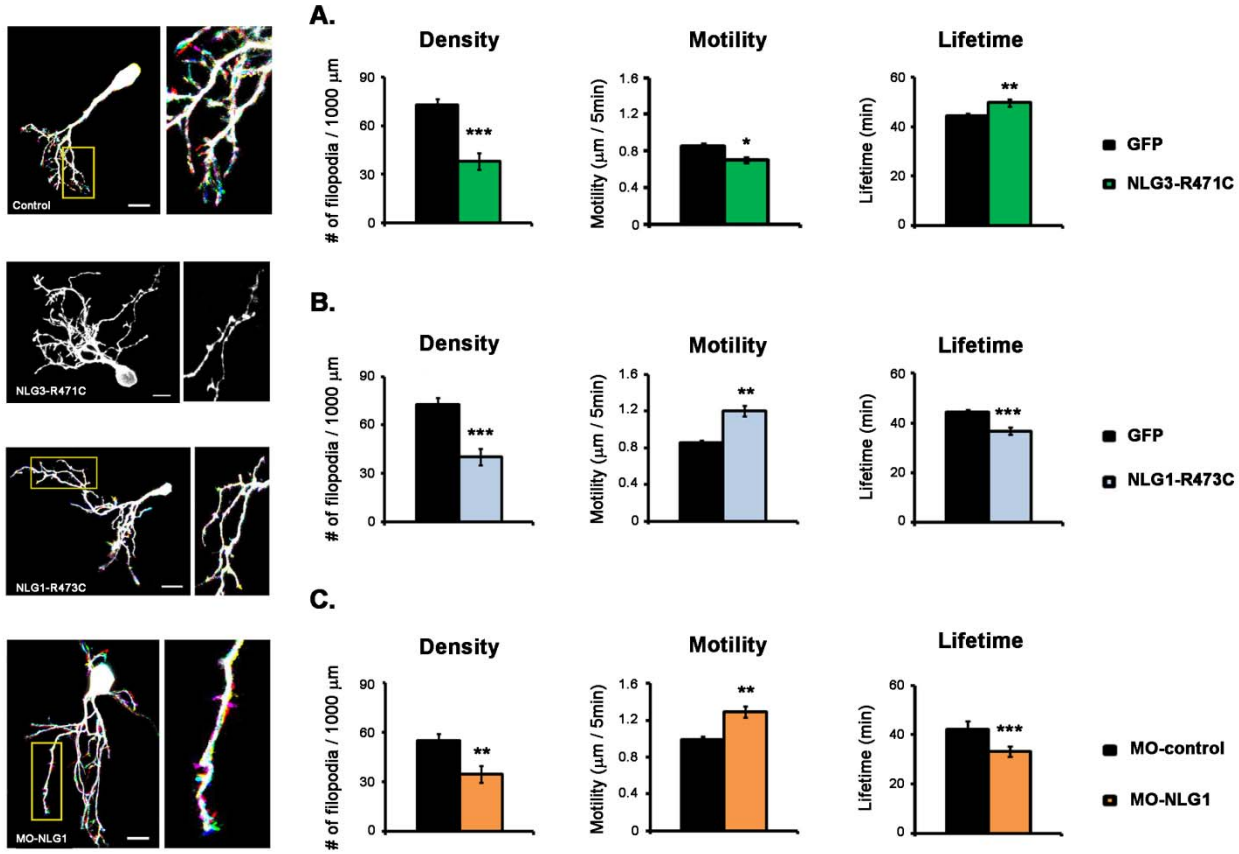

Figure 4.1 Expression of ASD-associated NLG Mutants Results in Simple and Less Complex Dendritic Arbors

Left Overlay of six successive images at 10 min intervals of tectal neurons over-expressing NLG3-R471C, NLG1-R473C, or MO-NLG1. *Right:* enlargement of boxed region of dendritic arbor Scale bar = 20 µm. **(A)** Morphometric analysis of dendritic filopodial dynamics of EGFP controls, neurons over-expressing NLG3-R471C **(B)** Morphometric analysis of dendritic filopodial dynamics of EGFP controls, neurons over-expressing NLG1-R473C **(C)** Morphometric analysis of dendritic filopodial dynamics of EGFP controls, neurons over-expressing MO-NLG1.

4.2.3. Role of NRX-NLG1 interactions on the functional properties and connectivities of neural circuit

During early embryonic development, *Xenopus* tectal neurons have large receptive fields (RFs) and respond optimally to visual stimuli such as sharp changes in illumination or movement of large black objects against a light-coloured background (Engert et al., 2002; Zhang et al., 2000). By presenting simple ON/OFF light flashes to unanesthetized tadpoles while performing *in vivo* two-photon calcium imaging of neuronal activity, the RF properties of neurons can be characterized throughout the tectum. Previous work in our laboratory has demonstrated that neurons with similar RF properties tend to cluster together, and this characteristic clustering pattern and distribution of RF responses are conserved across tadpoles (Dunfield and Haas, 2009). Hence, one future experiment could involve measuring the RFs of individual transfected tectal neurons with altered NRX-NLG1 interactions to determine effects on basic retinotectal circuit function. I expect neurons that are not capable of making proper axo-dendritic contacts will not be properly integrated into the visual circuit and will have reduced or abnormal RFs. In contrast, neurons that over-express WT-NLG1 and have complex, yet less plastic dendritic arbors will have strong responses to visual stimuli, yet with very broad and immature RF properties.

4.2.4. Identifying molecular cascades downstream of MEF2

The identification of MEF2 as a master regulator of the metaplastic state or plasticity threshold suggests orchestration of downstream effectors through altered transcriptional regulation. The Greenberg Lab has recently conducted screens for genes,

microRNA and proteins regulated by MEF2 in mouse hippocampal neurons (Fiore et al., 2009; Flavell et al., 2008). They identified MEF2 target genes associated with synapses, including the plasticity-associated activity-regulated cytoskeletal-related gene (Arc), synaptic RAS GTPase-activating protein (synGAP), and genes associated with ASDs, epilepsy, and mental retardation (lgi1, arhgef9, kcna1, ube3a, slc9a6, pcdh10, c3orf58) (Flavell et al., 2008). MEF2 was also found to regulate transcription of the miR379-410 cluster of microRNAs, which in turn, regulate the translational repressor such as Pumilio2 (Pum2) (Fiore et al., 2009). MEF2-dependent transcription thus may represent a mechanism in developing brain neurons to coordinate local and global gene and miRNA transcription to modulate neuronal sensitivity and responses to plasticity-inducing stimuli, without altering neuronal growth and physiology directly. Identification of protein targets downstream of MEF2 that mediates WN metaplasticity will be essential to provide important insights into precisely how sensory experience alters neuronal sensitivity to further plasticity-inducing stimuli.

4.3. Significance

The experiments in this thesis contribute to the field of developmental neurobiology by demonstrating how sensory experience and synapse formation regulate brain neuron morphological maturation during critical periods of neural circuit formation. First, I demonstrated that the cell adhesion molecules, NRX and NLGs, well known for their roles in synapse formation and maturation, also play an important role in the larger context of directing brain neuron dendritic arbor structural growth. This has clinical implications since genetic mutations in NRXs and NLGs have been identified in patients with familial ASDs. Understanding how normal and specific ASD-associated NLGs

influence brain neuron growth and functional development will help us to further understand of how neural circuits of ASD patients may be altered, both functionally and structurally due to perturbations during brain development. Currently, the field of neurodevelopmental disorders is overly focused on a role for synapse dysfunction as the primary source of pathophysiology, while ignoring larger effects of mutated synaptic proteins on neural circuit structural development.

Moreover, my discovery of the rapid and dramatic degradation of transcription factor MEF2A/D in response to brief WN visual stimulation in Chapter 3 is intriguing and important for new avenues of research on plasticity and metaplasticity. My experiments demonstrate that levels of MEF2 mediate the metaplastic shift in threshold for visual experience induced brain plasticity. Further, my identification of a novel non-apoptotic role of caspase-mediated MEF2 degradation sensitive to natural sensory experience may provide new targets for design of novel therapeutics to regulate brain plasticity. Such drugs in combination with training could also treat cognitive deficits, dementia, and promote enhanced recovery from stroke, by specifically strengthening circuits targeted by training, while avoiding confounding nonspecific network alterations

REFERENCES

Abel, T., Nguyen, P.V., Barad, M., Deuel, T.A., Kandel, E.R., and Bourtchouladze, R. (1997). Genetic demonstration of a role for PKA in the late phase of LTP and in hippocampus-based long-term memory. Cell *88*, 615-626.

Abraham, W.C. (2008). Metaplasticity: tuning synapses and networks for plasticity. Nat Rev Neurosci *9*, 387.

Abraham, W.C., and Huggett, A. (1997). Induction and reversal of long-term potentiation by repeated high-frequency stimulation in rat hippocampal slices. Hippocampus *7*, 137-145.

Abraham, W.C., Mason-Parker, S.E., Bear, M.F., Webb, S., and Tate, W.P. (2001). Heterosynaptic metaplasticity in the hippocampus in vivo: a BCM-like modifiable threshold for LTP. Proc Natl Acad Sci U S A *98*, 10924-10929.

Abraham, W.C., and Williams, J.M. (2003). Properties and mechanisms of LTP maintenance. Neuroscientist *9*, 463-474.

Ahmari, S.E., Buchanan, J., and Smith, S.J. (2000). Assembly of presynaptic active zones from cytoplasmic transport packets. Nat Neurosci *3*, 445-451.

Aizawa, H., Hu, S.C., Bobb, K., Balakrishnan, K., Ince, G., Gurevich, I., Cowan, M., and Ghosh, A. (2004). Dendrite development regulated by CREST, a calcium-regulated transcriptional activator. Science *303*, 197-202.

Aizenman, C.D., and Cline, H.T. (2007). Enhanced visual activity in vivo forms nascent synapses in the developing retinotectal projection. J Neurophysiol *97*, 2949-2957.

Antonova, I., Arancio, O., Trillat, A.C., Wang, H.G., Zablow, L., Udo, H., Kandel, E.R., and Hawkins, R.D. (2001). Rapid increase in clusters of presynaptic proteins at onset of long-lasting potentiation. Science *294*, 1547-1550.

Atasoy, D., Schoch, S., Ho, A., Nadasy, K.A., Liu, X., Zhang, W., Mukherjee, K., Nosyreva, E.D., Fernandez-Chacon, R., Missler, M.*, et al.* (2007). Deletion of CASK in mice is lethal and impairs synaptic function. Proc Natl Acad Sci U S A *104*, 2525-2530.

Baker, R.E., Dijkhuizen, P.A., Van Pelt, J., and Verhaagen, J. (1998). Growth of pyramidal, but not non-pyramidal, dendrites in long-term organotypic explants of neonatal rat neocortex chronically exposed to neurotrophin-3. Eur J Neurosci *10*, 1037-1044.

Baker, R.E., Wolters, P., and van Pelt, J. (1997). Chronic blockade of glutamate-mediated bioelectric activity in long-term organotypic neocortical explants differentially effects pyramidal/non-pyramidal dendritic morphology. Brain Res Dev Brain Res *104*, 31-39.

Bamji, S.X., Shimazu, K., Kimes, N., Huelsken, J., Birchmeier, W., Lu, B., and Reichardt, L.F. (2003). Role of beta-catenin in synaptic vesicle localization and presynaptic assembly. Neuron *40*, 719-731.

Banovic, D., Khorramshahi, O., Owald, D., Wichmann, C., Riedt, T., Fouquet, W., Tian, R., Sigrist, S.J., and Aberle, H. Drosophila neuroligin 1 promotes growth and postsynaptic differentiation at glutamatergic neuromuscular junctions. Neuron *66*, 724-738.

Barbosa, A.C., Kim, M.S., Ertunc, M., Adachi, M., Nelson, E.D., McAnally, J., Richardson, J.A., Kavalali, E.T., Monteggia, L.M., Bassel-Duby, R.*, et al.* (2008). MEF2C, a transcription factor that facilitates learning and memory by negative regulation of synapse numbers and function. Proc Natl Acad Sci U S A *105*, 9391-9396.

Barrow, S.L., Constable, J.R., Clark, E., El-Sabeawy, F., McAllister, A.K., and Washbourne, P. (2009). Neuroligin1: a cell adhesion molecule that recruits PSD-95 and NMDA receptors by distinct mechanisms during synaptogenesis. Neural Dev *4*, 17.

Baudet, M.L., Zivraj, K.H., Abreu-Goodger, C., Muldal, A., Armisen, J., Blenkiron, C., Goldstein, L.D., Miska, E.A., and Holt, C.E. (2011). miR-124 acts through CoREST to control onset of Sema3A sensitivity in navigating retinal growth cones. Nat Neurosci *15*, 29-38.

Bestman, J.E., Ewald, R.C., Chiu, S.L., and Cline, H.T. (2006). In vivo single-cell electroporation for transfer of DNA and macromolecules. Nat Protoc *1*, 1267-1272.

Biederer, T., Sara, Y., Mozhayeva, M., Atasoy, D., Liu, X., Kavalali, E.T., and Sudhof, T.C. (2002). SynCAM, a synaptic adhesion molecule that drives synapse assembly. Science *297*, 1525-1531.

Bienenstock, E.L., Cooper, L.N., and Munro, P.W. (1982). Theory for the development of neuron selectivity: orientation specificity and binocular interaction in visual cortex. J Neurosci *2*, 32-48.

Black, B.L., and Olson, E.N. (1998). Transcriptional control of muscle development by myocyte enhancer factor-2 (MEF2) proteins. Annu Rev Cell Dev Biol *14*, 167-196.

Bliss, T.V., and Collingridge, G.L. (1993). A synaptic model of memory: long-term potentiation in the hippocampus. Nature *361*, 31-39.

Bloodgood, B.L., and Sabatini, B.L. (2007). Ca(2+) signaling in dendritic spines. Curr Opin Neurobiol *17*, 345-351.

Blundell, J., Blaiss, C.A., Etherton, M.R., Espinosa, F., Tabuchi, K., Walz, C., Bolliger, M.F., Sudhof, T.C., and Powell, C.M. Neuroligin-1 deletion results in impaired spatial memory and increased repetitive behavior. J Neurosci *30*, 2115-2129.

Blundell, J., Tabuchi, K., Bolliger, M.F., Blaiss, C.A., Brose, N., Liu, X., Sudhof, T.C., and Powell, C.M. (2009). Increased anxiety-like behavior in mice lacking the inhibitory synapse cell adhesion molecule neuroligin 2. Genes Brain Behav *8*, 114-126.

Bolliger, M.F., Frei, K., Winterhalter, K.H., and Gloor, S.M. (2001). Identification of a novel neuroligin in humans which binds to PSD-95 and has a widespread expression. Biochem J *356*, 581-588.

Borodinsky, L.N., Root, C.M., Cronin, J.A., Sann, S.B., Gu, X., and Spitzer, N.C. (2004). Activity-dependent homeostatic specification of transmitter expression in embryonic neurons. Nature *429*, 523-530.

Boucard, A.A., Chubykin, A.A., Comoletti, D., Taylor, P., and Sudhof, T.C. (2005). A splice code for trans-synaptic cell adhesion mediated by binding of neuroligin 1 to alpha- and beta-neurexins. Neuron *48*, 229-236.

Bredt, D.S., and Nicoll, R.A. (2003). AMPA receptor trafficking at excitatory synapses. Neuron *40*, 361-379.

Bresler, T., Shapira, M., Boeckers, T., Dresbach, T., Futter, M., Garner, C.C., Rosenblum, K., Gundelfinger, E.D., and Ziv, N.E. (2004). Postsynaptic density assembly is fundamentally different from presynaptic active zone assembly. J Neurosci *24*, 1507-1520.

Brigidi, G.S., and Bamji, S.X. (2011). Cadherin-catenin adhesion complexes at the synapse. Curr Opin Neurobiol *21*, 208-214.

Budreck, E.C., and Scheiffele, P. (2007). Neuroligin-3 is a neuronal adhesion protein at GABAergic and glutamatergic synapses. Eur J Neurosci *26*, 1738-1748.

Carlisle, H.J., and Kennedy, M.B. (2005). Spine architecture and synaptic plasticity. Trends Neurosci *28*, 182-187.

Cases-Langhoff, C., Voss, B., Garner, A.M., Appeltauer, U., Takei, K., Kindler, S., Veh, R.W., De Camilli, P., Gundelfinger, E.D., and Garner, C.C. (1996). Piccolo, a novel 420 kDa protein associated with the presynaptic cytomatrix. Eur J Cell Biol *69*, 214-223.

Chadman, K.K., Gong, S., Scattoni, M.L., Boltuck, S.E., Gandhy, S.U., Heintz, N., and Crawley, J.N. (2008). Minimal aberrant behavioral phenotypes of neuroligin-3 R451C knockin mice. Autism Res *1*, 147-158.

Chen, L., Chetkovich, D.M., Petralia, R.S., Sweeney, N.T., Kawasaki, Y., Wenthold, R.J., Bredt, D.S., and Nicoll, R.A. (2000). Stargazin regulates synaptic targeting of AMPA receptors by two distinct mechanisms. Nature *408*, 936-943.

Chen, S.X., Tari, P.K., She, K., and Haas, K. (2010). Neurexin-neuroligin cell adhesion complexes contribute to synaptotropic dendritogenesis via growth stabilization mechanisms in vivo. Neuron *67*, 967-983.

Chen, W.S., and Bear, M.F. (2007). Activity-dependent regulation of NR2B translation contributes to metaplasticity in mouse visual cortex. Neuropharmacology *52*, 200-214.

Chih, B., Afridi, S.K., Clark, L., and Scheiffele, P. (2004). Disorder-associated mutations lead to functional inactivation of neuroligins. Hum Mol Genet *13*, 1471-1477.

Chih, B., Engelman, H., and Scheiffele, P. (2005). Control of excitatory and inhibitory synapse formation by neuroligins. Science *307*, 1324-1328.

Chih, B., Gollan, L., and Scheiffele, P. (2006). Alternative splicing controls selective trans-synaptic interactions of the neuroligin-neurexin complex. Neuron *51*, 171-178.

Chiu, S.L., Chen, C.M., and Cline, H.T. (2008). Insulin receptor signaling regulates synapse number, dendritic plasticity, and circuit function in vivo. Neuron *58*, 708-719.

Christie, B.R., and Abraham, W.C. (1992). Priming of associative long-term depression in the dentate gyrus by theta frequency synaptic activity. Neuron *9*, 79-84.

Chubykin, A.A., Atasoy, D., Etherton, M.R., Brose, N., Kavalali, E.T., Gibson, J.R., and Sudhof, T.C. (2007). Activity-dependent validation of excitatory versus inhibitory synapses by neuroligin-1 versus neuroligin-2. Neuron *54*, 919-931.

Chubykin, A.A., Liu, X., Comoletti, D., Tsigelny, I., Taylor, P., and Sudhof, T.C. (2005). Dissection of synapse induction by neuroligins: effect of a neuroligin mutation associated with autism. J Biol Chem *280*, 22365-22374.

Cingolani, L.A., and Goda, Y. (2008). Actin in action: the interplay between the actin cytoskeleton and synaptic efficacy. Nat Rev Neurosci *9*, 344-356.

Cline, H., and Haas, K. (2008). The regulation of dendritic arbor development and plasticity by glutamatergic synaptic input: a review of the synaptotrophic hypothesis. J Physiol *586*, 1509-1517.

Cline, H.T. (1991). Activity-dependent plasticity in the visual systems of frogs and fish. Trends Neurosci *14*, 104-111.

Coleman, P.D., and Riesen, A.H. (1968). Evironmental effects on cortical dendritic fields. I. Rearing in the dark. J Anat *102*, 363-374.

Collingridge, G.L., Peineau, S., Howland, J.G., and Wang, Y.T. (2010). Long-term depression in the CNS. Nat Rev Neurosci *11*, 459-473.

Comoletti, D., De Jaco, A., Jennings, L.L., Flynn, R.E., Gaietta, G., Tsigelny, I., Ellisman, M.H., and Taylor, P. (2004). The Arg451Cys-neuroligin-3 mutation associated with autism reveals a defect in protein processing. J Neurosci *24*, 4889-4893.

Craig, A.M., Graf, E.R., and Linhoff, M.W. (2006). How to build a central synapse: clues from cell culture. Trends Neurosci *29*, 8-20.

Dakoji, S., Tomita, S., Karimzadegan, S., Nicoll, R.A., and Bredt, D.S. (2003). Interaction of transmembrane AMPA receptor regulatory proteins with multiple membrane associated guanylate kinases. Neuropharmacology *45*, 849-856.

Dalva, M.B., Ghosh, A., and Shatz, C.J. (1994). Independent control of dendritic and axonal form in the developing lateral geniculate nucleus. J Neurosci *14*, 3588-3602.

Dalva, M.B., McClelland, A.C., and Kayser, M.S. (2007). Cell adhesion molecules: signalling functions at the synapse. Nat Rev Neurosci *8*, 206-220.

Datwani, A., McConnell, M.J., Kanold, P.O., Micheva, K.D., Busse, B., Shamloo, M., Smith, S.J., and Shatz, C.J. (2009). Classical MHCI molecules regulate retinogeniculate refinement and limit ocular dominance plasticity. Neuron *64*, 463-470.

Daw, M.I., Chittajallu, R., Bortolotto, Z.A., Dev, K.K., Duprat, F., Henley, J.M., Collingridge, G.L., and Isaac, J.T. (2000). PDZ proteins interacting with C-terminal GluR2/3 are involved in a PKC-dependent regulation of AMPA receptors at hippocampal synapses. Neuron *28*, 873-886.

Dean, C., and Dresbach, T. (2006). Neuroligins and neurexins: linking cell adhesion, synapse formation and cognitive function. Trends Neurosci *29*, 21-29.

Dean, C., Scholl, F.G., Choih, J., DeMaria, S., Berger, J., Isacoff, E., and Scheiffele, P. (2003). Neurexin mediates the assembly of presynaptic terminals. Nat Neurosci *6*, 708-716.

della Gaspera, B., Armand, A.S., Sequeira, I., Lecolle, S., Gallien, C.L., Charbonnier, F., and Chanoine, C. (2009). The Xenopus MEF2 gene family: evidence of a role for XMEF2C in larval tendon development. Dev Biol *328*, 392-402.

Denk, W., Strickler, J.H., and Webb, W.W. (1990). Two-photon laser scanning fluorescence microscopy. Science *248*, 73-76.

Derkach, V., Barria, A., and Soderling, T.R. (1999). Ca2+/calmodulin-kinase II enhances channel conductance of alpha-amino-3-hydroxy-5-methyl-4-isoxazolepropionate type glutamate receptors. Proc Natl Acad Sci U S A *96*, 3269-3274.

Derkach, V.A., Oh, M.C., Guire, E.S., and Soderling, T.R. (2007). Regulatory mechanisms of AMPA receptors in synaptic plasticity. Nat Rev Neurosci *8*, 101-113.

Dimitrova, S., Reissaus, A., and Tavosanis, G. (2008). Slit and Robo regulate dendrite branching and elongation of space-filling neurons in Drosophila. Dev Biol *324*, 18-30.

Dong, H., O'Brien, R.J., Fung, E.T., Lanahan, A.A., Worley, P.F., and Huganir, R.L. (1997). GRIP: a synaptic PDZ domain-containing protein that interacts with AMPA receptors. Nature *386*, 279-284.

Dong, W., Lee, R.H., Xu, H., Yang, S., Pratt, K.G., Cao, V., Song, Y.K., Nurmikko, A., and Aizenman, C.D. (2009). Visual avoidance in Xenopus tadpoles is correlated with the maturation of visual responses in the optic tectum. J Neurophysiol *101*, 803-815.

Dresbach, T., Neeb, A., Meyer, G., Gundelfinger, E.D., and Brose, N. (2004). Synaptic targeting of neuroligin is independent of neurexin and SAP90/PSD95 binding. Mol Cell Neurosci *27*, 227-235.

Dudanova, I., Tabuchi, K., Rohlmann, A., Sudhof, T.C., and Missler, M. (2007). Deletion of alpha-neurexins does not cause a major impairment of axonal pathfinding or synapse formation. J Comp Neurol *502*, 261-274.

Dudek, S.M., and Bear, M.F. (1992). Homosynaptic long-term depression in area CA1 of hippocampus and effects of N-methyl-D-aspartate receptor blockade. Proc Natl Acad Sci U S A *89*, 4363-4367.

Dunfield, D., and Haas, K. (2009). Metaplasticity governs natural experience-driven plasticity of nascent embryonic brain circuits. Neuron *64*, 240-250.

Dunfield, D., and Haas, K. (2010). In vivo single-cell excitability probing of neuronal ensembles in the intact and awake developing Xenopus brain. Nat Protoc *5*, 841-848.

Durand, C.M., Betancur, C., Boeckers, T.M., Bockmann, J., Chaste, P., Fauchereau, F., Nygren, G., Rastam, M., Gillberg, I.C., Anckarsater, H*., et al.* (2007). Mutations in the gene encoding the synaptic scaffolding protein SHANK3 are associated with autism spectrum disorders. Nat Genet *39*, 25-27.

Ehlers, M.D. (2000). Reinsertion or degradation of AMPA receptors determined by activity-dependent endocytic sorting. Neuron *28*, 511-525.

Engert, F., and Bonhoeffer, T. (1999). Dendritic spine changes associated with hippocampal long-term synaptic plasticity. Nature *399*, 66-70.

Engert, F., Tao, H.W., Zhang, L.I., and Poo, M.M. (2002). Moving visual stimuli rapidly induce direction sensitivity of developing tectal neurons. Nature *419*, 470-475.

Espinosa, J.S., Wheeler, D.G., Tsien, R.W., and Luo, L. (2009). Uncoupling dendrite growth and patterning: single-cell knockout analysis of NMDA receptor 2B. Neuron *62*, 205-217.

Ewald, R.C., Van Keuren-Jensen, K.R., Aizenman, C.D., and Cline, H.T. (2008). Roles of NR2A and NR2B in the development of dendritic arbor morphology in vivo. J Neurosci *28*, 850-861.

Feller, M.B., and Scanziani, M. (2005). A precritical period for plasticity in visual cortex. Curr Opin Neurobiol *15*, 94-100.

Feng, J., Schroer, R., Yan, J., Song, W., Yang, C., Bockholt, A., Cook, E.H., Jr., Skinner, C., Schwartz, C.E., and Sommer, S.S. (2006). High frequency of neurexin 1beta signal peptide structural variants in patients with autism. Neurosci Lett *409*, 10-13.

Fenster, S.D., Chung, W.J., Zhai, R., Cases-Langhoff, C., Voss, B., Garner, A.M., Kaempf, U., Kindler, S., Gundelfinger, E.D., and Garner, C.C. (2000). Piccolo, a presynaptic zinc finger protein structurally related to bassoon. Neuron *25*, 203-214.

Fiore, R., Khudayberdiev, S., Christensen, M., Siegel, G., Flavell, S.W., Kim, T.K., Greenberg, M.E., and Schratt, G. (2009). Mef2-mediated transcription of the miR379-410 cluster regulates activity-dependent dendritogenesis by fine-tuning Pumilio2 protein levels. EMBO J *28*, 697-710.

Flavell, S.W., Cowan, C.W., Kim, T.K., Greer, P.L., Lin, Y., Paradis, S., Griffith, E.C., Hu, L.S., Chen, C., and Greenberg, M.E. (2006). Activity-dependent regulation of MEF2 transcription factors suppresses excitatory synapse number. Science *311*, 1008-1012.

Flavell, S.W., Kim, T.K., Gray, J.M., Harmin, D.A., Hemberg, M., Hong, E.J., Markenscoff-Papadimitriou, E., Bear, D.M., and Greenberg, M.E. (2008). Genome-wide analysis of MEF2 transcriptional program reveals synaptic target genes and neuronal activity-dependent polyadenylation site selection. Neuron *60*, 1022-1038.

Friedman, H.V., Bresler, T., Garner, C.C., and Ziv, N.E. (2000). Assembly of new individual excitatory synapses: time course and temporal order of synaptic molecule recruitment. Neuron *27*, 57-69.

Fujii, S., Kuroda, Y., Miura, M., Furuse, H., Sasaki, H., Kaneko, K., Ito, K., Chen, Z., and Kato, H. (1996). The long-term suppressive effect of prior activation of synaptic inputs by low-frequency stimulation on induction of long-term potentiation in CA1 neurons of guinea pig hippocampal slices. Exp Brain Res *111*, 305-312.

Gao, F.B. (2007). Molecular and cellular mechanisms of dendritic morphogenesis. Curr Opin Neurobiol *17*, 525-532.

Garner, C.C., Zhai, R.G., Gundelfinger, E.D., and Ziv, N.E. (2002). Molecular mechanisms of CNS synaptogenesis. Trends Neurosci *25*, 243-251.

Gaudilliere, B., Konishi, Y., de la Iglesia, N., Yao, G., and Bonni, A. (2004). A CaMKII-NeuroD signaling pathway specifies dendritic morphogenesis. Neuron *41*, 229-241.

Gerber, S.H., Garcia, J., Rizo, J., and Sudhof, T.C. (2001). An unusual C(2)-domain in the active-zone protein piccolo: implications for Ca(2+) regulation of neurotransmitter release. EMBO J *20*, 1605-1619.

Gerrow, K., and El-Husseini, A. (2006). Cell adhesion molecules at the synapse. Front Biosci *11*, 2400-2419.

Glynn, M.W., Elmer, B.M., Garay, P.A., Liu, X.B., Needleman, L.A., El-Sabeawy, F., and McAllister, A.K. (2011). MHCI negatively regulates synapse density during the establishment of cortical connections. Nat Neurosci *14*, 442-451.

Goddard, C.A., Butts, D.A., and Shatz, C.J. (2007). Regulation of CNS synapses by neuronal MHC class I. Proc Natl Acad Sci U S A *104*, 6828-6833.

Goodman, L.A., and Model, P.G. (1990). Eliminating afferent impulse activity does not alter the dendritic branching of the amphibian Mauthner cell. J Neurobiol *21*, 283-294.

Graf, E.R., Kang, Y., Hauner, A.M., and Craig, A.M. (2006). Structure function and splice site analysis of the synaptogenic activity of the neurexin-1 beta LNS domain. J Neurosci *26*, 4256-4265.

Graf, E.R., Zhang, X., Jin, S.X., Linhoff, M.W., and Craig, A.M. (2004). Neurexins induce differentiation of GABA and glutamate postsynaptic specializations via neuroligins. Cell *119*, 1013-1026.

Grueber, W.B., Jan, L.Y., and Jan, Y.N. (2003). Different levels of the homeodomain protein cut regulate distinct dendrite branching patterns of Drosophila multidendritic neurons. Cell *112*, 805-818.

Haas, K., Jensen, K., Sin, W.C., Foa, L., and Cline, H.T. (2002). Targeted electroporation in Xenopus tadpoles in vivo--from single cells to the entire brain. Differentiation *70*, 148-154.

Haas, K., Li, J., and Cline, H.T. (2006). AMPA receptors regulate experience-dependent dendritic arbor growth in vivo. Proc Natl Acad Sci U S A *103*, 12127-12131.

Haas, K., Sin, W.C., Javaherian, A., Li, Z., and Cline, H.T. (2001). Single-cell electroporation for gene transfer in vivo. Neuron *29*, 583-591.

Hand, R., Bortone, D., Mattar, P., Nguyen, L., Heng, J.I., Guerrier, S., Boutt, E., Peters, E., Barnes, A.P., Parras, C*., et al.* (2005). Phosphorylation of Neurogenin2 specifies the migration properties and the dendritic morphology of pyramidal neurons in the neocortex. Neuron *48*, 45-62.

He, H.Y., Hodos, W., and Quinlan, E.M. (2006). Visual deprivation reactivates rapid ocular dominance plasticity in adult visual cortex. J Neurosci *26*, 2951-2955.

Heine, M., Thoumine, O., Mondin, M., Tessier, B., Giannone, G., and Choquet, D. (2008). Activity-independent and subunit-specific recruitment of functional AMPA receptors at neurexin/neuroligin contacts. Proc Natl Acad Sci U S A *105*, 20947-20952.

Hewapathirane, D.S., Dunfield, D., Yen, W., Chen, S., and Haas, K. (2008). In vivo imaging of seizure activity in a novel developmental seizure model. Exp Neurol *211*, 480-488.

Heynen, A.J., and Bear, M.F. (2001). Long-term potentiation of thalamocortical transmission in the adult visual cortex in vivo. J Neurosci *21*, 9801-9813.

Hines, R.M., Wu, L., Hines, D.J., Steenland, H., Mansour, S., Dahlhaus, R., Singaraja, R.R., Cao, X., Sammler, E., Hormuzdi, S.G.*, et al.* (2008). Synaptic imbalance, stereotypies, and impaired social interactions in mice with altered neuroligin 2 expression. J Neurosci *28*, 6055-6067.

Hofer, S.B., Mrsic-Flogel, T.D., Bonhoeffer, T., and Hubener, M. (2009). Experience leaves a lasting structural trace in cortical circuits. Nature *457*, 313-317.

Holt, C.E., and Harris, W.A. (1993). Position, guidance, and mapping in the developing visual system. J Neurobiol *24*, 1400-1422.

Horch, H.W., Kruttgen, A., Portbury, S.D., and Katz, L.C. (1999). Destabilization of cortical dendrites and spines by BDNF. Neuron *23*, 353-364.

Hossain, S., Hewapathirane, D.S., and Haas, K. (2011). Dynamic Morphometrics reveals contributions of dendritic growth cones and filopodia to dendritogenesis in the intact and awake embryonic brain. Dev Neurobiol.

Hrabetova, S., and Sacktor, T.C. (2001). Transient translocation of conventional protein kinase C isoforms and persistent downregulation of atypical protein kinase Mzeta in long-term depression. Brain Res Mol Brain Res *95*, 146-152.

Hsieh, H., Boehm, J., Sato, C., Iwatsubo, T., Tomita, T., Sisodia, S., and Malinow, R. (2006). AMPAR removal underlies Abeta-induced synaptic depression and dendritic spine loss. Neuron *52*, 831-843.

Hu, B., Nikolakopoulou, A.M., and Cohen-Cory, S. (2005). BDNF stabilizes synapses and maintains the structural complexity of optic axons in vivo. Development *132*, 4285-4298.

Huang, Y.Y., Colino, A., Selig, D.K., and Malenka, R.C. (1992). The influence of prior synaptic activity on the induction of long-term potentiation. Science *255*, 730-733.

Huh, G.S., Boulanger, L.M., Du, H., Riquelme, P.A., Brotz, T.M., and Shatz, C.J. (2000). Functional requirement for class I MHC in CNS development and plasticity. Science *290*, 2155-2159.

Ichtchenko, K., Hata, Y., Nguyen, T., Ullrich, B., Missler, M., Moomaw, C., and Sudhof, T.C. (1995). Neuroligin 1: a splice site-specific ligand for beta-neurexins. Cell *81*, 435-443.

Ichtchenko, K., Nguyen, T., and Sudhof, T.C. (1996). Structures, alternative splicing, and neurexin binding of multiple neuroligins. J Biol Chem *271*, 2676-2682.

Iden, S., and Collard, J.G. (2008). Crosstalk between small GTPases and polarity proteins in cell polarization. Nat Rev Mol Cell Biol *9*, 846-859.

Inan, M., and Crair, M.C. (2007). Development of cortical maps: perspectives from the barrel cortex. Neuroscientist *13*, 49-61.

Irie, M., Hata, Y., Takeuchi, M., Ichtchenko, K., Toyoda, A., Hirao, K., Takai, Y., Rosahl, T.W., and Sudhof, T.C. (1997). Binding of neuroligins to PSD-95. Science *277*, 1511-1515.

Isaac, J.T., Crair, M.C., Nicoll, R.A., and Malenka, R.C. (1997). Silent synapses during development of thalamocortical inputs. Neuron *18*, 269-280.

Jamain, S., Quach, H., Betancur, C., Rastam, M., Colineaux, C., Gillberg, I.C., Soderstrom, H., Giros, B., Leboyer, M., Gillberg, C*., et al.* (2003). Mutations of the X-linked genes encoding neuroligins NLGN3 and NLGN4 are associated with autism. Nat Genet *34*, 27-29.

Jan, Y.N., and Jan, L.Y. (2010). Branching out: mechanisms of dendritic arborization. Nat Rev Neurosci *11*, 316-328.

Jinushi-Nakao, S., Arvind, R., Amikura, R., Kinameri, E., Liu, A.W., and Moore, A.W. (2007). Knot/Collier and cut control different aspects of dendrite cytoskeleton and synergize to define final arbor shape. Neuron *56*, 963-978.

Kameyama, K., Lee, H.K., Bear, M.F., and Huganir, R.L. (1998). Involvement of a postsynaptic protein kinase A substrate in the expression of homosynaptic long-term depression. Neuron *21*, 1163-1175.

Katz, L.C., and Shatz, C.J. (1996). Synaptic activity and the construction of cortical circuits. Science *274*, 1133-1138.

Kerschensteiner, D., Morgan, J.L., Parker, E.D., Lewis, R.M., and Wong, R.O. (2009). Neurotransmission selectively regulates synapse formation in parallel circuits in vivo. Nature *460*, 1016-1020.

Kessels, H.W., and Malinow, R. (2009). Synaptic AMPA receptor plasticity and behavior. Neuron *61*, 340-350.

Kim, E., and Sheng, M. (2004). PDZ domain proteins of synapses. Nat Rev Neurosci *5*, 771-781.

Kim, S., Burette, A., Chung, H.S., Kwon, S.K., Woo, J., Lee, H.W., Kim, K., Kim, H., Weinberg, R.J., and Kim, E. (2006). NGL family PSD-95-interacting adhesion molecules regulate excitatory synapse formation. Nat Neurosci *9*, 1294-1301.

Kirkwood, A., Rioult, M.C., and Bear, M.F. (1996). Experience-dependent modification of synaptic plasticity in visual cortex. Nature *381*, 526-528.

Komiyama, T., Sweeney, L.B., Schuldiner, O., Garcia, K.C., and Luo, L. (2007). Graded expression of semaphorin-1a cell-autonomously directs dendritic targeting of olfactory projection neurons. Cell *128*, 399-410.

Laurie, D.J., and Seeburg, P.H. (1994). Ligand affinities at recombinant N-methyl-D-aspartate receptors depend on subunit composition. Eur J Pharmacol *268*, 335-345.

Lee, M.C., Yasuda, R., and Ehlers, M.D. (2010). Metaplasticity at single glutamatergic synapses. Neuron *66*, 859-870.

Levinson, J.N., Chery, N., Huang, K., Wong, T.P., Gerrow, K., Kang, R., Prange, O., Wang, Y.T., and El-Husseini, A. (2005). Neuroligins mediate excitatory and inhibitory synapse formation: involvement of PSD-95 and neurexin-1beta in neuroligin-induced synaptic specificity. J Biol Chem *280*, 17312-17319.

Li, J., Erisir, A., and Cline, H. (2011). In vivo time-lapse imaging and serial section electron microscopy reveal developmental synaptic rearrangements. Neuron *69*, 273-286.

Li, M., Linseman, D.A., Allen, M.P., Meintzer, M.K., Wang, X., Laessig, T., Wierman, M.E., and Heidenreich, K.A. (2001). Myocyte enhancer factor 2A and 2D undergo phosphorylation and caspase-mediated degradation during apoptosis of rat cerebellar granule neurons. J Neurosci *21*, 6544-6552.

Li, W., Wang, F., Menut, L., and Gao, F.B. (2004). BTB/POZ-zinc finger protein abrupt suppresses dendritic branching in a neuronal subtype-specific and dosage-dependent manner. Neuron *43*, 823-834.

Li, Z., Aizenman, C.D., and Cline, H.T. (2002). Regulation of rho GTPases by crosstalk and neuronal activity in vivo. Neuron *33*, 741-750.

Li, Z., Jo, J., Jia, J.M., Lo, S.C., Whitcomb, D.J., Jiao, S., Cho, K., and Sheng, M. (2010). Caspase-3 activation via mitochondria is required for long-term depression and AMPA receptor internalization. Cell *141*, 859-871.

Liao, D., Hessler, N.A., and Malinow, R. (1995). Activation of postsynaptically silent synapses during pairing-induced LTP in CA1 region of hippocampal slice. Nature *375*, 400-404.

Lim, B.K., Matsuda, N., and Poo, M.M. (2008). Ephrin-B reverse signaling promotes structural and functional synaptic maturation in vivo. Nature Neuroscience *11*, 160-169.

Ling, D.S., Benardo, L.S., and Sacktor, T.C. (2006). Protein kinase Mzeta enhances excitatory synaptic transmission by increasing the number of active postsynaptic AMPA receptors. Hippocampus *16*, 443-452.

Ling, D.S., Benardo, L.S., Serrano, P.A., Blace, N., Kelly, M.T., Crary, J.F., and Sacktor, T.C. (2002). Protein kinase Mzeta is necessary and sufficient for LTP maintenance. Nat Neurosci *5*, 295-296.

Linhoff, M.W., Lauren, J., Cassidy, R.M., Dobie, F.A., Takahashi, H., Nygaard, H.B., Airaksinen, M.S., Strittmatter, S.M., and Craig, A.M. (2009). An unbiased expression screen for synaptogenic proteins identifies the LRRTM protein family as synaptic organizers. Neuron *61*, 734-749.

Lise, M.F., and El-Husseini, A. (2006). The neuroligin and neurexin families: from structure to function at the synapse. Cell Mol Life Sci *63*, 1833-1849.

Liu, X.F., Tari, P.K., and Haas, K. (2009). PKM zeta restricts dendritic arbor growth by filopodial and branch stabilization within the intact and awake developing brain. J Neurosci *29*, 12229-12235.

Lledo, P.M., Hjelmstad, G.O., Mukherji, S., Soderling, T.R., Malenka, R.C., and Nicoll, R.A. (1995). Calcium/calmodulin-dependent kinase II and long-term potentiation enhance synaptic transmission by the same mechanism. Proc Natl Acad Sci U S A *92*, 11175-11179.

Luo, L. (2000). Rho GTPases in neuronal morphogenesis. Nat Rev Neurosci *1*, 173-180.

Lyons, G.E., Micales, B.K., Schwarz, J., Martin, J.F., and Olson, E.N. (1995). Expression of mef2 genes in the mouse central nervous system suggests a role in neuronal maturation. J Neurosci *15*, 5727-5738.

Majewska, A., Tashiro, A., and Yuste, R. (2000). Regulation of spine calcium dynamics by rapid spine motility. J Neurosci *20*, 8262-8268.

Malenka, R.C., and Bear, M.F. (2004). LTP and LTD: an embarrassment of riches. Neuron *44*, 5-21.

Malenka, R.C., Kauer, J.A., Perkel, D.J., Mauk, M.D., Kelly, P.T., Nicoll, R.A., and Waxham, M.N. (1989). An essential role for postsynaptic calmodulin and protein kinase activity in long-term potentiation. Nature *340*, 554-557.

Malinow, R., Schulman, H., and Tsien, R.W. (1989). Inhibition of postsynaptic PKC or CaMKII blocks induction but not expression of LTP. Science *245*, 862-866.

Mao, Z., Bonni, A., Xia, F., Nadal-Vicens, M., and Greenberg, M.E. (1999). Neuronal activity-dependent cell survival mediated by transcription factor MEF2. Science *286*, 785-790.

Mao, Z., and Wiedmann, M. (1999). Calcineurin enhances MEF2 DNA binding activity in calcium-dependent survival of cerebellar granule neurons. J Biol Chem *274*, 31102-31107.

Matsuzaki, M., Honkura, N., Ellis-Davies, G.C., and Kasai, H. (2004). Structural basis of long-term potentiation in single dendritic spines. Nature *429*, 761-766.

Mattila, P.K., and Lappalainen, P. (2008). Filopodia: molecular architecture and cellular functions. Nat Rev Mol Cell Biol *9*, 446-454.

McAllister, A.K. (2000). Cellular and molecular mechanisms of dendrite growth. Cereb Cortex *10*, 963-973.

McAllister, A.K. (2007). Dynamic aspects of CNS synapse formation. Annu Rev Neurosci *30*, 425-450.

McAllister, A.K., Lo, D.C., and Katz, L.C. (1995). Neurotrophins regulate dendritic growth in developing visual cortex. Neuron *15*, 791-803.

McFarlane, S., and Lom, B. (2011). The Xenopus retinal ganglion cell as a model neuron to study the establishment of neuronal connectivity. Dev Neurobiol.

McKinsey, T.A., Zhang, C.L., and Olson, E.N. (2002). MEF2: a calcium-dependent regulator of cell division, differentiation and death. Trends Biochem Sci *27*, 40-47.

Meyer, R.L. (1998). Roger Sperry and his chemoaffinity hypothesis. Neuropsychologia *36*, 957-980.

Missler, M., Zhang, W., Rohlmann, A., Kattenstroth, G., Hammer, R.E., Gottmann, K., and Sudhof, T.C. (2003). Alpha-neurexins couple Ca2+ channels to synaptic vesicle exocytosis. Nature *423*, 939-948.

Molkentin, J.D., Black, B.L., Martin, J.F., and Olson, E.N. (1995). Cooperative activation of muscle gene expression by MEF2 and myogenic bHLH proteins. Cell *83*, 1125-1136.

Monyer, H., Sprengel, R., Schoepfer, R., Herb, A., Higuchi, M., Lomeli, H., Burnashev, N., Sakmann, B., and Seeburg, P.H. (1992). Heteromeric NMDA receptors: molecular and functional distinction of subtypes. Science *256*, 1217-1221.

Moser, E.I., Krobert, K.A., Moser, M.B., and Morris, R.G. (1998). Impaired spatial learning after saturation of long-term potentiation. Science *281*, 2038-2042.

Mulkey, R.M., Endo, S., Shenolikar, S., and Malenka, R.C. (1994). Involvement of a calcineurin/inhibitor-1 phosphatase cascade in hippocampal long-term depression. Nature *369*, 486-488.

Mulkey, R.M., Herron, C.E., and Malenka, R.C. (1993). An essential role for protein phosphatases in hippocampal long-term depression. Science *261*, 1051-1055.

Mulkey, R.M., and Malenka, R.C. (1992). Mechanisms underlying induction of homosynaptic long-term depression in area CA1 of the hippocampus. Neuron *9*, 967-975.

Murakoshi, H., Lee, S.J., and Yasuda, R. (2008). Highly sensitive and quantitative FRET-FLIM imaging in single dendritic spines using improved non-radiative YFP. Brain Cell Biol *36*, 31-42.

Murakoshi, H., Wang, H., and Yasuda, R. (2011). Local, persistent activation of Rho GTPases during plasticity of single dendritic spines. Nature *472*, 100-104.

Nam, C.I., and Chen, L. (2005). Postsynaptic assembly induced by neurexin-neuroligin interaction and neurotransmitter. Proc Natl Acad Sci U S A *102*, 6137-6142.

Nevin, L.M., Taylor, M.R., and Baier, H. (2008). Hardwiring of fine synaptic layers in the zebrafish visual pathway. Neural Dev *3*, 36.

Nguyen, T., and Sudhof, T.C. (1997). Binding properties of neuroligin 1 and neurexin 1beta reveal function as heterophilic cell adhesion molecules. J Biol Chem *272*, 26032-26039.

Niell, C.M. (2006). Theoretical analysis of a synaptotropic dendrite growth mechanism. J Theor Biol *241*, 39-48.

Niell, C.M., Meyer, M.P., and Smith, S.J. (2004). In vivo imaging of synapse formation on a growing dendritic arbor. Nat Neurosci *7*, 254-260.

Nowak, L., Bregestovski, P., Ascher, P., Herbet, A., and Prochiantz, A. (1984). Magnesium gates glutamate-activated channels in mouse central neurones. Nature *307*, 462-465.

Okabe, S., Miwa, A., and Okado, H. (2001). Spine formation and correlated assembly of presynaptic and postsynaptic molecules. J Neurosci *21*, 6105-6114.

Okamoto, K., Nagai, T., Miyawaki, A., and Hayashi, Y. (2004). Rapid and persistent modulation of actin dynamics regulates postsynaptic reorganization underlying bidirectional plasticity. Nat Neurosci *7*, 1104-1112.

Okamoto, S., Li, Z., Ju, C., Scholzke, M.N., Mathews, E., Cui, J., Salvesen, G.S., Bossy-Wetzel, E., and Lipton, S.A. (2002). Dominant-interfering forms of MEF2 generated by caspase cleavage contribute to NMDA-induced neuronal apoptosis. Proc Natl Acad Sci U S A *99*, 3974-3979.

Olson, E.N., Perry, M., and Schulz, R.A. (1995). Regulation of muscle differentiation by the MEF2 family of MADS box transcription factors. Dev Biol *172*, 2-14.

Osten, P., Hrabetova, S., and Sacktor, T.C. (1996a). Differential downregulation of protein kinase C isoforms in spreading depression. Neurosci Lett *221*, 37-40.

Osten, P., Khatri, L., Perez, J.L., Kohr, G., Giese, G., Daly, C., Schulz, T.W., Wensky, A., Lee, L.M., and Ziff, E.B. (2000). Mutagenesis reveals a role for ABP/GRIP binding to GluR2 in synaptic surface accumulation of the AMPA receptor. Neuron *27*, 313-325.

Osten, P., Valsamis, L., Harris, A., and Sacktor, T.C. (1996b). Protein synthesis-dependent formation of protein kinase Mzeta in long-term potentiation. J Neurosci *16*, 2444-2451.

Paoletti, P., and Neyton, J. (2007). NMDA receptor subunits: function and pharmacology. Curr Opin Pharmacol *7*, 39-47.

Parrish, J.Z., Kim, M.D., Jan, L.Y., and Jan, Y.N. (2006). Genome-wide analyses identify transcription factors required for proper morphogenesis of Drosophila sensory neuron dendrites. Genes Dev *20*, 820-835.

Perez, J.L., Khatri, L., Chang, C., Srivastava, S., Osten, P., and Ziff, E.B. (2001). PICK1 targets activated protein kinase Calpha to AMPA receptor clusters in spines of hippocampal neurons and reduces surface levels of the AMPA-type glutamate receptor subunit 2. J Neurosci *21*, 5417-5428.

Pettit, D.L., Perlman, S., and Malinow, R. (1994). Potentiated transmission and prevention of further LTP by increased CaMKII activity in postsynaptic hippocampal slice neurons. Science *266*, 1881-1885.

Philibert, R.A., Winfield, S.L., Sandhu, H.K., Martin, B.M., and Ginns, E.I. (2000). The structure and expression of the human neuroligin-3 gene. Gene *246*, 303-310.

Philpot, B.D., Cho, K.K., and Bear, M.F. (2007). Obligatory role of NR2A for metaplasticity in visual cortex. Neuron *53*, 495-502.

Philpot, B.D., Espinosa, J.S., and Bear, M.F. (2003). Evidence for altered NMDA receptor function as a basis for metaplasticity in visual cortex. J Neurosci *23*, 5583-5588.

Pittenger, C., and Kandel, E.R. (2003). In search of general mechanisms for long-lasting plasticity: Aplysia and the hippocampus. Philos Trans R Soc Lond B Biol Sci *358*, 757-763.

Podgorski, K., Dunfield, D., and Haas, K. (2011). Functional clustering drives encoding improvement in a developing brain network during awake visual learning PLoS Biol *under revision*.

Polleux, F., Morrow, T., and Ghosh, A. (2000). Semaphorin 3A is a chemoattractant for cortical apical dendrites. Nature *404*, 567-573.

Portera-Cailliau, C., Pan, D.T., and Yuste, R. (2003). Activity-regulated dynamic behavior of early dendritic protrusions: evidence for different types of dendritic filopodia. J Neurosci *23*, 7129-7142.

Potthoff, M.J., Arnold, M.A., McAnally, J., Richardson, J.A., Bassel-Duby, R., and Olson, E.N. (2007). Regulation of skeletal muscle sarcomere integrity and postnatal muscle function by Mef2c. Mol Cell Biol *27*, 8143-8151.

Rajan, I., and Cline, H.T. (1998). Glutamate receptor activity is required for normal development of tectal cell dendrites in vivo. J Neurosci *18*, 7836-7846.

Rajan, I., Witte, S., and Cline, H.T. (1999). NMDA receptor activity stabilizes presynaptic retinotectal axons and postsynaptic optic tectal cell dendrites in vivo. J Neurobiol *38*, 357-368.

Ramdya, P., and Engert, F. (2008). Emergence of binocular functional properties in a monocular neural circuit. Nat Neurosci *11*, 1083-1090.

Redmond, L., Kashani, A.H., and Ghosh, A. (2002). Calcium regulation of dendritic growth via CaM kinase IV and CREB-mediated transcription. Neuron *34*, 999-1010.

Reichardt, L.F. (2006). Neurotrophin-regulated signalling pathways. Philos Trans R Soc Lond B Biol Sci *361*, 1545-1564.

Riccio, R.V., and Matthews, M.A. (1987). Effects of intraocular tetrodotoxin on the postnatal development of the dorsal lateral geniculate nucleus of the rat: a Golgi analysis. J Neurosci Res *17*, 440-451.

Ridley, A.J. (2001). Rho GTPases and cell migration. J Cell Sci *114*, 2713-2722.

Rose, G.M., and Dunwiddie, T.V. (1986). Induction of hippocampal long-term potentiation using physiologically patterned stimulation. Neurosci Lett *69*, 244-248.

Ruthazer, E.S., Akerman, C.J., and Cline, H.T. (2003). Control of axon branch dynamics by correlated activity in vivo. Science *301*, 66-70.

Ruthazer, E.S., and Cline, H.T. (2004). Insights into activity-dependent map formation from the retinotectal system: a middle-of-the-brain perspective. J Neurobiol *59*, 134-146.

Ruthazer, E.S., Li, J., and Cline, H.T. (2006). Stabilization of axon branch dynamics by synaptic maturation. J Neurosci *26*, 3594-3603.

Sabatini, B.L., Maravall, M., and Svoboda, K. (2001). Ca(2+) signaling in dendritic spines. Curr Opin Neurobiol *11*, 349-356.

Sabo, S.L., Gomes, R.A., and McAllister, A.K. (2006). Formation of presynaptic terminals at predefined sites along axons. J Neurosci *26*, 10813-10825.

Sakaguchi, D.S., and Murphey, R.K. (1985). Map formation in the developing Xenopus retinotectal system: an examination of ganglion cell terminal arborizations. J Neurosci *5*, 3228-3245.

Sanchez, A.L., Matthews, B.J., Meynard, M.M., Hu, B., Javed, S., and Cohen Cory, S. (2006). BDNF increases synapse density in dendrites of developing tectal neurons in vivo. Development *133*, 2477-2486.

Scheiffele, P., Fan, J., Choih, J., Fetter, R., and Serafini, T. (2000). Neuroligin expressed in nonneuronal cells triggers presynaptic development in contacting axons. Cell *101*, 657-669.

Schwartz, N., Schohl, A., and Ruthazer, E.S. (2009). Neural activity regulates synaptic properties and dendritic structure in vivo through calcineurin/NFAT signaling. Neuron *62*, 655-669.

Shalizi, A., Gaudilliere, B., Yuan, Z., Stegmuller, J., Shirogane, T., Ge, Q., Tan, Y., Schulman, B., Harper, J.W., and Bonni, A. (2006). A calcium-regulated MEF2 sumoylation switch controls postsynaptic differentiation. Science *311*, 1012-1017.

Shalizi, A.K., and Bonni, A. (2005). brawn for brains: the role of MEF2 proteins in the developing nervous system. Curr Top Dev Biol *69*, 239-266.

Sheng, M., and Hoogenraad, C.C. (2007). The postsynaptic architecture of excitatory synapses: a more quantitative view. Annu Rev Biochem *76*, 823-847.

Shi, S., Hayashi, Y., Esteban, J.A., and Malinow, R. (2001). Subunit-specific rules governing AMPA receptor trafficking to synapses in hippocampal pyramidal neurons. Cell *105*, 331-343.

Siddiqui, T.J., and Craig, A.M. (2011). Synaptic organizing complexes. Curr Opin Neurobiol *21*, 132-143.

Siddiqui, T.J., Pancaroglu, R., Kang, Y., Rooyakkers, A., and Craig, A.M. (2011). LRRTMs and neuroligins bind neurexins with a differential code to cooperate in glutamate synapse development. J Neurosci *30*, 7495-7506.

Silva, A.J., Kogan, J.H., Frankland, P.W., and Kida, S. (1998). CREB and memory. Annu Rev Neurosci *21*, 127-148.

Sin, W.C., Haas, K., Ruthazer, E.S., and Cline, H.T. (2002). Dendrite growth increased by visual activity requires NMDA receptor and Rho GTPases. Nature *419*, 475-480.

Skolnick, P. (2002). Modulation of glutamate receptors: strategies for the development of novel antidepressants. Amino Acids *23*, 153-159.

Slee, E.A., Adrain, C., and Martin, S.J. (1999). Serial killers: ordering caspase activation events in apoptosis. Cell Death Differ *6*, 1067-1074.

Song, I., and Huganir, R.L. (2002). Regulation of AMPA receptors during synaptic plasticity. Trends Neurosci *25*, 578-588.

Song, J.Y., Ichtchenko, K., Sudhof, T.C., and Brose, N. (1999). Neuroligin 1 is a postsynaptic cell-adhesion molecule of excitatory synapses. Proc Natl Acad Sci U S A *96*, 1100-1105.

Sperry, R.W. (1963). Chemoaffinity in the Orderly Growth of Nerve Fiber Patterns and Connections. Proc Natl Acad Sci U S A *50*, 703-710.

Spruston, N. (2008). Pyramidal neurons: dendritic structure and synaptic integration. Nat Rev Neurosci *9*, 206-221.

Srivastava, S., Osten, P., Vilim, F.S., Khatri, L., Inman, G., States, B., Daly, C., DeSouza, S., Abagyan, R., Valtschanoff, J.G.*, et al.* (1998). Novel anchorage of GluR2/3 to the postsynaptic density by the AMPA receptor-binding protein ABP. Neuron *21*, 581-591.

Stevens, B., Allen, N.J., Vazquez, L.E., Howell, G.R., Christopherson, K.S., Nouri, N., Micheva, K.D., Mehalow, A.K., Huberman, A.D., Stafford, B.*, et al.* (2007). The classical complement cascade mediates CNS synapse elimination. Cell *131*, 1164-1178.

Sudhof, T.C. (2008). Neuroligins and neurexins link synaptic function to cognitive disease. Nature *455*, 903-911.

Sugimura, K., Satoh, D., Estes, P., Crews, S., and Uemura, T. (2004). Development of morphological diversity of dendrites in Drosophila by the BTB-zinc finger protein abrupt. Neuron *43*, 809-822.

Sun, Y., Aiga, M., Yoshida, E., Humbert, P.O., and Bamji, S.X. (2009). Scribble interacts with beta-catenin to localize synaptic vesicles to synapses. Mol Biol Cell *20*, 3390-3400.

Sun, Y., and Bamji, S.X. (2011). beta-Pix modulates actin-mediated recruitment of synaptic vesicles to synapses. J Neurosci *31*, 17123-17133.

Sweeney, L.B., Chou, Y.H., Wu, Z., Joo, W., Komiyama, T., Potter, C.J., Kolodkin, A.L., Garcia, K.C., and Luo, L. (2011). Secreted Semaphorins from Degenerating Larval ORN Axons Direct Adult Projection Neuron Dendrite Targeting. Neuron *72*, 734-747.

Tabuchi, K., Blundell, J., Etherton, M.R., Hammer, R.E., Liu, X., Powell, C.M., and Sudhof, T.C. (2007). A neuroligin-3 mutation implicated in autism increases inhibitory synaptic transmission in mice. Science *318*, 71-76.

Tan, Z.J., Peng, Y., Song, H.L., Zheng, J.J., and Yu, X. (2010). N-cadherin-dependent neuron-neuron interaction is required for the maintenance of activity-induced dendrite growth. Proc Natl Acad Sci U S A *107*, 9873-9878.

Tao, H.W., Zhang, L.I., Engert, F., and Poo, M. (2001). Emergence of input specificity of ltp during development of retinotectal connections in vivo. Neuron *31*, 569-580.

tom Dieck, S., Sanmarti-Vila, L., Langnaese, K., Richter, K., Kindler, S., Soyke, A., Wex, H., Smalla, K.H., Kampf, U., Franzer, J.T.*, et al.* (1998). Bassoon, a novel zinc-finger CAG/glutamine-repeat protein selectively localized at the active zone of presynaptic nerve terminals. J Cell Biol *142*, 499-509.

Tomita, S., Fukata, M., Nicoll, R.A., and Bredt, D.S. (2004). Dynamic interaction of stargazin-like TARPs with cycling AMPA receptors at synapses. Science *303*, 1508-1511.

Trachtenberg, J.T., Chen, B.E., Knott, G.W., Feng, G., Sanes, J.R., Welker, E., and Svoboda, K. (2002). Long-term in vivo imaging of experience-dependent synaptic plasticity in adult cortex. Nature *420*, 788-794.

Tropea, D., Kreiman, G., Lyckman, A., Mukherjee, S., Yu, H., Horng, S., and Sur, M. (2006). Gene expression changes and molecular pathways mediating activity-dependent plasticity in visual cortex. Nat Neurosci *9*, 660-668.

van Dam, E.J., Ruiter, B., Kamal, A., Ramakers, G.M., Gispen, W.H., and de Graan, P.N. (2002). N-methyl-D-aspartate-induced long-term depression is associated with a decrease in postsynaptic protein kinase C substrate phosphorylation in rat hippocampal slices. Neurosci Lett *320*, 129-132.

Varoqueaux, F., Aramuni, G., Rawson, R.L., Mohrmann, R., Missler, M., Gottmann, K., Zhang, W., Sudhof, T.C., and Brose, N. (2006). Neuroligins determine synapse maturation and function. Neuron *51*, 741-754.

Varoqueaux, F., Jamain, S., and Brose, N. (2004). Neuroligin 2 is exclusively localized to inhibitory synapses. Eur J Cell Biol *83*, 449-456.

Vaughn, J.E. (1989). Fine structure of synaptogenesis in the vertebrate central nervous system. Synapse *3*, 255-285.

Vetere, G., Restivo, L., Cole, C.J., Ross, P.J., Ammassari-Teule, M., Josselyn, S.A., and Frankland, P.W. (2011). Spine growth in the anterior cingulate cortex is necessary for the consolidation of contextual fear memory. Proc Natl Acad Sci U S A *108*, 8456-8460.

Volkmar, F.R., and Greenough, W.T. (1972a). Rearing complexity affects branching of dendrites in the visual cortex of the rat. Science *176*, 1445-1447.

Volkmar, F.R., and Greenough, W.T. (1972b). Rearing complexity affects branching of dendrites in the visual cortex of the rat. Science *176*, 1445-1447.

Wang, X.B., Yang, Y., and Zhou, Q. (2007). Independent expression of synaptic and morphological plasticity associated with long-term depression. J Neurosci *27*, 12419-12429.

Washbourne, P., Bennett, J.E., and McAllister, A.K. (2002). Rapid recruitment of NMDA receptor transport packets to nascent synapses. Nat Neurosci *5*, 751-759.

Washbourne, P., Dityatev, A., Scheiffele, P., Biederer, T., Weiner, J.A., Christopherson, K.S., and El-Husseini, A. (2004). Cell adhesion molecules in synapse formation. J Neurosci *24*, 9244-9249.

Wiesel, T.N., and Hubel, D.H. (1963). Effects of Visual Deprivation on Morphology and Physiology of Cells in the Cats Lateral Geniculate Body. J Neurophysiol *26*, 978-993.

Williams, K., Russell, S.L., Shen, Y.M., and Molinoff, P.B. (1993). Developmental switch in the expression of NMDA receptors occurs in vivo and in vitro. Neuron *10*, 267-278.

Wong, R.O., and Ghosh, A. (2002). Activity-dependent regulation of dendritic growth and patterning. Nat Rev Neurosci *3*, 803-812.

Wong, W.T., Faulkner-Jones, B.E., Sanes, J.R., and Wong, R.O. (2000). Rapid dendritic remodeling in the developing retina: dependence on neurotransmission and reciprocal regulation by Rac and Rho. J Neurosci *20*, 5024-5036.

Wu, G., Malinow, R., and Cline, H.T. (1996). Maturation of a central glutamatergic synapse. Science *274*, 972-976.

Wu, G.Y., and Cline, H.T. (1998). Stabilization of dendritic arbor structure in vivo by CaMKII. Science *279*, 222-226.

Wu, G.Y., and Cline, H.T. (2003). Time-lapse in vivo imaging of the morphological development of Xenopus optic tectal interneurons. J Comp Neurol *459*, 392-406.

Xiao, T., Staub, W., Robles, E., Gosse, N.J., Cole, G.J., and Baier, H. (2011). Assembly of lamina-specific neuronal connections by slit bound to type IV collagen. Cell *146*, 164-176.

Yan, J., Oliveira, G., Coutinho, A., Yang, C., Feng, J., Katz, C., Sram, J., Bockholt, A., Jones, I.R., Craddock, N.*, et al.* (2005). Analysis of the neuroligin 3 and 4 genes in autism and other neuropsychiatric patients. Mol Psychiatry *10*, 329-332.

Yang, Y., Wang, X.B., Frerking, M., and Zhou, Q. (2008). Spine expansion and stabilization associated with long-term potentiation. J Neurosci *28*, 5740-5751.

Yashiro, K., Corlew, R., and Philpot, B.D. (2005). Visual deprivation modifies both presynaptic glutamate release and the composition of perisynaptic/extrasynaptic NMDA receptors in adult visual cortex. J Neurosci *25*, 11684-11692.

Yashiro, K., and Philpot, B.D. (2008). Regulation of NMDA receptor subunit expression and its implications for LTD, LTP, and metaplasticity. Neuropharmacology *55*, 1081-1094.

Yu, X., and Malenka, R.C. (2003). Beta-catenin is critical for dendritic morphogenesis. Nat Neurosci *6*, 1169-1177.

Yuste, R., and Denk, W. (1995). Dendritic spines as basic functional units of neuronal integration. Nature *375*, 682-684.

Zamir, E., and Geiger, B. (2001). Molecular complexity and dynamics of cell-matrix adhesions. J Cell Sci *114*, 3583-3590.

Zhai, R.G., Vardinon-Friedman, H., Cases-Langhoff, C., Becker, B., Gundelfinger, E.D., Ziv, N.E., and Garner, C.C. (2001). Assembling the presynaptic active zone: a characterization of an active one precursor vesicle. Neuron *29*, 131-143.

Zhang, L.I., Tao, H.W., Holt, C.E., Harris, W.A., and Poo, M. (1998). A critical window for cooperation and competition among developing retinotectal synapses. Nature *395*, 37-44.

Zhang, L.I., Tao, H.W., and Poo, M. (2000). Visual input induces long-term potentiation of developing retinotectal synapses. Nat Neurosci *3*, 708-715.

Zhang, W., Rohlmann, A., Sargsyan, V., Aramuni, G., Hammer, R.E., Sudhof, T.C., and Missler, M. (2005). Extracellular domains of alpha-neurexins participate in regulating synaptic transmission by selectively affecting N- and P/Q-type Ca2+ channels. J Neurosci *25*, 4330-4342.

Zhou, Q., Homma, K.J., and Poo, M.M. (2004). Shrinkage of dendritic spines associated with long-term depression of hippocampal synapses. Neuron *44*, 749-757.

Zhou, Q., Tao, H.W., and Poo, M.M. (2003). Reversal and stabilization of synaptic modifications in a developing visual system. Science *300*, 1953-1957.

Ziv, N.E. (2001). Recruitment of synaptic molecules during synaptogenesis. Neuroscientist *7*, 365-370.

Ziv, N.E., and Smith, S.J. (1996). Evidence for a role of dendritic filopodia in synaptogenesis and spine formation. Neuron *17*, 91-102.

Zoghbi, H.Y. (2003). Postnatal neurodevelopmental disorders: meeting at the synapse? Science *302*, 826-830.

Zou, D.J., and Cline, H.T. (1999). Postsynaptic calcium/calmodulin-dependent protein kinase II is required to limit elaboration of presynaptic and postsynaptic neuronal arbors. J Neurosci *19*, 8909-8918.